Study of the degradation of amine solvents used in the context of CO2 capture by chemical absorption : development of analytical methods

Auteur : Lefèbvre, Jean
Promoteur(s) : Léonard, Grégoire
Faculté : Faculté des Sciences appliquées
Diplôme : Master : ingénieur civil en chimie et science des matériaux, à finalité spécialisée en Chemical Engineering
Année académique : 2023-2024
URI/URL : http://hdl.handle.net/2268.2/20422

UNIVERSITY OF LIEGE
FACULTY OF APPLIED SCIENCES

Study of the degradation of amine solvents used in the context of CO_2 capture by chemical absorption: development of analytical methods

Jean LEFÈBVRE

Thesis presented for obtaining the Master's degree in
Chemical and Materials engineering

Supervisors
Loris BAGGIO
Grégoire LÉONARD

Academic Year : 2023 - 2024

Acknowledgments

This master's thesis has allowed me to glimpse the potential that a chemical engineer can acquire to contribute to a common goal. It marks the end of an era for me, made possible by the presence and actions of many individuals.

First and foremost, I would like to express my deepest gratitude to my distinguished supervisor, Professor Grégoire LÉONARD, for guiding me along this path and encouraging me to follow it as a true engineer would. His expert advice, rooted in his own experiences with similar challenges, has greatly enhanced my abilities, bringing me closer to his esteemed level of expertise.

I also wish to extend my heartfelt thanks to my mentor, Mr. Loris BAGGIO, for all his assistance throughout these months of experimentation, reading, and writing. His guidance led me to make the best possible decisions, provided solutions to my problems, and ensured I had the necessary equipment, chemicals, and samples for my experiments, as well as the pertinent documents. Without his support, none of my experiments would have been possible. I am also grateful for his assistance in the writing of this thesis.

My sincere thanks also go to Thierry SALMON and his colleagues, who introduced me to the laboratory environment. Their support was instrumental in enabling me to conduct my experiments efficiently.

Finally, I would like to acknowledge all those who have indirectly contributed to this thesis. An academic journey is incomplete without a social life. Therefore, I wish to thank my best friends, Quentin LAPERCHE and Maria FARCAS, for always believing in me and providing much-needed companionship and diversion during these long years.

Abstract

This master's thesis investigates the degradation of amine solvents used in CO_2 capture by chemical absorption, focusing on the development of analytical methods for assessing solvent degradation. The study addresses the pressing issue of global warming and the role of carbon capture and storage (CCS) technologies in mitigating CO_2 emissions.

The research is divided into several key areas: the identification and analysis of degradation products of various amine solvents, the application of these findings in real-world settings, and the development of precise analytical methods to measure solvent degradation. Specifically, the thesis examines the degradation of Monoethanolamine (MEA), Methyldiethanolamine (MDEA), and Piperazine (PZ), providing a comprehensive overview of their degradation products and the conditions under which these products form.

Analytical techniques such as titration with hydrochloric acid (HCl), high-performance liquid chromatography (HPLC), and methods for quantifying CO2 loading were developed and refined. These methods were applied to both fresh and degraded solvent samples to evaluate their effectiveness and reliability. The results indicate significant differences in the degradation patterns of the solvents, highlighting the importance of selecting appropriate analytical methods for accurate assessment. Additionally, differences of approximately 2 wt.-% between the results of the HPLC and HCl titration methods were observed for highly degraded samples.

The findings contribute to a better understanding of the stability and efficiency of amine solvents in CCS applications. The developed analytical methods offer a robust framework for future studies on solvent degradation, aiming to enhance the operational efficiency and environmental sustainability of CO_2 capture processes. Future work should focus on extending these methods to other amine solvents and exploring the implications of solvent degradation on the overall performance of CCS systems.

This research not only advances the technical knowledge in the field of chemical engineering but also underscores the critical role of innovative analytical techniques in addressing global environmental challenges.

Résumé

Ce travail de fin d'études étudie la dégradation des solvants amines utilisés dans la capture de CO_2 par absorption chimique, en se concentrant sur le développement de méthodes analytiques pour évaluer la dégradation des solvants. L'étude aborde la question urgente du réchauffement climatique et le rôle des technologies de capture et de stockage du carbone (CSC) dans la réduction des émissions de CO_2.

La recherche est divisée en plusieurs domaines clés : l'identification et l'analyse des produits de dégradation de divers solvants amines, l'application de ces résultats dans des contextes réels et le développement de méthodes analytiques précises pour mesurer la dégradation des solvants. Plus précisément, la thèse examine la dégradation de la Monoéthanolamine (MEA), de la Méthyldiéthanolamine (MDEA) et de la Pipérazine (PZ), fournissant une vue d'ensemble complète de leurs produits de dégradation et des conditions dans lesquelles ces produits se forment.

Des techniques analytiques telles que la titration avec de l'acide chlorhydrique (HCl), la chromatographie liquide à haute performance (HPLC) et des méthodes de quantification de la charge de CO_2 ont été développées et perfectionnées. Ces méthodes ont été appliquées à des échantillons de solvants frais et dégradés pour évaluer leur efficacité et leur fiabilité. Les résultats indiquent des différences significatives dans les schémas de dégradation des solvants, soulignant l'importance de choisir des méthodes analytiques appropriées pour une évaluation précise. De plus, des différences d'environ 2 % en poids entre les résultats des méthodes de HPLC et de titration avec HCl ont été observées pour des échantillons fortement dégradés.

Les résultats contribuent à une meilleure compréhension de la stabilité et de l'efficacité des solvants amines dans les applications de CSC. Les méthodes analytiques développées offrent un cadre solide pour les études futures sur la dégradation des solvants, visant à améliorer l'efficacité opérationnelle et la durabilité environnementale des processus de capture de CO_2. Les travaux futurs devraient se concentrer sur l'extension de ces méthodes à d'autres solvants amines et explorer les implications de la dégradation des solvants sur la performance globale des systèmes CSC.

Cette recherche non seulement fait progresser les connaissances techniques dans le domaine du génie chimique, mais souligne également le rôle crucial des techniques analytiques innovantes dans la résolution des défis environnementaux mondiaux.

Contents

List of Figures

List of Tables

Chapter I

Introduction

I1. Overview of global warming problematic

Since the Industrial Revolution, humanity has enhanced the global human lifestyle through the development of new technologies. While these technologies offer significant advantages, many of them contribute to global warming by producing problematic gases known as greenhouse gases. The most important of these gases is carbon dioxide (CO_2). The primary source of these emissions is the intensive use of fossil resources, which are deeply embedded in our daily lives and industrial processes. This reliance on fossil fuels for energy and chemical production results in significant CO_2 emissions. Global warming has a negative impact on the environment and must be controlled by humans to protect the ecosystem from the consequences of this global issue.

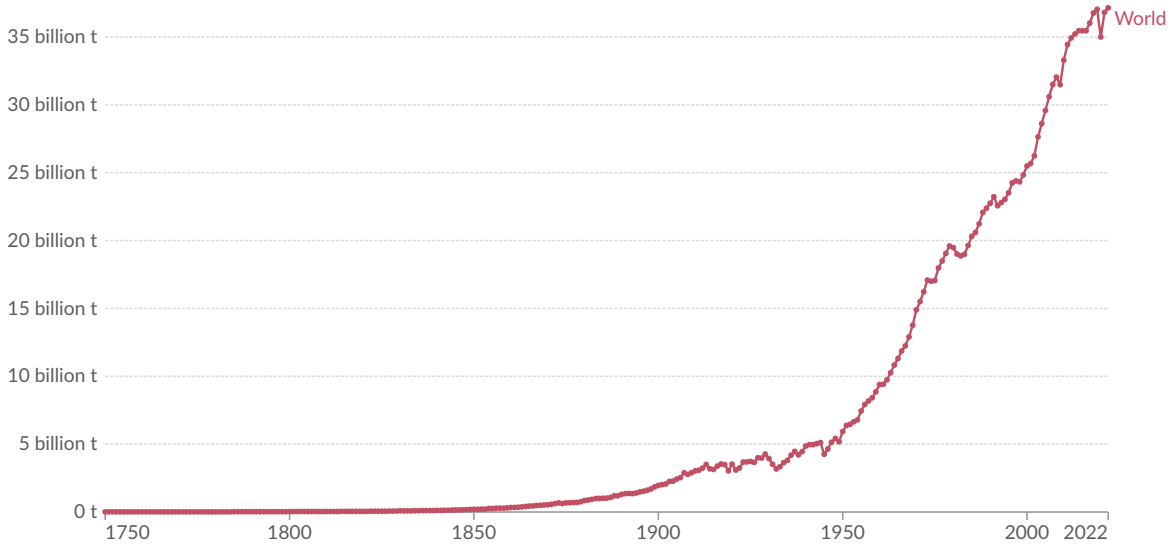

Figure I.1: Annual CO_2 emissions since 1750 (Ritchie et al. (2023))

According to Figure I.1, the annual CO_2 emission has been exponentially increased since the middle of the 19^{th} century. Global annual CO_2 emissions reached 35 billion tonnes of CO_2 per year around the 2020s, a value seven times greater than 70 years ago.

To mitigate global warming, several solutions are being considered. The first approach involves limiting CO_2 and other greenhouse gas emissions into the atmosphere by improving technologies and processes. This includes enhancing energy efficiency, transitioning to low-carbon industrial practices, and reducing emissions from transportation. The second approach focuses on maximizing the use of green or renewable energy sources, such as wind, solar, and hydroelectric power, to replace fossil fuels. Lastly, the third approach encompasses capturing carbon dioxide and utilizing it in various processes and products, thereby providing it with harmless functionality. This includes carbon capture and storage (CCS) and carbon capture, utilization, and storage (CCUS), where captured CO2 is used in the production of fuels, chemicals, and materials. These solutions correspond to the Trias Energetica model as depicted in Figure I.2. The Trias Energetica emphasizes reducing energy demand, utilizing renewable energy sources, and optimizing the use of fossil fuels. By integrating these strategies, a sustainable pathway to significantly reduce greenhouse gas emissions can be established.

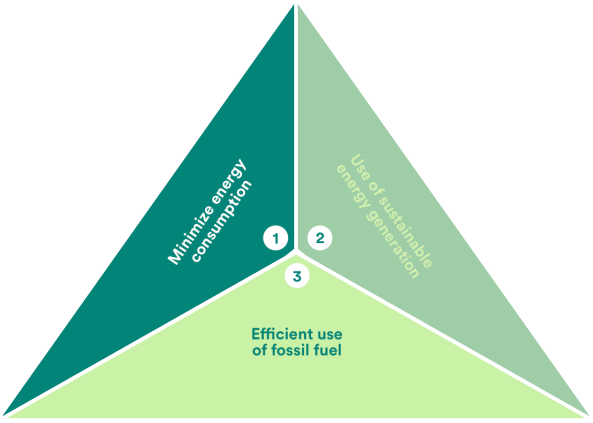

Figure I.2: Trias Energetica (Schurink (2022))

In this work, the focus will be on the capture of CO_2 as one of the solutions to climate change. Specifically, this research will explore analytical methods used to quantify the effectiveness of CO_2 capture processes. By analyzing the accuracy and reliability of these methods, the study aims to contribute to optimizing carbon capture technologies and understanding their impact on reducing greenhouse gas emissions. This examination will provide insights into applying various analytical techniques, which are crucial for evaluating the performance and efficiency of CO_2 capture systems. Through this detailed analysis, the goal is to enhance the sustainability and effectiveness of carbon capture initiatives.

I2. CO_2 capture

I.2.1 Introduction of CO_2 capture

Several technologies have been developed for CO_2 capture. Among these, Direct Air Capture (DAC) enables the extraction of CO_2 directly from the atmosphere using fans. In contrast, the predominant technologies are designed to capture CO_2 emissions from industrial sources. The CO_2 capture processes relevant to this master's thesis pertain to the treatment of exhaust gases, aiming to purify these emissions. This is commonly referred to as Carbon Capture and Storage (CCS) or Carbon Capture, Utilization, and Storage (CCUS), the latter incorporating the reutilization of CO_2 as a raw material for the synthesis of various products.

In order to illustrate, the Petra Nova project is a carbon capture initiative launched in 2017. It captures CO_2 emissions from the W. A. Parish power plant by using a chemical solvent to separate the CO_2 from flue gases. The captured CO_2 is then transported via pipeline to an underground oil reservoir for storage. This project captures approximately 1.6 million tons of CO_2 annually, which is used for enhanced oil recovery. (AgriTech (2023))

Another example is the Sleipner Project in the North Sea. It captures CO_2 produced during natural gas extraction and stores it beneath the seabed. Since its inception in 1996, the Sleipner Project has successfully captured over 25 million tonnes of CO_2 (AgriTech (2023)).

Several companies are demonstrating the potential of reusing captured CO_2 to manufacture a diverse range of products. For example, Twelve, a California-based startup, has developed an electrolyzer that converts CO_2 into synthesis gas (syngas). This syngas has been utilized to create fossil-free jet fuel in collaboration with the US Air Force, marking a significant milestone in carbon-neutral aviation. Additionally, Twelve has partnered with companies like Mercedes-Benz and Tide to explore manufacturing car parts and laundry detergent ingredients, respectively, using their syngas technology. Another notable example is Air Company, which produces vodka, perfume, and hand sanitisers from CO_2, showcasing the versatility of carbon-based products. These examples underscore the emerging carbon tech industry potential to transform waste CO_2 into valuable commodities, contributing to both environmental sustainability and product innovation (Guardian (2021)).

I.2.2 Different types of CO_2 capture technologies

For capturing CO_2, there are three main methods used in the industry:

- Post-Combustion Capture (regularly abbreviated as PCC)
- Pre-Combustion Capture
- Oxyfuel Combustion

Among these three methods, post-combustion capture (PCC) is considered one of the most easily applicable methods to existing industrial processes. The basic process for PCC involves chemical absorption using solvents. This master's thesis will focus on this method, particularly on the solvents used for CO_2 capture.

Post-combustion CO_2 capture allows the capture of CO_2 after the combustion of fuel and can be achieved through various methods such as solvent-based processes, membrane separation, and cryogenic techniques. Solvent-based processes are commonly used due to their ease of integration into existing systems, but they come with high costs and issues related to solvent degradation and energy-intensive regeneration. Membrane technologies offer an alternative by separating CO_2 through selective permeation, while cryogenic and low-temperature processes take advantage of the differences in boiling points to separate CO_2 from other gases. These methods include CO_2 liquefaction and anti-sublimation, which do not require solvents and can operate at very low temperatures (Léonard (2013)).

The pre-combustion method allows the capture of CO_2 before the combustion of the fuel by converting the carbonated fuel into CO_2 and H_2, which can be separated. It has the benefit of being a cost-effective method with high CO_2 removal efficiency but poses difficulties when integrating with some existing processes.

Oxyfuel combustion captures CO_2 by combusting the fuel using pure oxygen instead of air, which releases only CO_2 and steam. This method benefits from avoiding the exhaust gas separation step and can be easily added to existing processes but requires a pure oxygen production step, which still necessitates a separation unit (2022).

I.2.3 CO_2 capture by amine absorption

In this section, a brief description of an example of a post-combustion process is provided to demonstrate how amine solvents can be used to capture CO_2. Following this, a list of solvents that can be employed in this process is compiled before being detailed following different comparison points.

I.2.3.a Process description

The industrial process described by MacDowell et al. (2010) focuses on capturing CO_2 emissions from large stationary sources such as power plants and industrial facilities. This process aims to mitigate the effects of anthropogenic climate change by reducing the amount of CO_2 released into the atmosphere.

Figure I.3 is a simplified representation of the CO_2 capture process using amine-based chemical absorption, as described by MacDowell et al.:

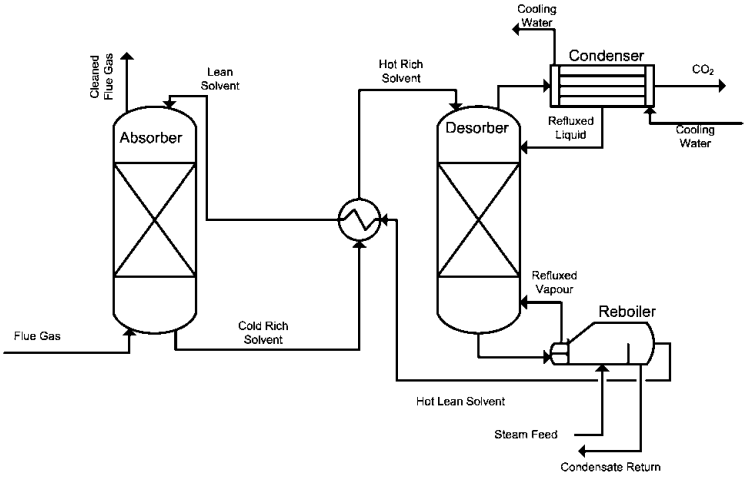

Figure I.3: Process flow diagram of a solvent-based CO_2 capture process (MacDowell et al. (2010))

The choice of amine is critical in the CO_2 capture process. MacDowell et al. highlight that primary, secondary, and tertiary amines each have distinct properties that influence their effectiveness. Monoethanolamine (MEA) is often used as a benchmark due to its high reactivity with CO2, but secondary amines like diethanolamine (DEA) and tertiary amines such as methyldiethanolamine (MDEA) are also considered for their lower energy requirements and stability.

The chemical reaction between an amine and CO_2 is essential for the absorption process. The general reactions are:

1. For primary and secondary amines, the reaction with CO_2 typically involves the formation of a carbamate:
$$CO_2 + 2\,R_1R_2NH \rightleftharpoons R_1R_2NCO_2^- + R_1R_2NH_2^+ \tag{I.1}$$

2. The carbamate can further react with water:
$$R_1R_2NCO_2^- + H_2O \rightleftharpoons R_1R_2NH + HCO_3^- \tag{I.2}$$

3. The direct reaction of CO2 with hydroxide ions:
$$CO_2 + OH^- \rightleftharpoons HCO_3^- \tag{I.3}$$

4. For tertiary amines, the reaction involves the formation of bicarbonate:
$$CO_2 + H_2O + R_1R_2R_3N \rightleftharpoons R_1R_2R_3NH^+ + HCO_3^- \tag{I.4}$$

The CO_2 capture process involves two main columns: the absorber and the stripper (or regenerator).

1. Absorber column :
    - Flue gas containing CO_2 is introduced at the bottom of the absorber column.
    - The gas rises through the column and contacts a counter-flowing amine solution.
    - The amine reacts with CO_2 to form a carbamate or bicarbonate, capturing CO_2 from the gas stream.
    - The treated gas, now depleted of CO_2, exits the top of the absorber.
2. Stripper column :
    - The rich amine solution, now loaded with CO_2, is pumped to the top of the stripper column.
    - In the stripper, the solution is heated, typically using steam.
    - The heat breaks the chemical bonds between the amine and CO_2, releasing CO_2 gas.
    - The lean amine, free of CO_2, is recycled back to the absorber for reuse.

This process is energy-intensive, primarily due to the heat required for regenerating the amine in the stripper column. However, advancements in amine formulations and process optimizations aim to reduce these energy penalties, improving the overall efficiency of the CO_2 capture process.

I.2.3.b Solvent overview

During the CO_2 capture step described in the previous section, the CO_2 separation method used was chemical absorption, which requires solvents. The most commonly used solvents for CO_2 capture are aqueous amine solutions. Amines can be classified as primary, secondary, or tertiary, and the reactions will vary depending on the type of amine.

The most common amine solvent is monoethanolamine (MEA), which has been extensively used in industrial applications. A notable industrial application of MEA is in urea production, where CO_2 captured using MEA is utilized as a feedstock. For instance, the use of MEA in the urea production process is well documented, with industrial applications capturing significant amounts of CO_2 for further chemical processes (Léonard (2021-2022)). Other notable amines include methyldiethanolamine (MDEA), 2-amino-2-methylpropanol (AMP), and piperazine (PZ). Additionally, mixtures of these amines can be utilized to optimize the CO_2 capture process, leveraging the strengths of each component.

In recent years, the development of new solvents has been a significant focus in the field of CO_2 capture. For example, BASF has introduced a solvent called OASE® blue, which promises lower energy consumption and reduced solvent degradation compared to traditional amine solutions (BASF (2022)). Mitsubishi has developed the KS-1 solvent, which similarly aims to improve efficiency and reduce environmental impact. These advancements in solvent technology are crucial for enhancing the feasibility and sustainability of CO_2 capture processes (Mitsubishi Heavy Industries, Ltd. (2022)).

These amine solvents thus hold significant potential for CO_2 capture. However, over time and under varying environmental conditions, these solvents tend to degrade. Consequently, certain analytical methods are employed to quantify the remaining amount of amine solvents, the different degradation compounds coming from the degradation as well as the capacity of the solvent to absorb CO_2, also known as the CO_2 loading. Among these, the primary focus of this master's thesis will be on the remaining amount of amine solvent and its CO_2 loading.

Chapter II

Literature Review

In this chapter, a general literature review of the different amine solvents used for CO_2 capture is done including their characteristics as well as the methods used to analyse the different components produced during the CO_2 absorption process with flue gases. This global review allows us to understand the different reactions occurring during the global process and then identify the experimental work required for bringing an interesting work that will contribute to an increase in the absorption CO_2 capture knowledge.

II1. Degradation of amine solvents

II.1.1 List of amine solvents and their degradation products

Through this literature review, different amine solvents will be discussed and presented. The benchmark amine solvent used for CO_2 capture is the monoethanolamine (MEA). This one has been used for several years and consists of the basic solvent and is the most commonly used (Langa et al. (2017)). The other amine solvents on which this work will focus are methyldiethanolamine (MDEA) and piperazine (PZ). Mixtures of those in different proportions are more and more studied. Apart from these solvents, 2-amino-2-methylpropanol (AMP), diethanolamine (DEA), and ethylenediamine (EDA) are other amine solvents used for CO_2 capture by chemical absorption.

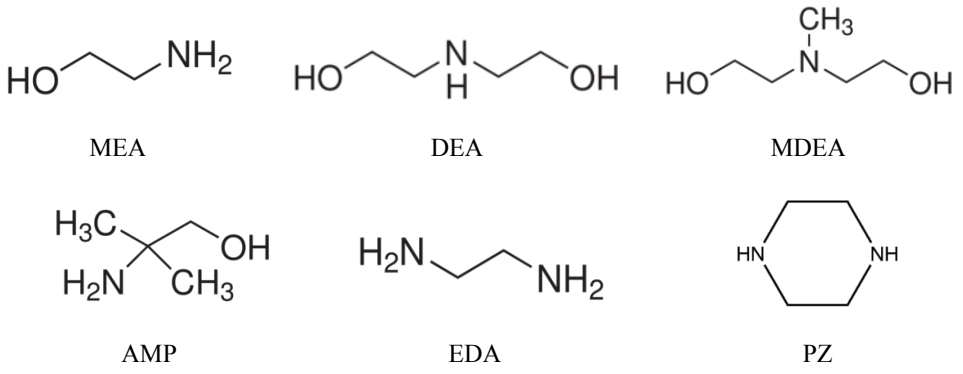

Figure II.1: Molecular formula of amine solvents used for CO_2 absorption (Léonard (2013))

II.1.1.a Monoethanolamine (MEA)

Most of the degradation products, the different reactions and mechanisms occurring with MEA and the influence of some parameters on the reactions have already been identified, as explained in various works (Léonard (2013), Lepaumier (2008)).

First, Figure II.2 shows the main identified degradation products of MEA.

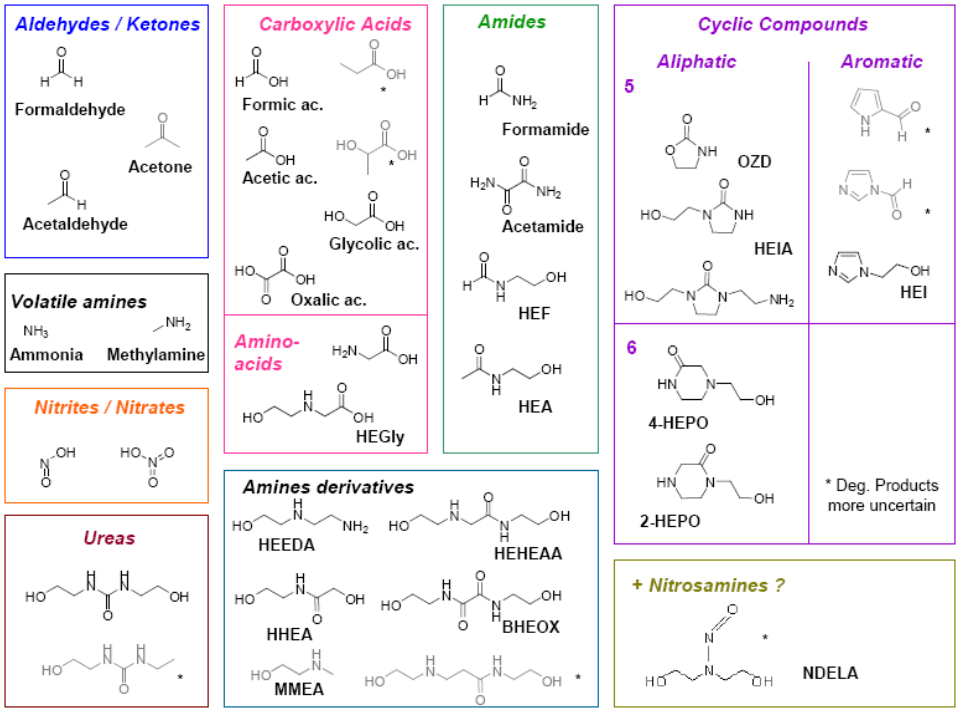

Figure II.2: List of the main degradation products of MEA (Léonard (2013))

According to Cuzuel et al. (2015), there are approximately 60 identified different degradation products including the rarest produced ones.

The previously identified degradation products are formed through various mechanisms. Four distinct types of degradation can be identified:

- Thermal decomposition
- Thermal degradation in the presence of CO_2
- Oxidative degradation
- Reactions of MEA with flue gas contaminants SO_x and NO_x

Thermal decomposition:

Thermal decomposition occurs at temperatures exceeding 200 °C. Since these temperatures are rarely reached during regeneration of the solvent, this degradation mechanism is not typically studied when discussing CO_2 capture.

Thermal decomposition in the presence of CO_2:

Thermal degradation with CO_2 involves irreversible reactions of amine with CO_2. During absorption, MEA carbamates (HO-CH_2-CH_2-NH-COO-) are formed due to enhanced interactions between gaseous CO_2 and the solvent. However, at stripper temperatures, carbamate species may undergo further irreversible reactions, forming degradation products. The main identified degradation products of MEA in the presence of CO_2 include HEIA (N-(2-hydroxyethyl)imidazolidone), HEEDA (2-(2-aminoethylamino)ethanol), and OZD (2-oxazolidinone) (Lepaumier (2008)).

The formation mechanism of oxazolidinone from MEA carbamate is depicted in Figure II.3.

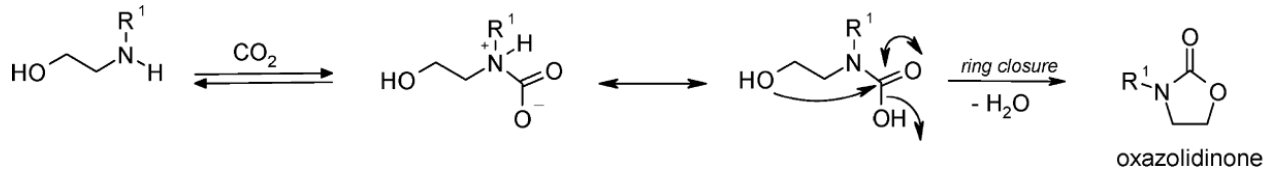

Figure II.3: Oxazolidinone formation mechanism from MEA carbamate (R^1=H) Lepaumier (2008)

The oxazolidinone is relatively unstable and can react with MEA to form HEEDA. Further, HEEDA can undergo additional reactions with CO_2, resulting in the formation of a carbamate that undergoes cyclization, ultimately leading to the formation of HEIA, the primary product of MEA thermal degradation with CO_2 Lepaumier (2008).

The formation mechanism of imidazolidinone from oxazolidinone is illustrated in Figure II.4.

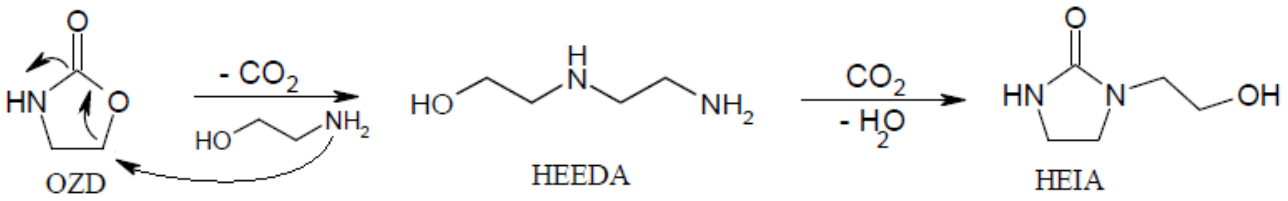

Figure II.4: Imidazolidinone formation from oxazolidinone (Lepaumier (2008)
)

HEIA contributes to 65.5% of the identified degradation products of MEA thermal degradation under CO_2, while HEEDA and OZD contribute 14.2% and 1.6% respectively (Lepaumier (2008)). Additionally, other identified degradation products include a second MEA addition product and its corresponding imidazolidinone.

Oxidative degradation:

Oxidative degradation of MEA is primarily a free radical chain reaction involving initiation, propagation, and termination steps (Lepaumier (2008), Bedell (2011), Voice and Rochelle (2011)).

During the initiation step, a free radical is generated through the cleavage of a homolytic covalent bond. This initiation can be caused by temperature, light, or the presence of metal catalysts (Delfort et al. (2011)). For example:

$$\mathrm{RH} \rightarrow \mathrm{R}\cdot + \mathrm{H}\cdot \quad \text{Initiation} \tag{II.1}$$

$$\mathrm{R\text{-}R} \rightarrow 2\mathrm{R}\cdot \tag{II.2}$$

These radicals subsequently react with oxygen to form peroxy radicals, which further react with a C-H bond via hydrogen abstraction, producing hydroperoxides. The chain reaction can continue through the cleavage of hydroperoxides into two radicals (Delfort et al. (2011)). For instance:

$$\mathrm{R}\cdot + \mathrm{O_2} \rightarrow \mathrm{ROO}\cdot \quad \text{Propagation} \tag{II.3}$$

$$\mathrm{ROO}\cdot + \mathrm{RH} \rightarrow \mathrm{ROOH} + \mathrm{R}\cdot \tag{II.4}$$

$$\mathrm{ROOH} \rightarrow \mathrm{RO}\cdot + \mathrm{HO}\cdot \tag{II.5}$$

$$2\mathrm{ROOH} \rightarrow \mathrm{ROO}\cdot + \mathrm{RO}\cdot + \mathrm{H_2O} \tag{II.6}$$

The termination step involves the recombination of two radicals to form a stable molecule, resulting in the final degradation product. In the case of MEA, the primary degradation products are ammonia and carboxylic acids such as formic, acetic, glycolic, and oxalic acids (Voice and Rochelle (2011)). Figure II.5 illustrates the free radical chain reaction for MEA (Delfort et al. (2011)).

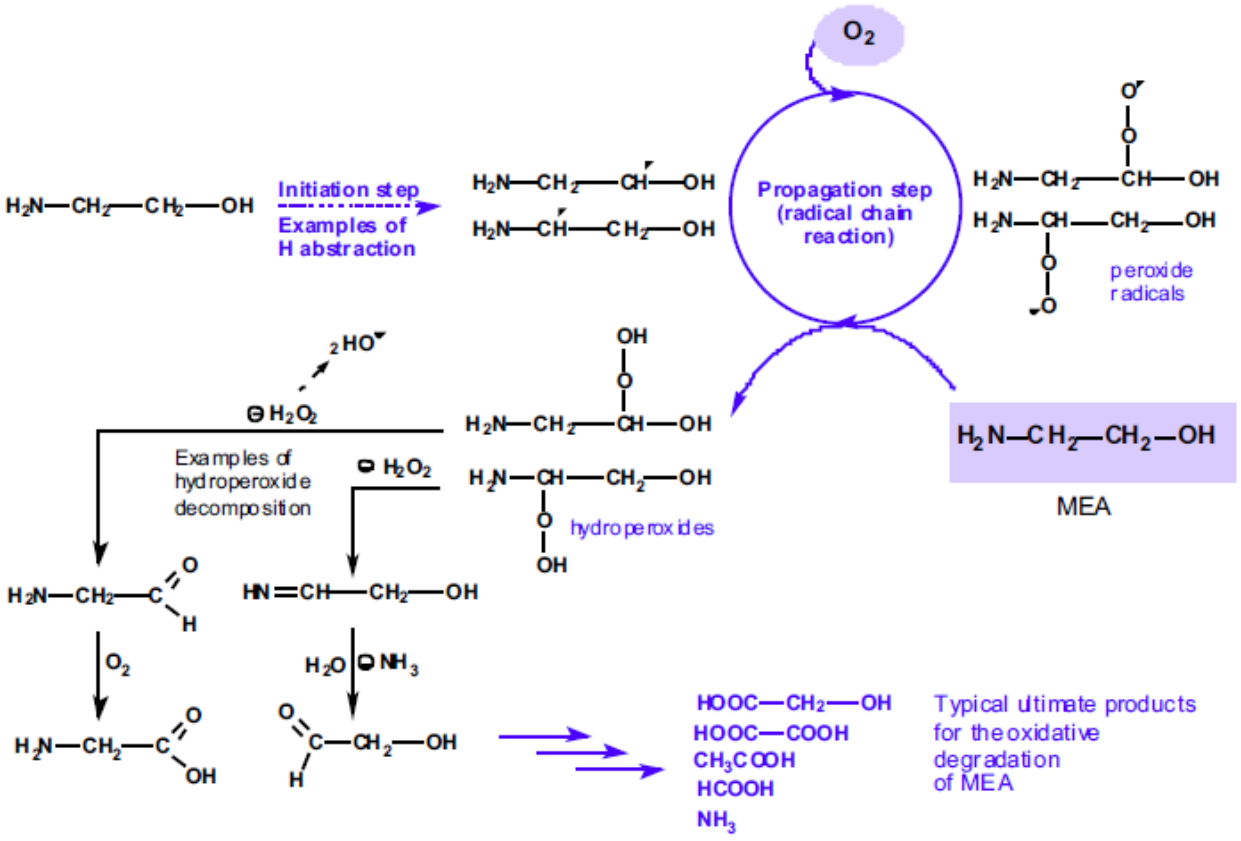

Figure II.5: Free radical chain reaction for MEA (Delfort et al. (2011))

Monoethanolamine (MEA) is prone to forming heat-stable salts (HSS) when it reacts with organic acids. These organic acids can arise from the oxidation of MEA itself or from impurities in the flue

gas. The formation of HSS is a significant degradation pathway because these salts do not regenerate and accumulate in the solvent, reducing its efficiency. These organic acids can further react by dehydration with MEA, leading to other degradation products such as HEF, HEA, HEHEEA, and BHEOX (Lepaumier (2008)). The pathways for these formations are illustrated in Figure II.6.

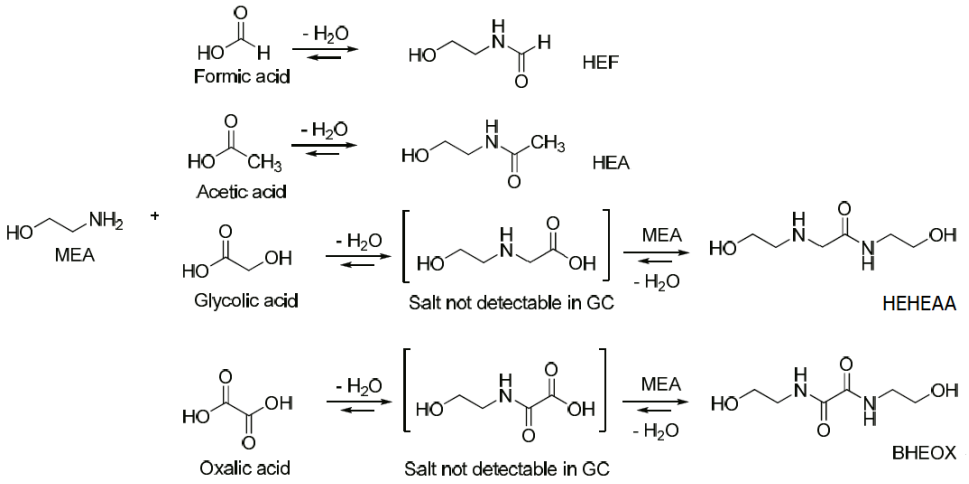

Figure II.6: MEA degradation reactions with organic acids

Additionally, HEPO (4-(2-hydroxyethyl)piperazin-2-one) has been identified as an important degradation product of MEA oxidative degradation, potentially formed by the cyclization of HEHEAA (N-(2-hydroxyethyl)-2-(2-hydroxyethylamino)acetamide) (Strazisar et al. (2003)).

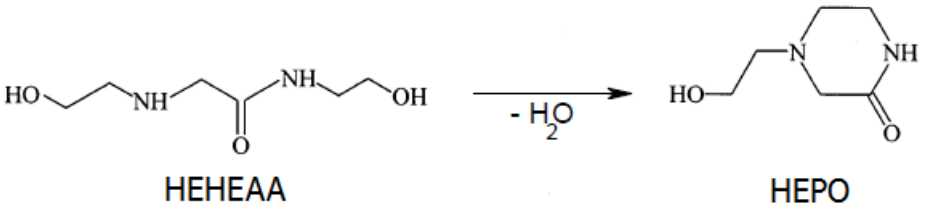

Figure II.7: Formation of HEPO

Finally, HEI (N-(2-hydroxyethyl)imidazole) is another significant degradation product of MEA, with its formation pathway still under investigation (Lepaumier (2008)). Voice et al. (2012) proposed a condensation mechanism between MEA/glyoxal imine and methanimine, as shown in Figure II.8.

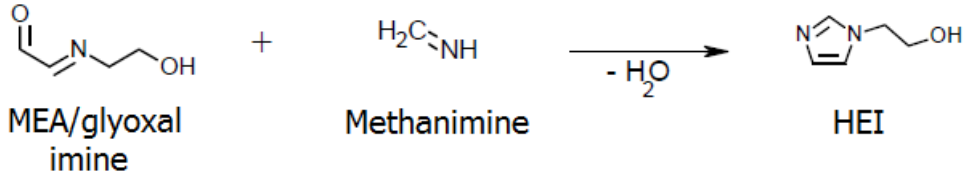

Figure II.8: Formation of HEI (Voice et al. (2012))

Other secondary oxidative degradation compounds such as HEA, HEF, HEGly, OZD and BHEOX may be produced by a further degradation of the solvent (Buvik et al. (2021)).

Reactions of MEA with flue gas contaminants SO_x and NO_x:

In addition to reacting with CO_2, monoethanolamine (MEA) can also react with contaminants such as sulfur oxides (SO_x) and nitrogen oxides (NO_x) present in flue gas. These reactions lead to the formation of various degradation products that are significantly different from those formed during reactions with CO_2.

When MEA is exposed to SO_x, particularly sulfur dioxide (SO_2), it forms non-reclaimable corrosive salts which can severely affect the operation of the CO_2 capture plant. SO_2 in the presence of MEA and oxygen can form heat stable salts (HSS) such as sulfate and bisulfate, which are difficult to remove and can cause operational issues. Additionally, SO_2 can react with MEA to form organosulfates and other degradation products, potentially leading to increased solvent losses and corrosion problems.

Similarly, MEA reacts with NO_x, particularly nitrogen dioxide (NO_2) and nitric oxide (NO), to form nitrosamines and nitramines. These compounds are hazardous, carcinogenic, and pose significant environmental and health risks. The presence of NO_x can lead to the formation of nitrosodiethanolamine (NDELA) and other harmful compounds, which must be carefully monitored and controlled. These reactions typically occur through complex mechanisms involving multiple steps and intermediate compounds.

However, it should be noted that modern flue gas treatment technologies, including flue gas desulfurization (FGD) and selective catalytic reduction (SCR) units, are highly effective at removing SO_x and NO_x from the flue gas before it reaches the CO_2 capture system. This significantly reduces the impact of these contaminants on MEA degradation. As a result, the focus of this work will be primarily on the degradation of MEA due to CO_2 and oxidative degradation, with less emphasis on the reactions with SO_x and NO_x (Ghosh (2023*a*)).

II.1.1.b Methyldiethanolamine (MDEA)

Methyldiethanolamine (MDEA) is widely used for CO_2 capture in post-combustion processes. It is a tertiary amine, which differs from primary amines like MEA and secondary amines like DEA (Diethanolamine).The reduced reactivity of MDEA with CO_2 correlates with lower heat demands during regeneration, positioning it as a favoured choice within select industrial contexts. (Langa et al. (2017)).

MDEA is generally more stable than MEA, but it still undergoes degradation through several pathways, including thermal and oxidative degradation. The primary degradation products of MDEA include:

- Diethanolamine (DEA)
- Bicine (bis-hydroxyethylglycine)
- Formate
- Formamide (Closmann and Rochelle (2011*a*))

Thermal degradation of MDEA typically occurs at higher temperatures than MEA (according to Langa et al. (2017), MEA has a boiling temperature of 171 °C and MDEA 247 °C), resulting in

the formation of formamide and methylformamide among other products. This process is less prominent in typical operational conditions due to the higher thermal stability of MDEA compared to MEA.

Oxidative degradation involves reactions with oxygen and can result in the formation of various organic acids and amides. The presence of oxidative agents in the flue gas can catalyze these reactions, although the resistance of MDEA to oxidative degradation is higher than that of MEA.

The comparison between MDEA and MEA highlights several key differences that influence their application in CO_2 capture processes. Indeed, MDEA has a lower specific heat demand (1 MJ/kg CO_2) compared to MEA (3.7 MJ/kg CO_2), making it more energy-efficient for solvent regeneration. Additionally, the lower heat duty of MDEA for the partial condenser indicates less energy required for cooling (Poluzzi et al. (2022)).

In addition, MDEA has a higher potential concerning CO_2 loading capacity to MEA. The maximum loading capacity of MEA is approximately 0.5 mol CO_2/mol amine, while MDEA can achieve nearly 1.0 mol CO_2/mol amine under optimal conditions. This higher capacity can improve the overall efficiency of CO_2 capture, potentially reducing the required solvent volumes and regeneration cycles (Santos et al. (2016)).

II.1.1.c Piperazine (PZ)

Concentrated piperazine (PZ) has emerged as a promising solvent for CO_2 capture in amine-based absorption/stripping processes. Previous studies have highlighted several key advantages of PZ, including fast CO_2 absorption rates, high CO_2 capacity, low volatility, and limited degradation under absorption/stripping process conditions. Despite these desirable characteristics, concentrated PZ systems do present certain drawbacks such as high viscosity, potential high amine cost, and the possibility of solid precipitation.

The resistance of concentrated PZ to thermal degradation has been extensively studied. PZ demonstrates exceptional resistance to degradation up to 150 °C, significantly higher than standard stripper operating conditions. However, at temperatures exceeding 150 °C, PZ begins to degrade at rates comparable to alkanolamines. Several structural characteristics contribute to the thermal stability of PZ. Notably, its six-membered ring structure with two secondary amino functions minimizes angle or torsional strain, enhancing stability. Moreover, the absence of an alcohol function, which typically enhances thermal degradation, further contributes to the resistance of PZ to degradation.

Comparative analysis between concentrated PZ and monoethanolamine (MEA) reveals significant differences in thermal degradation characteristics . PZ exhibits superior thermal stability compared to MEA, with resistance to degradation up to 150 °C. In contrast, MEA demonstrates lower thermal resistance and requires low-temperature applications to fully utilize its advantageous solvent characteristics. Additionally, the resistance of PZ to thermal degradation outperforms other well-studied alkanolamine solvents such as 2-amino-2-methyl-1-propanol (AMP) and methyldiethanolamine (MDEA). These findings underscore the potential of concentrated PZ as a robust solvent for CO_2 capture applications (Closmann and Rochelle (2011*b*)).

To illustrate the principle, an example of a process producing exhaust gases that contain CO_2 in a non-negligible concentration is taken. In this example, a natural gas power plant that produces energy requires fossil fuel and releases impurities and harmful gases such as SO_x and NO_x, and mainly carbon

dioxide. Some previous steps can remove impurities, SO_x, and NO_x, leaving mainly N_2, CO_2, water vapor, and small concentrations of other gases.

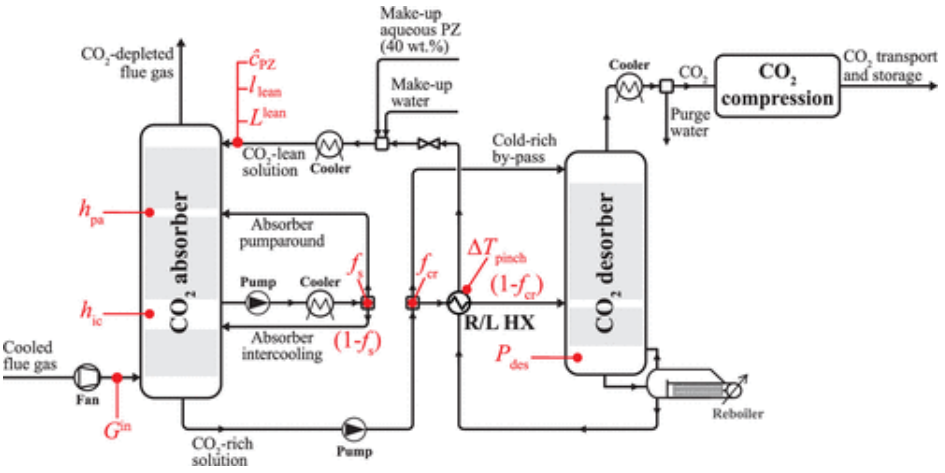

Figure II.9: Process flow diagram of a solvent-based CO_2 capture process (Zanco et al. (2021))

After some steps to condition the waste gases such as compression and cooling, the gases enter an absorption column that contains a liquid solvent. In this process, aqueous piperazine (PZ) has been selected as the solvent due to its superior performance compared to the benchmark aqueous monoethanolamine (MEA). The advantages of PZ include greater normalized CO_2 absorption capacity, faster absorption rate, better resistance to oxidative and thermal degradation, lower energy demand for solvent regeneration, lower amine volatility, and reduced corrosive effects.

In the absorption column, the exhaust gases flow upward in counter-current to the downward-flowing PZ solution. A chemical reaction occurs, capturing CO_2 from the gas into the liquid solvent.

$$PZ + CO_2 + H_2O \rightarrow PZCOO^- + H^+ \tag{II.7}$$

The CO_2-rich solution is then transferred to a desorption column where thermal energy, usually provided by steam, regenerates the lean solvent by releasing the absorbed CO_2. This CO_2-rich gaseous stream, which contains significant amounts of water vapor, is cooled to separate the water by condensation and then compressed for transportation to storage or utilization. To minimize the thermal energy required for solvent regeneration, a heat exchanger (R/L HX) preheats the CO_2-rich solution using the heat from the hot CO_2-lean solution exiting the reboiler.

The standard absorber-desorber process has been enhanced with intercooling and partial pumparound recycle in the absorber, and a cold-rich bypass in the desorber to improve performance. The absorber is divided into three packing sections, with the liquid stream cooled and recycled to optimize CO_2 capture.

In the desorber, a cold-rich bypass and a single rich/lean heat exchanger are implemented. This configuration, while simpler than other proposed models, balances performance and capital costs effectively (Zanco et al. (2021)).

II.1.2 Application in ULiège

At the University of Liège, a degradation test rig (DTR) was developed to study oxidative degradation. The test rig is composed of different parts that can be seen in Figure II.10.

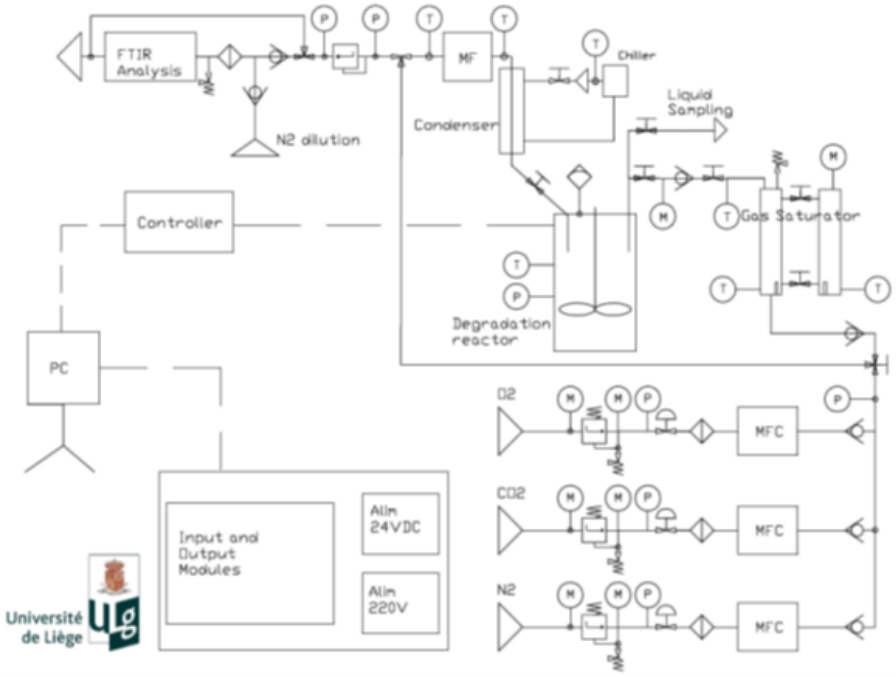

Figure II.10: Flowsheet of the degradation test rig

Those parts include the gas supply (Figures II.11 & II.12), the degradation reactor and the water balance control (gas saturator and condenser) represented in Figure II.13, as well as the data acquisition and control panel.

Figure II.11: Gas bottles

Figure II.12: Gas control system and data acquisition

The gas supply section consists of gas bottles containing oxygen, carbon dioxide, and nitrogen, which are essential for simulating the oxidative degradation environment. The gas control system ensures the precise mixing and flow rate of these gases, as shown in Figure II.12. This system is crucial for maintaining the desired experimental conditions throughout the degradation process.

Figure II.13: Degradation reactor and water balance control parts

The degradation reactor, depicted in Figure II.13, is designed to withstand high temperatures and pressures, providing a controlled environment for the oxidative degradation of MEA. It includes features such as a gas saturator and a condenser, which are part of the water balance control system. This setup ensures that the gas entering the reactor is properly saturated with water vapor, and the condensate is efficiently removed, maintaining the stability of the system.

Data acquisition and control are integral to the DTR, enabling continuous monitoring and adjustment of the experimental parameters. The control panel allows for real-time data collection and logging, facilitating detailed analysis of the degradation process.

The DTR design incorporates several safety and efficiency measures, such as automated shut-off valves and pressure relief systems, to prevent accidents and ensure smooth operation. These features, along with the precise control of experimental conditions, make the DTR a robust platform for studying the oxidative degradation of amine solvents under simulated industrial conditions.

This test rig has been instrumental in various studies, providing valuable insights into the mechanisms and kinetics of solvent degradation, and helping to develop strategies for minimizing degradation in industrial applications.

The work of Léonard (2013) has demonstrated the effectiveness of the DTR in accelerating solvent degradation to obtain experimental data within a reasonable timeframe while maintaining conditions representative of real CO_2 capture environments. The test rig facilitated detailed studies on the oxidative degradation of MEA, confirming that oxidative degradation is a significant pathway in industrial CO_2 capture scenarios. The research highlighted the influence of process parameters such as oxygen concentration, agitation rate, and temperature on the degradation rate, providing a comprehensive understanding of the degradation mechanisms.

Continuous efforts at ULiège aim to study the degradation of SO_x and NO_x, illustrating the broader applicability of the DTR in understanding and quantifying the degradation phenomena of various pollutants. The ongoing work, including the research in this master thesis, aims to enhance the comprehension of degradation processes and improve the quantification of degradation products. This will contribute to more effective mitigation strategies for solvent degradation in industrial applications, supporting the overall objective of optimizing CO_2 capture processes and ensuring the long-term stability and efficiency of amine solvents.

II2. Analytical methods used to characterize solvent degradation

This section provides an overview of the various analytical techniques employed to identify and quantify the degradation of solvents used in CO_2 capture processes. Specifically, there are two types of methods: those that determine the concentration of amine and those that quantify the CO_2 loading in the solvent.

II.2.1 Analytical methods used to quantify amine concentration

In this subsection, the focus is on the degradation of amines, examining how their concentrations change over time. These methods are employed to accurately measure the remaining quantity of amines, thereby characterizing the extent of solvent degradation.

II.2.1.a Titration with HCl

The process of HCl titration involves an acid-base reaction between an amine solvent and HCl. In this procedure, the employed coloured indicator could be orange methyl. The quantification of amine solvent via HCl titration often involves the utilization of the Chittick Apparatus, which facilitates the measurement of CO_2 loading. For further elucidation on this topic, comprehensive details are provided in Section II.2.2.b.

The reaction mechanisms between a strong acid and an amine solvent, whether charged or uncharged, are outlined below using MEA and H_3O^+ as examples:

$$MEA + H_3O^+ \rightarrow MEAH^+ + H_2O \tag{II.8}$$

$$MEACOO^- + H_3O^+ \rightarrow MEACOOH + H_2O \tag{II.9}$$

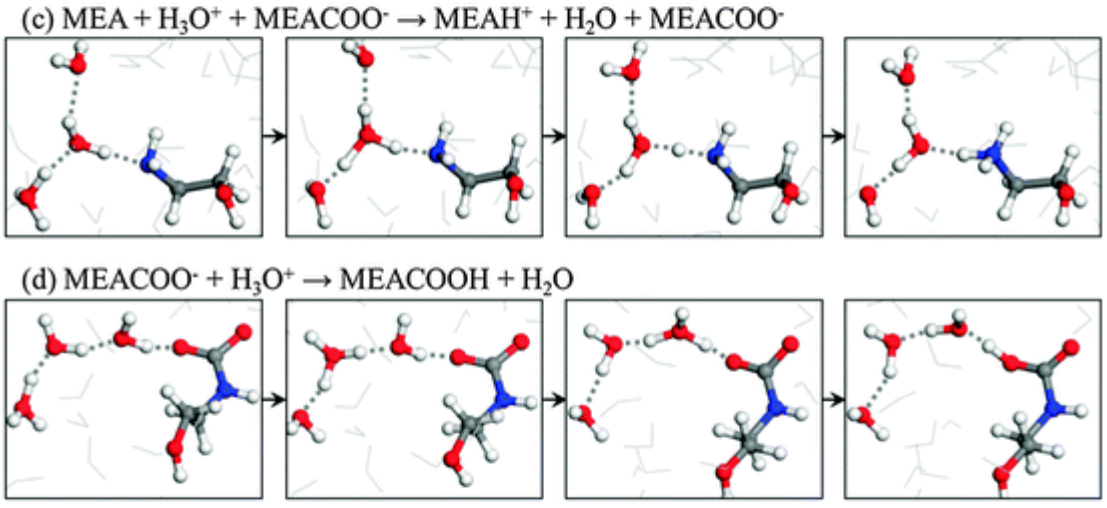

Figure II.14: Elementary reaction steps between MEA and H_3O^+ (Hwang et al. (2015))

In this process, a proton is donated to the non CO_2 charged MEA molecule to obtain protonated MEA ($MEAH^+$) and if the amine is charged, the carbamate ($MEACOO^-$) can react with acid proton to form carbamic acid (MEACOOH). Hydrochloric acid, being a common strong acid, is employed for solvent quantification. The mentioned equations can thus be rearranged, and proton donation occurs

alongside the release of a chloride ion (Cl^-). Due to the sharp pH drop at the equivalence point, methyl orange is utilized for endpoint detection. Methyl orange transitions from yellow to orange/pink within an acidic pH range of 3.1 to 4.4 (Hwang et al. (2015)).

A detailed methodology outlining the HCl titration process is presented in Section III1..

II.2.1.b High-Performance Liquid Chromatography HPLC

High-Performance Liquid Chromatography (HPLC) is a powerful analytical technique used to separate, identify, and quantify components in a mixture. This method relies on high-pressure pumps to pass a liquid solvent containing the sample mixture through a column filled with a solid adsorbent material. Each component in the sample interacts differently with the adsorbent material, leading to different flow rates for each component and thus separating them as they flow out of the column.

The fundamental principle of HPLC is based on the distribution of analytes between a mobile phase and a stationary phase. The mobile phase is a liquid solvent that carries the sample through the column. The stationary phase is a solid material within the column that interacts with the analytes. The degree of interaction between each analyte and the stationary phase determines the retention time of the analyte, which is the time taken for the analyte to pass through the column and reach the detector.

Retention time (t_R) is a crucial parameter in HPLC. It is the time taken for a specific analyte to elute from the column after the injection of the sample. The retention time depends on the nature of the analyte, the stationary phase, the mobile phase composition, and the flow rate of the mobile phase. Analytes with stronger interactions with the stationary phase have longer retention times, while those with weaker interactions elute faster (Ali (2022) and Delft (2024)).

An HPLC system typically comprises the following components:

- **Solvent Reservoir:** Holds the mobile phase, which can be a single solvent or a mixture of solvents.
- **Pump:** Generates the high pressure required to push the mobile phase through the column.
- **Injector:** Introduces the sample into the mobile phase stream.
- **Column:** Contains the stationary phase and separates the analytes.
- **Detector:** Detects the separated analytes as they elute from the column.
- **Data System:** Records and analyzes the detector signals to produce chromatograms. A chromatogram is a graph that displays the response of the detector from HPLC as a function of time. The compounds in a sample are separated within the column and sequentially detected, producing peaks on the chromatogram, with each peak representing a specific compound. The position and size of these peaks provide qualitative and quantitative information about the compounds present in the sample (Ali (2022)).

HPLC is widely used in various fields including pharmaceuticals, environmental analysis, food and beverage industry, and clinical testing. It is employed to:

- Analyze complex mixtures.
- Purify compounds.

- Quantify components in a mixture.
- Identify compounds based on their retention times and spectral data.

HPLC plays a pivotal role in the analysis of amines used in CO_2 capture processes. This technique is particularly valuable for identifying and quantifying the degradation products of amines, which are critical for evaluating the efficiency and longevity of CO_2 capture solvents. By separating the various degradation products, HPLC allows for the precise quantification of the remaining amine concentration in the samples. This capability is essential for assessing the extent of amine degradation over time. Furthermore, HPLC can differentiate between multiple types of degradation products, providing a detailed profile of the chemical changes occurring within the solvent. For instance, in CO_2 capture applications, HPLC can identify and quantify specific degradation compounds, such as heat-stable salts and other byproducts, which directly impact the performance and environmental footprint of the capture process. This method's sensitivity and accuracy make it indispensable for ongoing research and operational monitoring in CO_2 capture technology.

II.2.1.c Gas Chromatography (GC)

Gas chromatography (GC) is a crucial analytical technique widely used for the identification and quantification of organic compounds in various samples. This method is particularly valuable in the study of solvent degradation products.

In gas chromatography, a liquid sample is first vaporized and then injected into a capillary column housed within an oven. The temperature of the oven is meticulously controlled and gradually increased during the analysis. As the sample passes through the column, it interacts with the stationary phase, leading to the separation of its components based on their different affinities with the column material.

The separated compounds are then detected as they elute from the column, usually by a Flame Ionization Detector (FID) or other types of detectors. The FID works by ionizing the compounds as they burn in a hydrogen flame, producing ions that create an electrical signal proportional to the amount of the compound (Léonard (2013)).

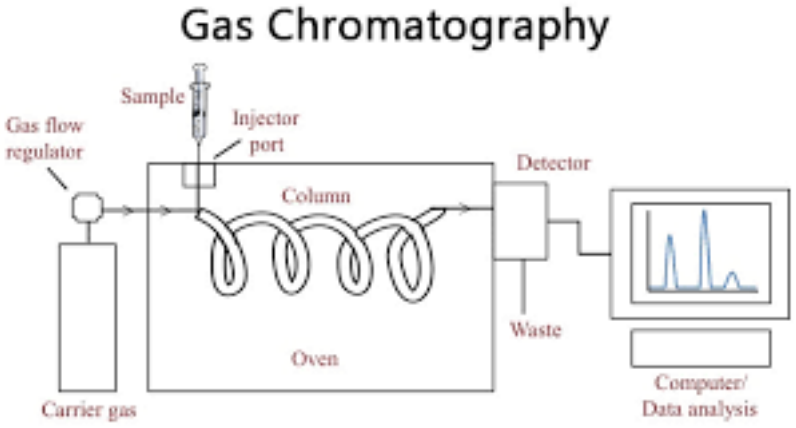

Figure II.15: Gas chromatography units (Aryal (2024)

II.2.1.d Ion Chromatography (IC)

Ion chromatography (IC) is an essential analytical technique for the identification and quantification of ionic compounds in various solutions. This method is particularly useful in the analysis of degradation products of amines used in CO_2 capture processes. The fundamental principle of IC is based on the separation of ions according to their interactions with a charged stationary phase and a liquid mobile phase. A sample is injected into a separation column containing an ion-exchange resin. The ions in the sample migrate through the column at different rates based on their charges and affinities for the resin, allowing for their separation.

IC employs conductivity detectors to identify and quantify the separated ions. The detector measures the electrical conductivity of the ions in solution after their elution from the column. This method is highly sensitive and can detect ion concentrations at the ppb (parts per billion) level. In addition to its sensitivity, IC is rapid and precise, enabling the analysis of numerous samples in a short period. This technique is commonly used to analyze degraded amines in CO_2 capture processes, allowing for the monitoring of amine concentrations and the identification of degradation products such as thermostable salts and other by-products

IC is a subcategory of liquid chromatography, widely utilized for amine analysis. These systems can analyze samples without special preparation, except for dilution. Optimized IC methods allow for the precise determination of amines (Bruckner (2006)).

II.2.2 Methods used to quantify CO_2 concentration

In this subsection, the focus is on the CO_2 loading of amines, examining how the CO_2 loading of solvents changes over time. These methods are employed to accurately measure the remaining absorbed CO_2 into the solvent, thereby characterizing the discharge of CO_2.

II.2.2.a Titration with $BaCl_2$

The objective of the $BaCl_2$ titration is to introduce known reagents that react with CO_2-loaded compounds, forming new products that can be analyzed. These new products precipitate and are collected for quantification. The quantification method employed is an acid-base titration.

The titration using $BaCl_2$ involves several steps. Firstly, the CO_2 from the sample is converted from bicarbonate and carbamate forms into carbonate, as shown in equations II.10 and II.11:

$$HCO_3^- + OH^- \rightleftharpoons CO_3^{2-} + H_2O \tag{II.10}$$

$$MEACOO^- + OH^- \rightleftharpoons CO_3^{2-} + MEA \tag{II.11}$$

Next, the addition of a certain amount of $BaCl_2$ leads to the precipitation of carbonate as barium carbonate, depicted in equation II.12:

$$BaCl_2 + CO_3^{2-} \rightleftharpoons BaCO_3 + 2\,Cl^- \tag{II.12}$$

The precipitated barium carbonate is then recovered via vacuum filtration. Subsequently, a known excess of HCl is added to the filtrate to dissolve it, as represented by equation II.13:

$$BaCO_3 + 2\,H^+ \rightleftharpoons Ba^{2+} + CO_2 + H_2O \tag{II.13}$$

Finally, a back-titration is performed to determine the excess acid used. This involves using NaOH as a titrant and a pH meter, with the equivalence point occurring at a pH near 5.2 (Dubois (2023); Hoff (2003)).

For improved accuracy and reduced manipulation errors, replacing the pH meter with an automatic titrator is a more optimal solution. Comprehensive formulas and data are available, and detailed methodology is provided in Section IV1..

II.2.2.b Titration with Chittick Apparatus

This titration method enables the calculation of both CO_2 loading and amine concentration. The apparatus depicted in Figure II.16 operates on the principle of measuring the release of CO_2 through liquid displacement. The sample is contained within a hermetically sealed flask placed on a magnetic stirrer and is connected to a graduated burette or pipette containing hydrogen chloride (HCl). Additionally, a second connection is established with the flask using a measuring burette, a leveling bulb, and a leveling stopcock (Cerato (2023); Dubois (2023); Zhang et al. (2017); Horwitz (1970)).

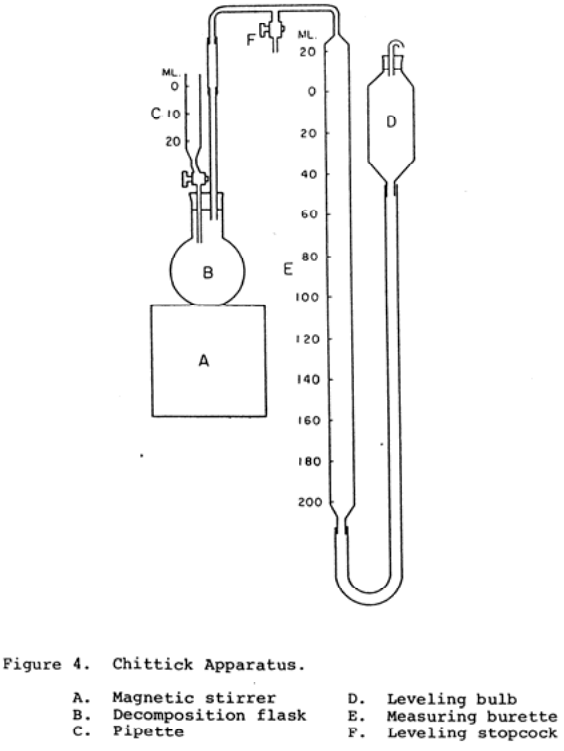

Figure 4. Chittick Apparatus.

A. Magnetic stirrer
B. Decomposition flask
C. Pipette
D. Leveling bulb
E. Measuring burette
F. Leveling stopcock

Figure II.16: Chittick Apparatus (Cerato (2023))

The liquid reservoir contains a mixture of NaCl, $NaHCO_3$ and methyl orange. This solution avoids the absorption of CO_2 in the liquid, but enables the displacement inside the burette to show the release of CO_2. All details related to the preparation of the liquid reservoir are located in the Appendix A.

Finally, the manipulation consists of doing a titration with HCl as a titrate and methyl orange as

an indicator. After adding a certain amount of HCl, the solution becomes pink which corresponds to the equivalent point and some CO_2 is released to the burette. Adding a excess amount of HCl allows to release all of the absorbed CO_2. The released CO_2 has pushed the reservoir fluid.

As a result, the reservoir fluid displacement allows to calculate the CO_2 volume in the sample and so the concentration in the sample. The added volume of HCl for the equivalent point allows to calculate the concentration of amine in the sample. Here are the equations used to calculate the CO_2 loading:

$$V_{CO_2} = V_{total} - V_{HCl,titration} - V_{HCl,excess} \tag{II.14}$$

where
V_{CO_2} is the volume of CO_2 ;
V_{total} is the total volume of displacement of the liquid reservoir ;
$V_{HCl,titration}$ is the volume of HCl added until the color change of the indicator ;
$V_{HCl,excess}$ is the excess HCl used after the color change of the indicator.

For accurate calculations, it is crucial to control the pressure and temperature of the environment, ensuring precise determination of CO_2 quantity from its volume.

For the experimentation chapter, several articles provide numerical values related to the preparation of consumables, including the concentration and volume of samples and titrants required to replicate the protocols. Additionally, formulas for calculating amine and CO_2 concentrations are available. However, due to the unavailability of the Chittick Apparatus for the tests, only the amine concentration data could be collected.

II.2.2.c Density correlation

The relationship between the density of a carbonated amine solution and its CO_2 loading is a fundamental aspect in understanding the behaviour of these solutions in CO_2 capture processes. The density of an amine solution increases with the CO_2 loading due to the additional mass of CO_2 being dissolved and the subsequent formation of carbamates and bicarbonates, which occupy space within the solution, thereby increasing its overall density.

As CO_2 is absorbed by the amine solution, it reacts with the amine to form carbamate (in the case of primary and secondary amines) or bicarbonate (in the case of tertiary amines). This reaction increases the mass of the solution without significantly increasing the volume, resulting in a higher density. The density of the solution, therefore, is a direct indicator of the amount of CO_2 absorbed, which is crucial for determining the efficiency of CO_2 capture in industrial applications.

Furthermore, the temperature of the solution also affects the density. As temperature increases, the density of the solution typically decreases due to the thermal expansion of the liquid and increased molecular motion, which reduces the solution's density (Spietz et al. (2018)).

The density of the solution can be predicted knowing some parameters as followed:

$$\rho_S = AT + B\alpha + D_0 \tag{II.15}$$

where A, B, and D_0 designate model parameters, ρ_S is the density of carbonated solution (g/cm^3), t

is the temperature of the solution (in [°C]) and α is the CO_2 loading (mole CO_2 per mole of amine) (Spietz et al. (2018)).
As a result, the CO_2 loading can be calculated for different densities.
In the reference, some tables containing measured data are available (an example is in Figure II.17). It contains the values of densities at different temperatures and CO_2 loading.

CO_2 loading, mol CO_2/mol amine	Density (g/cm^3) at temperature:					
	20°C	25°C	30°C	40°C	50°C	60°C
0.00	1.01248	1.01036	1.00836	1.00342	0.99802	0.99222
0.10	1.03210	1.02993	1.02767	1.02285	1.01757	1.01189
0.20	1.05149	1.04933	1.04708	1.04234	1.03713	1.03155
0.30	1.07210	1.06986	1.06769	1.06253	1.05717	1.05161
0.40	1.09288	1.09052	1.08808	1.08285	1.07749	1.07179
0.51	1.11255	1.11023	1.10787	1.10278	1.09758	1.09197

Figure II.17: Densities of carbonated aqueous solutions of 30 wt.-% monoethanolamine (Spietz et al. (2018))

II.2.2.d Other methods

This subsection contains 3 other analytical methods used to determine CO_2 loading with lacks of information but may be used in a comparison objective.

A first analytical method is an KOH titration. The only available information from Saleh et al. (2021) is the reference method : Reference method DOW43000055, the manipulation steps : add 100 mL of methanol into the solution then titrate the solution with KOH and the CO_2 loading calculation :

$$(\frac{V_1}{W_1} - \frac{V_2}{W_2}) \cdot N \cdot 4.4 = \%\ CO_2\ in\ amine \tag{II.16}$$

Where:
V_1 = mL of KOH to titrate sample, up to 0.05 mL;
V_2 = mL of KOH to titrate fresh solution, up to 0.05 mL;
W_1 = g of sample titrated, up to 0.0001g;
W_2 = g of lean solution titrated, up to 0.0001g;
N = normality of KOH (0.5 N suggested), up to 0.0001N.

The second method is a MeONa titration. According to Masohan et al. (2009), this method refers to the UOP method 829-82 which determines of CO_2 in ethanolamine and consists of dissolving the sample using anhydrous methanol, then applying a titration with methanolic sodium hydroxide (MeONa) as a titrate and thymolphthalein as the indicator.

A final potential analytical method is the pH correlation. In the study from Nakagaki et al. (2014), the correlation between pH and CO_2 loading in aqueous monoethanolamine (MEA) solutions was evaluated, particularly under conditions of oxidative degradation. Oxidative degradation in MEA solutions produces carboxylic acids, which negatively impact the CO_2 absorption characteristics. The study shows a decrease of the pH with the increase of the CO_2 loading. However, the production of carboxylic acids due to the degradation of amine led to a lower pH in the degraded MEA solution compared to the normal MEA solution at the same CO2 loading. As a result, the pH correlation is not valid when the amine is degraded.

Chapter III

Development of analytical methods used to quantify the amine concentration

III1. Titration using HCl

The titration of hydrochloric acid (HCl) was employed as a method for determining the concentration of amines in experiments, owing to the accessibility of this technique. Firstly, a detailed protocol, including all necessary materials, chemicals, and procedural steps, as well as the calculations required to determine the amine concentration, is provided in the following section. Subsequently, information concerning potential sources of precision error is discussed after the data calculation.

III.1.1 Materials and chemicals

Materials:

- Beakers (200 mL suggested) ;
- Clamp stand ;
- Burette (25 mL or 10 mL) ;
- Graduated pipette (1 or 2 mL) ;
- Wash bottle ;
- Magnetic stirrer.

Chemicals:

- Methyl orange (0.04 % in aqueous solution, supplied by VMR Chemicals) ;
- Distilled water ;
- HCl (1M, supplied by EMD Millipore Corporation).

III.1.2 Manipulations

1. Take 2 mL[1] of a sample (V_{Amine}) using a graduated pipette and pour it into the beaker ;
2. Add a few drops of methyl orange;
3. Add distilled water in the beaker until the solution becomes pale yellow or colourless and the magnetic stir bar is immersed ;
4. Fill the burette with 1 M HCl (C_{HCl});
5. Begin titration until the solution changes colour titration until the solution changes colour (turns into pink if the starting solution is colourless or orange if the starting solution is pale yellow[2]) ;
6. Record the volume ($V_{HCl,titration}$) from the burette.

All of these steps take approximately 5-10 minutes for a single sample, excluding cleaning steps.

III.1.3 Data calculation

The titration of hydrochloric acid (HCl) is an acid-base reaction involving an acid (HCl) and a basic amine solvent. The fundamental equation governing acid-base titrations, which links the concentrations and volumes of both reactants, is given by $C_A V_A = C_B V_B$. This equation can be rearranged and generalized to apply to all amines. Consequently, the concentration of the amine can be determined using the following expression:

$$C_{amine} = \frac{C_{HCl} \cdot V_{HCl,titration}}{X \cdot V_{amine}} \tag{III.1}$$

Here, X represents the number of basic groups in the amine (e.g., 1 for MEA and MDEA; 2 for PZ).

III.1.4 Potential precision error sources

During the manipulation, certain steps may decrease the precision of the method:

- Sample collection: the utilisation of a graduated pipette may lose the precision of the sample volume taken due to the viscosity of some samples (highly concentrated and/or degraded amine solvents increase their viscosity) which results in some drops staying in the pipette or drops out of the burette which can lead to an excess of drops. For comparison, the pure MEA and MDEA viscosity at ambient temperature are respectively 24 mPa·s and 104 Pa·s as compared to 1 Pa·s for the water viscosity (Arachchige et al. (2013)).
- Less noticeable colour change: highly degraded amine samples have dark red or black colours which requires to addition of distilled water to have a solution colour close to the yellow but that can lead to a less noticeable colour change from yellow to orange.
- Precision of burette: the burette has a certain precision depending on the size of the drops. The tolerance of the burette is +/- 0.025 mL with a graduation of 0.05 mL for a 10 mL burette.

[1] This volume value can be changed to increase precision.
[2] Examples of typical colour solutions are available in Appendix B

III2. High Performance Liquid chromatography

III.2.1 List of devices

High-Performance Liquid Chromatography (HPLC) is composed of different devices and the combination with a Refraction index detector (RID) allows quantifying amine solvents. The various components of the sample are eluted at different retention times, depending on their affinity with the column stationary phase and the mobile phase (eluent). Then, each component is detected and quantified. The main elements of the HPLC analytical unit are listed in Table III.1.

Device	**Specification(s)**	**Type**
HPLC pump	Flow rate: 1.0 mL/min	Waters 515
Automatic injector	Injection volume: 5 μ L Injection time: 20 min	Waters 717+
Column thermostat	Temperature: 30 °C	Merck T-6300
Refractive index detector (RID)	Sensitivity: 16 Scale Factor: 11 Temperature: 30 °C	Waters 410
UV-visible detector	Detection wavelength: 210 nm	Merck Hitachi L-4200
Data acquisition unit	n.a.	PowerChrom 280, version 2.5.13
HPLC column	Hydrophilic Interaction Liquid Chromatography (HILIC)	Phenomenex HILIC HPLC

Table III.1: Specifications of different components of HPLC unit

Each part of the HPLC unit is described below.

HPLC pump: This component allows to injection of eluent in the column at a constant flow rate (set at 1 mL/minute) and at a high pressure (between 88 bars and 100 bars). The HPLC pump can be seen in Figure III.1 on the left of the erlenmeyer which contains eluent.

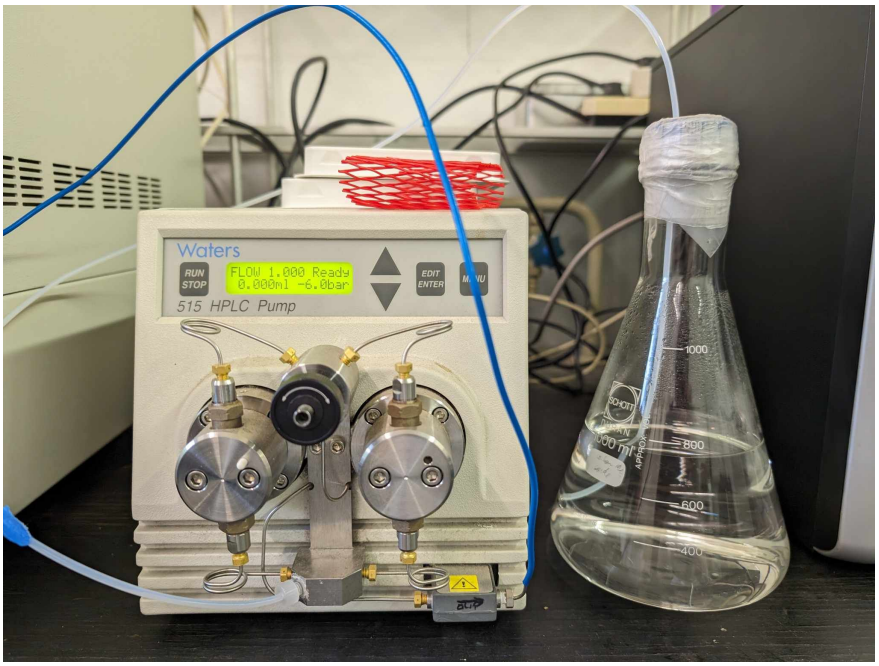

Figure III.1: HPLC pump

Automatic injector unit: This component allows to inject samples in the column. As can be seen in Figure III.2, the injector unit contains a carousel that contains samples. Figure III.3 shows the carousel with samples in flasks.

Figure III.2: Automatic injector unit

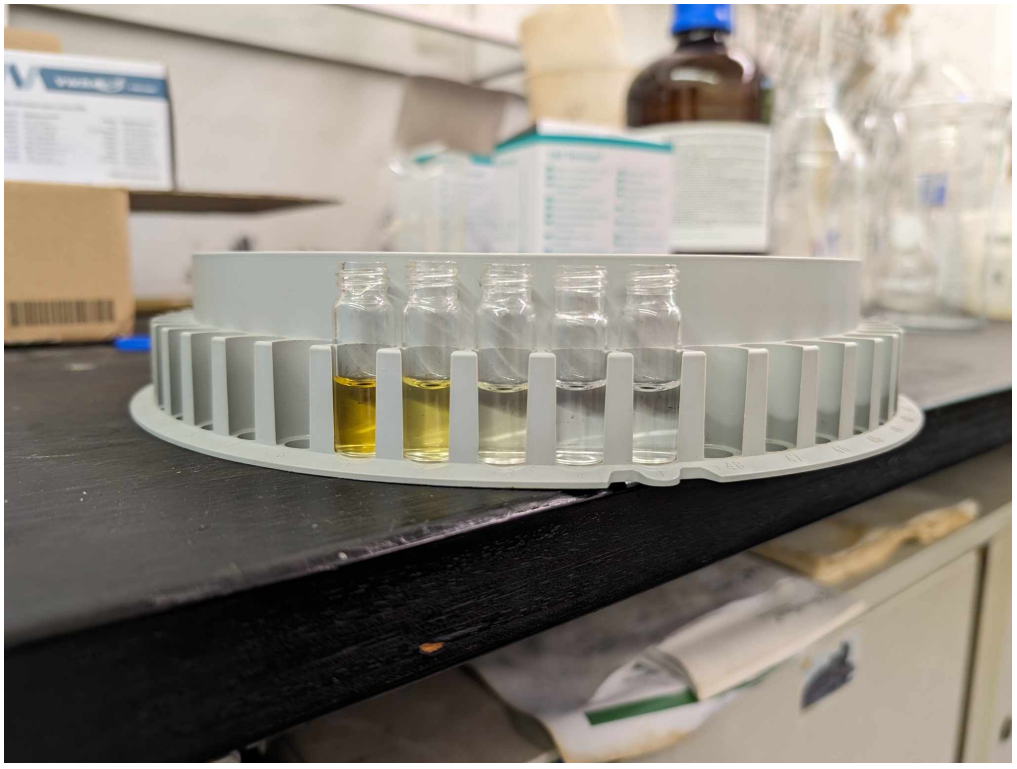

Figure III.3: Carousel

Column thermostat: This component allows us to fix the temperature of the column. The temperature is usually fixed at 30 °C ensuring the operational efficiency and accuracy of the column throughout the chromatographic process.

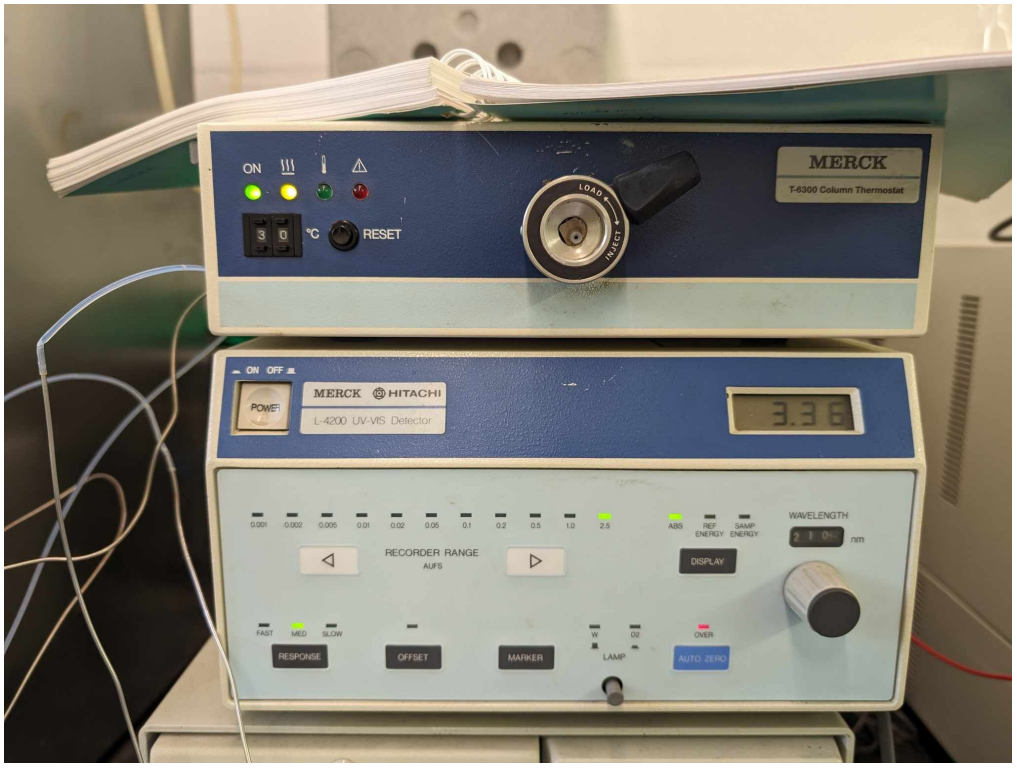

Figure III.4: Column thermostat

Refractive index detector (RID): This component allows to detection of constituents of the sample in the mobile phase and so to quantify the studied amine.

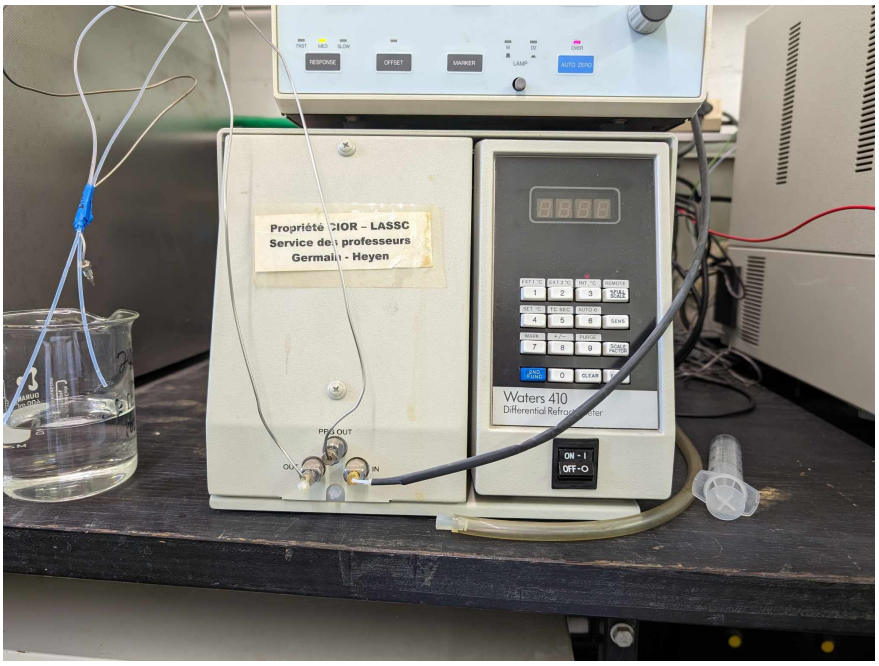

Figure III.5: Refractive index detector (RID)

HPLC column: The column housing the stationary phase comprising a packing material, serves as the conduit through which the mobile phase, containing the sample, is introduced. This interaction culminates in the creation of a chromatogram, where analytes are separated based on their distinct retention times (Ghosh (2023*b*)).

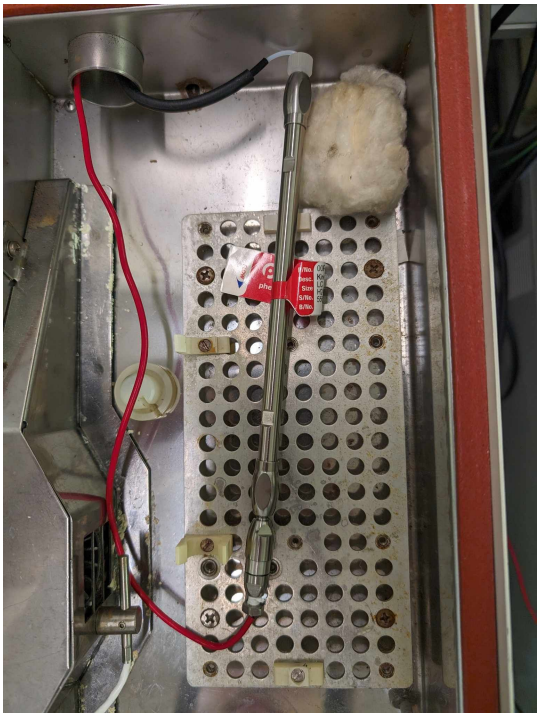

Figure III.6: HPLC column

The column used for HPLC analysis is the HILIC HPLC column produced by Phenomenex. Hydrophilic Interaction Liquid Chromatography (HILIC) is particularly advantageous for the separation of polar organic compounds, which often cannot be effectively retained using conventional reversed-phase methods. In reversed-phase chromatography, polar compounds frequently co-elute with the solvent front or elute in regions with significant ion suppression, complicating their analysis. HILIC HPLC/UHPLC columns address this issue by drawing and retaining a water-enriched layer on the surface of the silica stationary phase. This water layer facilitates enhanced interaction between polar compounds and the stationary phase, thereby increasing their retention and improving separation efficiency.

III.2.2 Eluent preparation

This operating procedure refers to a previous work done at the University of Liège by Proneet Ghosh (Ghosh (2023*b*)) and it was based on the PhD thesis of Grégoire Léonard (Léonard (2013)).

III.2.2.a Materials and chemicals

Materials:

- Beaker (200 mL suggested) ;
- 100 mL cylinder ;
- Magnetic stirrer ;
- pH meter ;
- Vacuum filtration kit: void pump, clamp, vacuum flask, diaphragm, Büchner funnel, filter ;
- 0.45 μm nylon or PTFE filters ;
- Vacuum pump ;
- Erlenmeyer with pipe connection (1 L) ;
- Ultrasonic bath ;
- Bottle.

Chemicals:

- Ammonium formate (NH_4HCO_2) (supplied by VWR) ;
- Milli-Q water[3] ;
- Concentrated formic acid (supplied by EMD Millipore Corporation) ;
- HPLC-grade acetonitrile (supplied by EMD Millipore Corporation).

[3]Due to the unavailability of this chemical, it was replaced by distilled water. Milli-Q water through filtration is unnecessary

III.2.2.b Manipulations

1. Weigh 0.3153g of ammonium formate in a clean, dry 200ml beaker ;
2. Measured 100ml of Milli-Q water in a dry cylinder.
3. Add the measured water to the beaker to dissolve the ammonium formate ;
4. Stir the mixture using a magnetic stirrer for at least 5 minutes until complete dissolution ;
5. While stirring, 500 μL of concentrated formic acid is added using a 200 μL pipette to attain a pH of 3.2, monitored with a pre-calibrated pH meter[4] ;
6. Once the desired pH is reached, then 900ml of HPLC-grade acetonitrile is added ;
7. Filter the solution through a dry Büchner filter with 0.45 μm nylon or PTFE filters and a vacuum pump ;
8. Transfer the filtered solution to a 1 L Erlenmeyer flask with a vacuum pump connection ;
9. De-gas the solution under vacuum for $\geq$5 minutes using an ultrasonic bath ;
10. Pour the degassed solution into a labeled, sterile bottle with accurate records of solution details, concentration, pH, date, and operator initials.

III.2.3 Samples preparation

For MEA samples, a dilution of 1:10 with distilled water is required before launching HPLC analysis in order to avoid the overloading of the column due to the high concentration of amine. For MDEA samples, dilution of 1:8 with distilled water is required before adding it into the engine.

III.2.4 Utilisation of the devices

These are the steps to do during an HPLC.

1. Turn on the following devices: HPLC pump, automatic injector unit, column thermostat, refractive index detector (RID), computer ;
2. Put all the flasks containing the diluted samples in the carousel and put the carousel in the automatic injector unit and close the trapdoor ;
3. Verify that the value of flowrate is 1 mL/min and 88 bars, then press "RUN STOP" in the HPLC pump. Wait until the pressure reaches at 88 bars and remains constant ;
4. To zero the refractive index detector, press the "2ND FUNC" button followed by pressing the number 6 button ;
5. Launch PowerChrom on the computer, choose a method on the "easy access" window, then click "inject" ;

[4]For MDEA samples, it is suggested to add more formic acid to obtain a pH of 2.7 instead of 3.2 (Chiarella (2018 - 2019))

6. Press "AUTO PAGE" on the automatic injector to choose which samples will be analysed, choose the number of samples to inject and press "START AUTO" to start the analysis;

7. At the end of the run, press "RUN STOP" in the HPLC pump, and save the file on the computer.

During the analysis, the Refractive Index Detector (RID) regularly sends signals to the computer, which are then processed by PowerChrom. These signals are measured in volts. Consequently, the software generates a graph of signal intensity over time. The higher the signal intensity, the more concentrated the sample is in a particular species. The concentrated species in the sample pass through the column in a very short duration, typically a few tens of seconds, resulting in an intensity peak in the program. The area under this peak is proportional to the quantity of the species passing through the column. The analysis of a single sample takes 20 minutes, and the analysis of multiple samples can be performed sequentially.

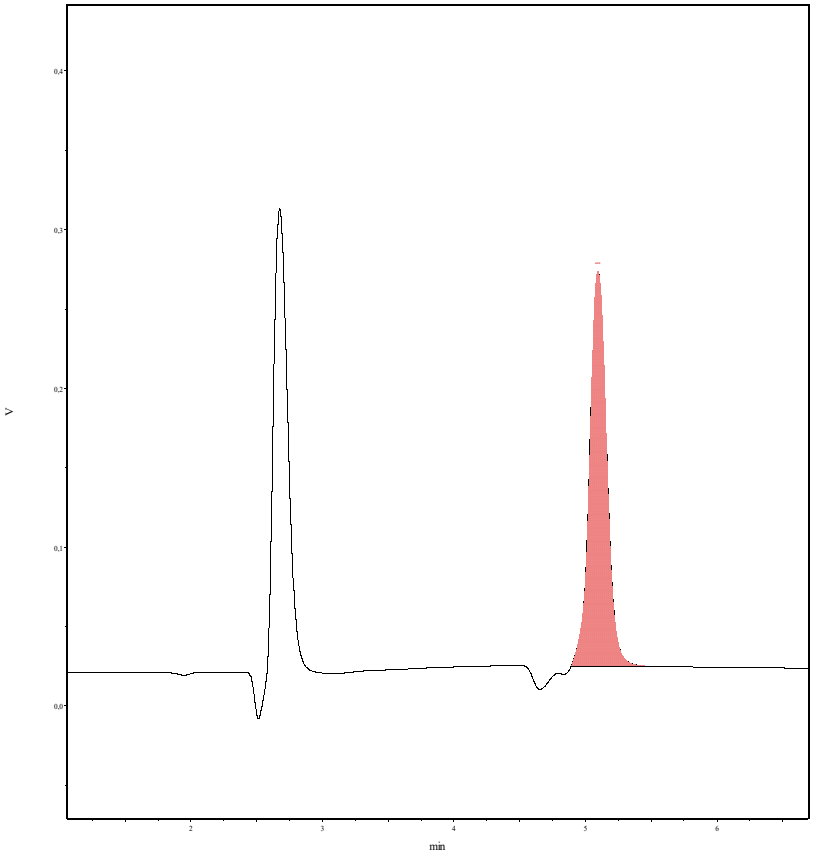

Figure III.7: MEA 30 % peak first calibration curve

For the area calculation, the software PowerChrom allows one to edit manually to measure the area under the intensity peak. Then, it is possible to collect all the area values by going to "Windows" and then "Peak Report".

III.2.5 Potential precision error sources

During the manipulation, some steps can reduce the precision of the method:

- Dilution step: this step may cause imprecision depending on how it is executed (utilisation of graduated pipette for example) which increases/decreases the ratio between samples and distilled water. By altering the water-to-sample ratio, the resulting concentration also changes, thereby skewing the results obtained during HPLC analysis. A potential solution to this issue would be to find an alternative to the graduated pipette, such as an analytical balance, to ensure the dilution has been performed correctly.
- flasks cleaning step: flasks can be not totally dried or clean which can dilute the sample or interact with it. To clean a flask, it is suggested to clean it with diluted HCl and dry it. However, a few drops may remain in the container, which can not only add to the volume and thus alter the concentration of the diluted sample but also react with the sample and produce other species. A solution to this problem is to first condition the flask with the diluted sample.
- Calibration age: depending on the age of the calibration, the calibration can be invalid due to a peak shape change which can be the case after an eluent change. To avoid this issue, it is recommended to perform calibration concurrently with the sample analysis.

Chapter IV

Development of analytical methods used to quantify the CO_2 loading

IV1. Titration using $BaCl_2$

The titration of barium chloride ($BaCl_2$) was employed as a method for determining the CO_2 loading in experiments, owing to the accessibility of this technique. Firstly, a detailed protocol, including all necessary materials, chemicals, and procedural steps, as well as the calculations required to determine the amine concentration, is provided in the following section. Subsequently, information concerning potential sources of precision error is discussed after the data calculation.

IV.1.1 Materials and chemicals

Materials:

- Beaker(s) (400 mL suggested) ;
- Burette (50 mL or less) ;
- Graduated pipette (0.5 mL) ;
- Pipette (25 mL suggested) ;
- Vacuum filtration kit: void pump, clamp, vacuum flask, diaphragm, Büchner funnel, filter ;
- pH meter ;
- pH paper ;
- Magnetic stirrer with hot plate ;

Chemicals:

- Amine sample
- NaOH (0.1 M, supplied by EMD Millipore Corporation) ;
- HCl (0.1 M, supplied by EMD Millipore Corporation) ;
- $BaCl_2$ (0.5 M, supplied by Analytichem) ;
- Distilled water

IV.1.2 Manipulations

1. Using an appropriate pipette, transfer 0.5 mL of the sample (V_S) into the beaker ;
2. Add 50 mL of 0.1 M NaOH followed by 25 mL of 0.5 M BaCl2;
3. Heat until boiling and bubbles production (reaching a temperature of approximately 300 °C). A white precipitate should form due to the different reactions between amine, NaOH and $BaCl_2$ occurring at high temperature ;
4. Pour the solution onto the filter used during vacuum filtration while activating the pump. The filter should retain the solid solution;
5. Rinse with distilled water (between 50 and 100 mL), checking that the permeate has a neutral pH using pH paper;
6. Remove the filter and place its contents into a beaker;
7. Dissolve the precipitate with excess HCl with a known volume V_{HCl} (10 mL for uncharged samples, 40 mL for charged samples or 30 mL for degraded samples) ;
8. Set up the equipment for the titration (add the pH meter, burette containing 0.1 M NaOH (C_{NaOH}), stirrer);
9. Pour the NaOH while monitoring the pH until a pH jump occurs (around 5.2). Identify the equivalence point and therefore the volume of NaOH added V_t;
10. Repeat all the steps with a sample that was not CO_2-charged (blind sample titration). Note the volumes of acid and base used to reach the equivalence point (V_{acid} and V_{base}).

All of these steps take approximately 30-40 minutes for a single sample, excluding cleaning steps.

IV.1.3 Data calculation

To find the CO_2 concentration, the next formula can be used:

$$C_{CO2} = \frac{V_{HCl} - V_t - \Delta V_b}{2 \times V_S} C_{HCl} \tag{IV.1}$$

where V_{HCl} is the total volume of HCl added to dissolve the precipitate ; V_t is the volume of NaOH added to reach the equivalence point during titration ; ΔV_b is the difference in volume between the total volume of HCl and NaOH used during the blind sample titration ; V_s is the volume of the sample.

To understand Equation IV.1, the reaction equation has similarities : $C_1V_1 = X \cdot C_2V_2$ with X depending of the stoichiometry of the reaction. The absorbed CO_2 has a form of carbamate and bicarbonate and has several reactions according to Section II.2.2.a with 1:1 stoichiometry except for reaction between precipitate and HCl with a stoichiometry of 1:2. As a result, the reaction between precipitate and HCl has the follow equation : $C_{CO2} = \frac{V_{HCl}}{2 \cdot V_S} \cdot C_{HCl}$. However, there is an excess of HCl added to totally dissolve the precipitate which has been verified by the back titration (V_t) and an excess of HCl that has reacted with CO_2 charge-less species and have precipitated which has been verified by a blank titration (ΔV_b). These two types of HCl excess are taken into account in Equation IV.1.

IV.1.4 Potential precision error sources

During the manipulation, some steps can reduce the precision of the method:

- Sample collection: the utilisation of a graduated pipette may lose the precision of the sample volume taken due to the viscosity of some samples (highly concentrated and/or degraded amine solvents increase their viscosity) which results in some drops staying in the pipette or drops out of the burette which can lead to an excess of drops. For comparison, the pure MEA and MDEA viscosity at ambient temperature are respectively 24 mPa·s and 104 Pa·s as compared to 1 Pa·s for the water viscosity (Arachchige et al. (2013)). The utilisation of an analytical balance instead of graduated pipette is one of the solution.
- Precipitate recuperation: after the filtration, the total recuperation of the precipitate can be more challenging when the sample is not charged. In this case, the residue is too small and stocks on the filter. To recuperate the global precipitate, an instrument such as a spoon spatula, accompanied by a rinse with distilled water, can reduce this precision error.
- Precision of burette: the burette has a certain precision depending on the size of the drops. The tolerance of the burette is +/- 0.03 mL with a graduation of 0.1 mL for a 50 mL burette.
- Amine concentration calculation: the CO_2 loading is calculated using CO_2 concentration and amine concentration. The precision depends on which analytical method is used to calculate the amine concentration.

IV2. Density correlation

This section discusses the use of density/CO_2 loading correlations developed by Spietz et al. (2018) to determine the CO_2 loading using only temperature and density. The use of sophisticated equipment is required for precise determination of density at a chosen temperature.

IV.2.1 Utilisation of the device

The device used to precisely measure the density is a Density and Sound Velocity Meter DSA 5000 M that can be seen in Figure IV.1.

Figure IV.1: Density and Sound Velocity Meter

The device is composed of many components such as the U-tube where the sample is introduced and analysed, the camera (U-View) to verify if there is no bubble in the U-tube and the thermobalance in order to stabilise the temperature. The DSA 5000 M measures density using an oscillating U-tube method, where a sample is introduced into a U-shaped glass tube that vibrates at a characteristic frequency, which changes with the sample's density. This frequency change is measured and converted mathematically to determine the sample's density.

To use this device some steps are necessary:

1. Check the method used by pressing the "Method" button and choose any density method. Then, press "OK".

2. Press the "Quick Settings" button to change the sample name and the temperature. Then, press "OK"

3. Inject the sample using a syringe in the hole on the left of the device until no bubble appears on the camera (4-6 mL is sufficient). Make sure that the syringe stays on the hole to avoid undertow.

4. Press the "Start" Button. Wait until the desired temperature is reached.

5. To clear the device, use the pump by putting its pipe in the hole and by pressing the "fan item" button. Then, inject distilled water with a syringe into the hole and reuse the pump as before. Redo this step three times.

These steps take approximately 15 minutes for a single sample and two different calculated temperatures, excluding cleaning steps.

IV.2.2 Data calculation

According to Spietz et al. (2018), the density is linearly proportional to the CO_2 loading due to the fact that loading CO_2 increases the solvent weight with a smaller increase of the volume which increases the density. As a result, by doing a linear regression on experimental data, a first order equation can be found. Only 30 wt.-% MEA samples with a loaded status are analyzed. The experimental data from Spietz et al. (2018) are shown in Figure IV.2

CO_2 loading, mol CO_2/mol amine	Density (g/cm^3) at temperature:					
	20°C	25°C	30°C	40°C	50°C	60°C
0.00	1.01248	1.01036	1.00836	1.00342	0.99802	0.99222
0.10	1.03210	1.02993	1.02767	1.02285	1.01757	1.01189
0.20	1.05149	1.04933	1.04708	1.04234	1.03713	1.03155
0.30	1.07210	1.06986	1.06769	1.06253	1.05717	1.05161
0.40	1.09288	1.09052	1.08808	1.08285	1.07749	1.07179
0.51	1.11255	1.11023	1.10787	1.10278	1.09758	1.09197

Figure IV.2: Densities of carbonated aqueous solutions of 30 wt.-% monoethanolamine (Spietz et al. (2018))

Finally, the loading equations for temperatures of 20°C and 25°C are expressed respectively in equations IV.2 and IV.3. The loading unit is expressed in mol of CO_2 per mol of amine and the density in g/cm^3.

$$CO_2\ loading\ (T = 20\ °C) = 5.04698 \cdot \rho_{sample} - 5.10957 \tag{IV.2}$$

$$CO_2\ loading\ (T = 25\ °C) = 5.05898 \cdot \rho_{sample} - 5.11104 \tag{IV.3}$$

IV.2.3 Potential precision error sources

This method presents several sources of precision error:

- Correlation determination: the experimental data in Figure IV.2 are derived from experiments conducted by Spietz et al. (2018), which mention an uncertainty in the determination of CO_2 loading.
- Non-linearity at high CO_2 loading: at elevated CO_2 loading, there is a greater formation of bicarbonate ions, which are significantly smaller than carbamate ions. Consequently, bicarbonate ions form a more compact hydration shell, resulting in a non-linear change in density with increasing CO_2 loading (Spietz et al. (2018)).
- Degradation influence on density: the correlation equations pertain to non-degraded samples and do not account for the influence of degradation, where degraded species may have different densities compared to amine molecules.

Chapter V

Results

V1. Determination of amine concentration

In this section, all results concerning the determination of the concentration of MEA, MDEA, and PZ in different samples (with and without degradation compounds) using HPLC and HCl titration are detailed.

V.1.1 Aqueous MEA samples

This section concerns the accuracy and the precision of the utilisation of the HCl titration method on aqueous MEA samples as well as the utilisation of these samples for an HPLC analysis as a calibration step.

The analysed samples have a known concentration respectively as followed: 10 wt.-% MEA ; 20 wt.-% MEA ; 30 wt.-% MEA ; 40 wt.-% MEA.

V.1.1.a HCl titration

For each type of sample, 3 HCl titrations have been made with a sample volume varying between 1 and 4 mL depending on the MEA concentration (the lower the concentration, the higher the suggested volume sample). Table V.1, V.2, V.3 and V.4 show results of titrations on each MEA sample. The relative error is calculated as followed :

$$\text{Relative error (\%)} = \frac{\text{Measured HCL volume (mL)} - \text{Predicted required volume (mL)}}{\text{Predicted required volume (mL)}} \cdot 100$$

Volume Sample (mL)	**Predicted required HCl volume (mL)**	**Measured HCl volume (mL)**	**Measured MEA concentration (wt.-%)**	**Relative error (%)**
2	3.28	3.30	10.08	0.75
3	4.91	4.85	9.87	-1.29
4	6.55	6.60	10.08	0.75

Table V.1: HCl titration results for 10 wt.-% MEA

Volume Sample (mL)	Predicted required HCl volume (mL)	Measured HCl volume (mL)	Measured MEA concentration (wt.-%)	Relative error (%)
2	6.54	6.60	20.19	0.93
3	9.81	9.90	20.19	0.93
4	13.08	13.40	20.49	2.46

Table V.2: HCl titration results for 20 wt.-% MEA

Volume Sample (mL)	Predicted required HCl volume (mL)	Measured HCl volume (mL)	Measured MEA concentration (wt.-%)	Relative error (%)
2	9.79	9.80	30.02	0.07
2	9.79	9.80	30.02	0.07
1	4.90	4.95	30.33	1.10

Table V.3: HCl titration results for 30 wt.-% MEA

Volume Sample (mL)	Predicted required HCl volume (mL)	Measured HCl volume (mL)	Measured MEA concentration (wt.-%)	Relative error (%)
2	13.04	13.50	41.44	3.59
1	6.52	6.80	41.75	4.37
2	13.04	13.50	41.44	3.59

Table V.4: HCl titration results for 40 wt.-% MEA

According to the results, the relative error between predicted and measured data is close to 1 % except for 40 wt.-% MEA samples where the relative error is at least 3.5 %. The relative error is mainly caused by the precision of the burette (± 0.03 mL of error) which depends on the size of the drop. Due to the high difference in the 40 wt.-%, it should be noted that it also may be due to an error during the preparation of the sample, as all the previous samples had relative error lower than 1%.

V.1.1.b High Performance Liquid Chromatography

During the HPLC, 3 valid calibration curves have been made and can be seen in Figure V.1, V.2 and V.3. This high number of calibration curves is the causality of eluent changes and column performance changes. The first one has been made for the first and second experiments on the degradation of MEA. The second one is used for the third experiment as well as for repeatability validation. The third calibration curve is used for the two last experiments. Finally, a previous calibration was made for the 3 last experiments V.4. However, this calibration was not made at the same time as the sample analysis.

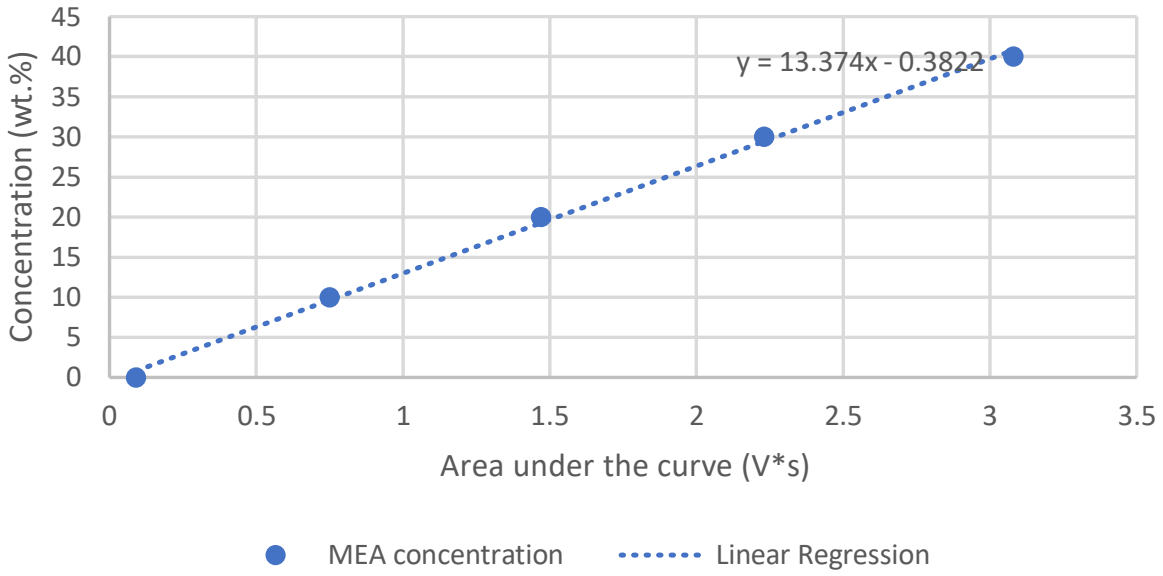

Figure V.1: Calibration curve for experiments 1 and 2

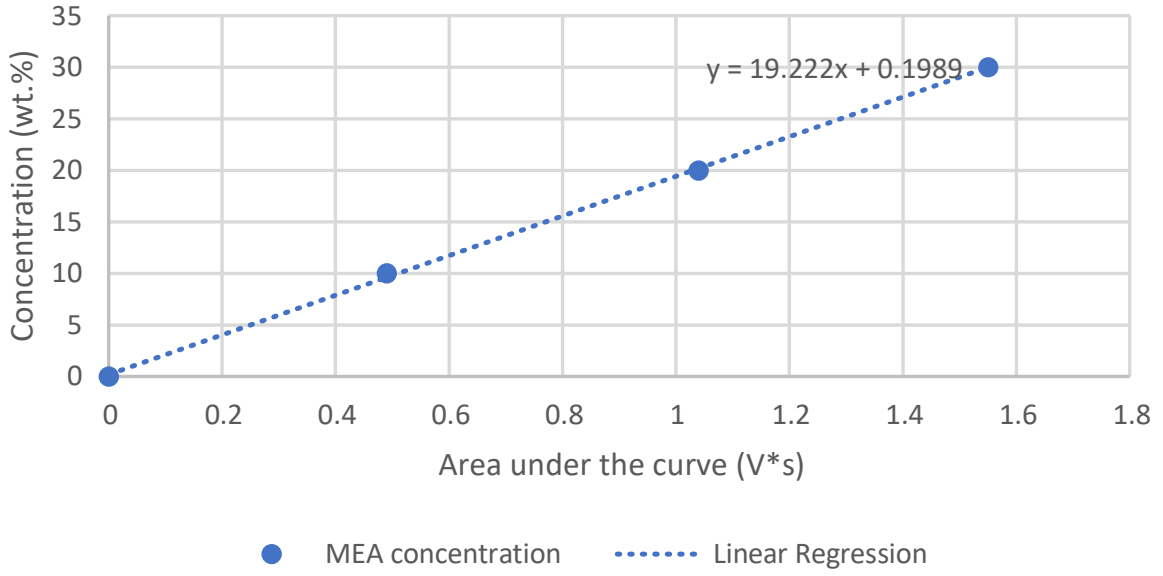

Figure V.2: Calibration curve for experiment 3

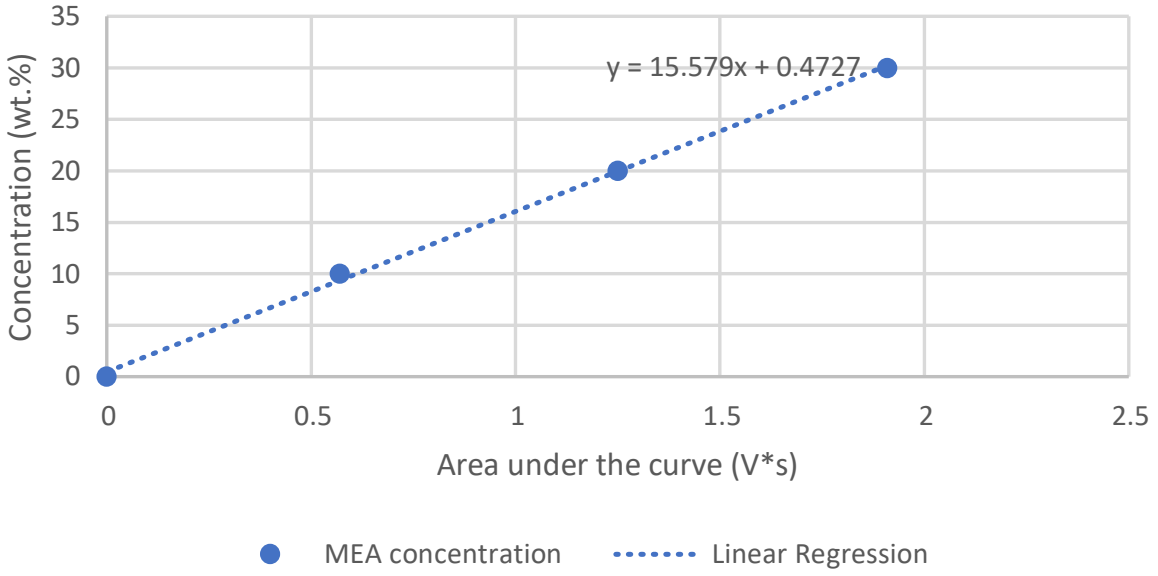

Figure V.3: Calibration curve for experiments 4 and 5

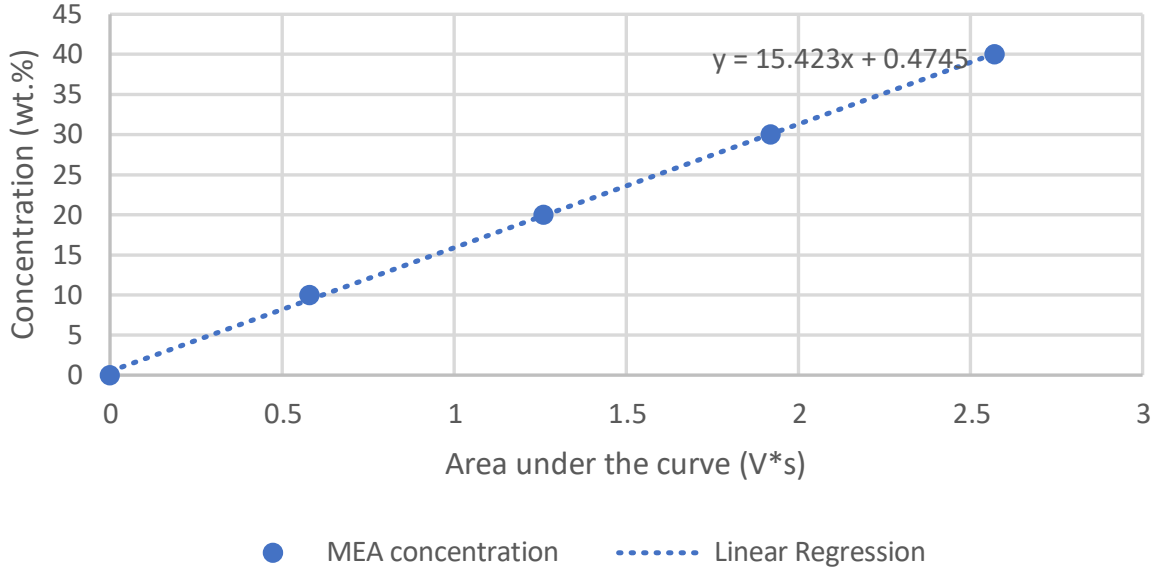

Figure V.4: Old calibration curve for experiments 3, 4 and 5

The 3 calibration curves show that intensity peaks can have different shapes depending on the past of the column. A significant difference between peaks can be observed between the first and second calibration curves where the peaks from the first calibration are narrower, come sooner and have a higher max intensity as compared to peaks from the other calibrations. Examples of intensity peaks are located in Appendix C. According to the different areas under the peaks, the equations correlating the area under the curve with concentration differ significantly for certain calibrations. These discrepancies arise from the altered behavior of the column following the change of eluent. Consequently, it is recommended to perform a calibration immediately prior to sample analysis.

V.1.2 Degraded MEA samples

Firstly, an HPLC analysis is conducted on several highly degraded samples to verify the repeatability of the HPLC method and to determine the potential variation in the results. Subsequently, a comprehensive analysis of samples from the various experiments is performed. The application of HPLC and HCl titration analytical methods is as follows: for each day of the experiment, a sample is taken and analyzed using both HPLC and HCl titration to determine its concentration. This approach allows for monitoring the evolution of MEA concentration and its degradation over the course of the experiment, thus enabling a comparison of the two analytical methods.

For each MEA experiment, a detailed protocol for each experiment is documented in Appendix F. All tables compile values of MEA concentration calculated using both methods. The differences in their values and their relative differences are calculated as follows:

$$\text{wt.-\% difference (wt.-\%)} = \text{Concentration HCl (wt.-\%)} - \text{Concentration HPLC (wt.-\%)}$$

$$\text{Relative difference (\%)} = \frac{\text{Concentration HCl (wt.-\%) - Concentration HPLC (wt.-\%)}}{\text{Concentration HPLC (wt.-\%)}} \cdot 100$$

V.1.2.a Repeatability in HPLC for MEA samples

In this part, final degraded samples from previous experiments have been analysed in HPLC multiple times to check the repeatability of the method. These samples come from the end of experiments 3 and 4. To verify if the calibration curve used[1] is still valid, a 30 wt.-% MEA sample is analysed at the same time. A minor correction was applied to the equation relating the area under the curve to concentration.

Experiment number	**Area under the curve (V· s)**	**Concentration (wt.-%)**	**Mean area (V· s)**	**Highest area gap (V· s)**	**Highest concentration gap (wt.-%)**
3	1.33	25.77	1.33	0.07	1.35
3	1.37	26.53			
3	1.30	25.19			
4	1.34	25.96	1.29	0.10	1.92
4	1.29	25.00			
4	1.24	24.03			

Table V.5: Repeatability on MEA degraded samples in HPLC

According to Table V.5, the new calculated weight percentage concentrations can fluctuate of 1.3 or 2 wt.-% which may be caused by the influence of the precision errors during the dilution step.

[1] Second calibration was used. The calibration was made one day before this analysis

V.1.2.b MEA concentration from experiment 1

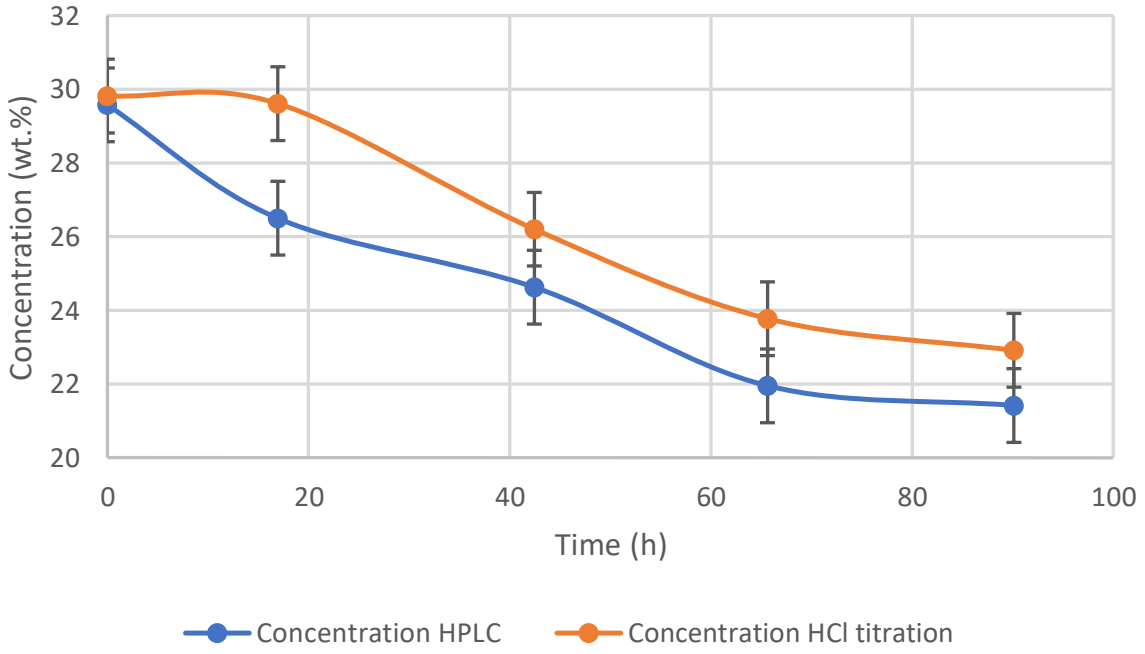

Figure V.5: MEA concentration through experiment 1

Time (h)	Concentration HPLC (wt.-%)	Concentration HCl titration (wt.-%)	wt.-% difference (%)	Relative difference (%)
0	29.58	29.82	0.24	0.82
17	26.50	29.61	3.11	11.74
43	24.63	26.20	1.57	6.39
66	21.95	23.77	1.82	8.30
90	21.42	22.91	1.49	6.98

Table V.6: MEA concentration through experiment 1

Figure V.5 and Table V.6 show similar curvature tendency between HPLC and HCl titration results. The differences between data from both analytical methods are non-negligible due to the significant variations in concentration values, with differences ranging from 0.24 % to 3.11 % MEA wt.

The highest differences between both methods come from the second sample concentration values with a 3.11 wt.-% difference. This significant difference may result from precision errors during one of the analytical methods used, or from the early degradation processes that can occur even within the first 17 hours of the experiment, as indicated by the HPLC results. It is important to note that after almost 17 hours of experimentation, degradation is indeed significant, as shown by the HPLC data.

For other samples, the weight percentage differences between both methods range from 1.49 % to 1.82 % wt.-%, which are still noticeable and indicate that variations exist, but these are relatively lower compared to the second sample. This suggests that while the methods are somewhat consistent, there are still inherent discrepancies likely due to analytical precision and degradation effects over time.

V.1.2.c MEA concentration from experiment 2

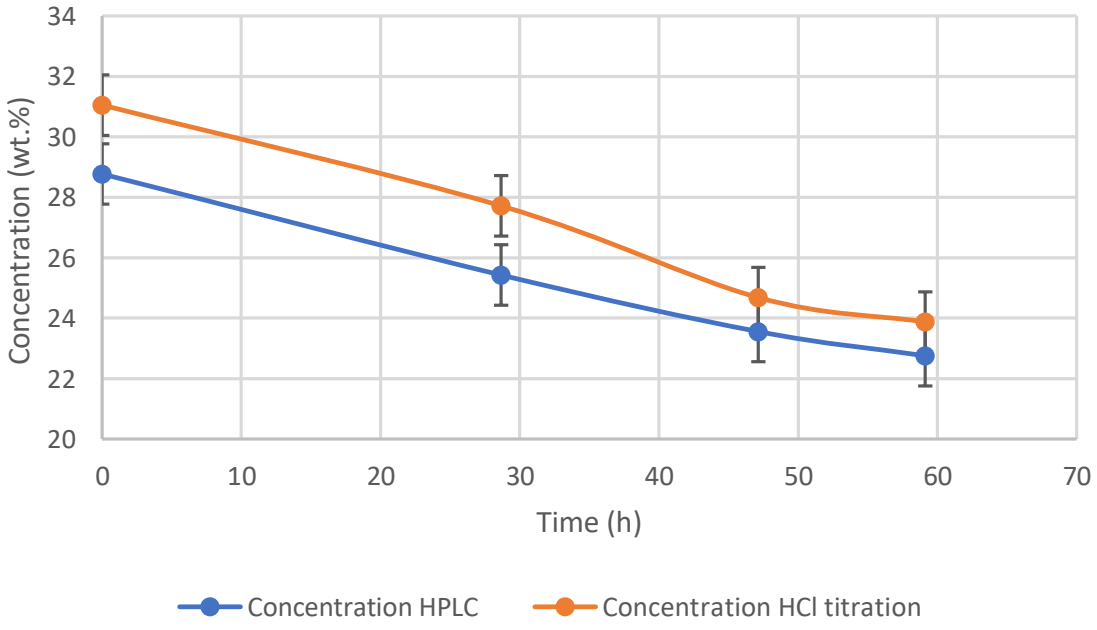

Figure V.6: MEA concentration through experiment 2

Time (h)	Concentration HPLC (wt.-%)	Concentration HCl titration (wt.-%)	wt.-% difference (%)	Relative difference (%)
0	28.77	31.05	2.28	7.92
29	25.43	27.72	2.29	9.00
47	23.56	24.68	1.12	4.79
59	22.76	23.88	1.12	4.92
90	21.42	22.91	1.49	6.99

Table V.7: MEA concentration through experiment 2

Figure V.6 and Table V.7 show similar curvature tendency between HPLC and HCl titration results. The differences between data from both analytical methods are non-negligible when compared to the expected precision from repeatability tests. Before delving into these differences, it is crucial to highlight that repeatability tests for HPLC on degraded samples showed a fluctuation range of 1.3 to 2 wt.-% due to precision errors during the dilution step. Given this context, the observed differences between the HPLC and HCl titration results, which range from 1.49 % to 3.11 %, indicate significant discrepancies likely due to both analytical precision and degradation effects over time.

A first non-negligible error appears right at the beginning of the experiment where both analytical methods have a difference weight percentage value of at least 1 wt.-% of the true value which is 30 wt.-%: HPLC is 1.23 wt.-% lower than 30 wt.-% and HCl titration is 1 wt.-% higher than 30 wt.-%. This error can result to the calibration used which was not created at the same time than the HPLC analysis of the experiment 2 samples or the potential dilution step errors for HPLC method.

The wt.-% differen between both methods decreases of 1 wt.-% for high degraded samples with relative differences of 5-7 % instead of 8-9 %.

V.1.2.d MEA concentration from experiment 3

Regarding the analysis of samples from Experiment 3, an initial HPLC analysis was performed using the previous calibration (see Figure V.4), which was conducted a few days earlier. However, as the results were significantly different from those obtained by HCl titration, a new HPLC analysis was performed concurrently with a new calibration (see Figure V.2). This approach allows for verification of whether the large discrepancies were due to the calibration.

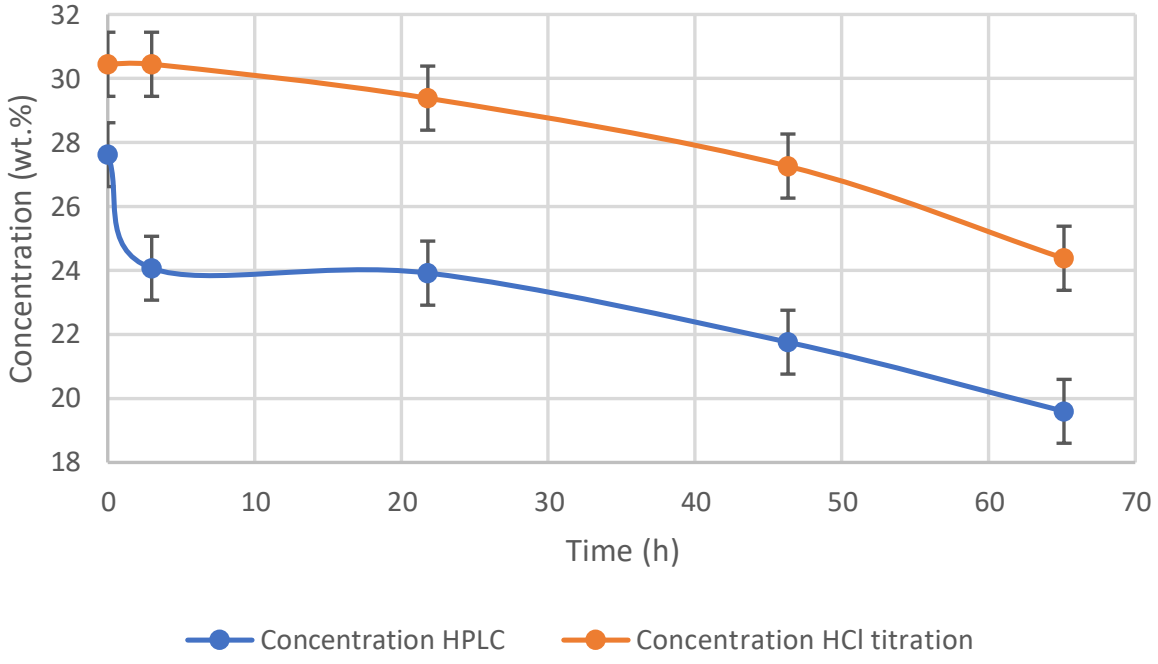

Figure V.7: MEA concentration through experiment 3 using old calibration

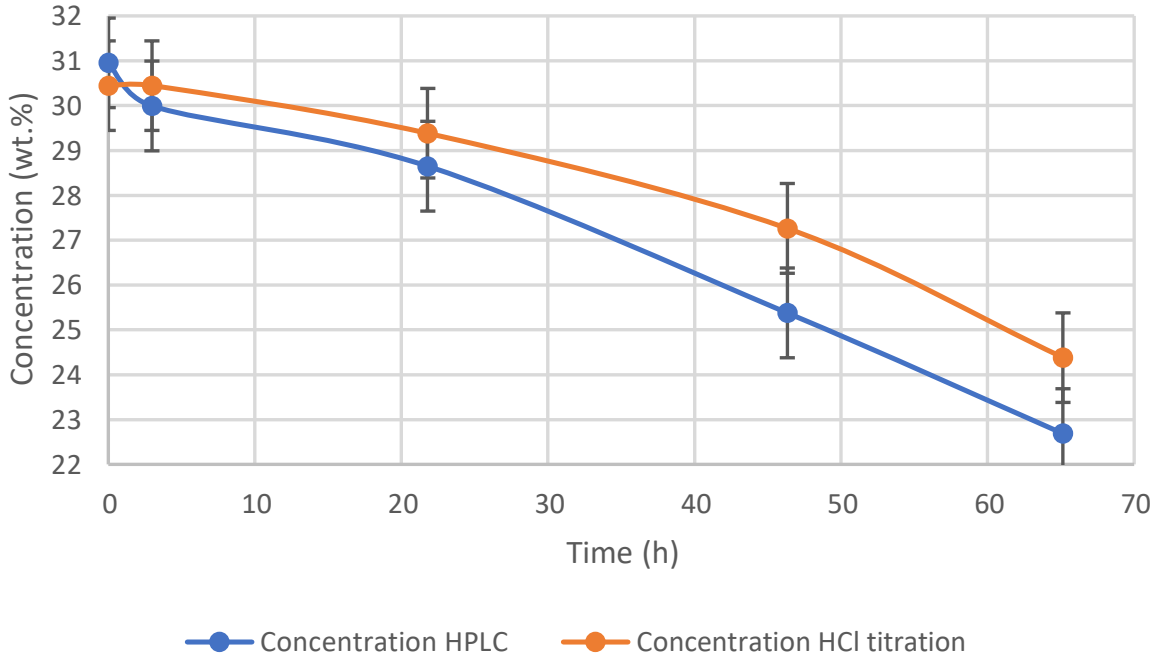

Figure V.8: MEA concentration through experiment 3

Time (h)	Concentration HPLC (wt.-%)	Concentration HCl titration (wt.-%)	wt.-% difference (%)	Relative difference (%)
0	27.62	30.45	2.83	10.23
3	24.07	30.45	6.37	26.48
22	23.92	29.38	5.47	22.86
46	21.76	27.26	5.50	25.30
65	19.60	24.38	4.78	24.40

Table V.8: MEA concentration through experiment 3 using old calibration curve

Time (h)	Concentration HPLC (wt.-%)	Concentration HCl titration (wt.-%)	wt.-% difference (%)	Relative difference (%)
0	30.95	30.45	-0.50	-1.65
3	29.99	30.45	0.46	1.51
22	28.65	29.38	0.73	2.57
46	25.38	27.26	1.88	7.42
65	22.69	24.38	1.69	7.46

Table V.9: MEA concentration through experiment 3

Figures V.7 and V.8 alongside Tables V.8 and V.9 illustrate the MEA concentration throughout experiment 3, using both the old and recent calibration curves for HPLC analysis.

The results from the HPLC using the recent calibration (Figure V.8 and Table V.9) show a closer agreement with the HCl titration method compared to the old calibration (Figure V.7 and Table V.8). Initially, the HPLC results using the old calibration showed a significant deviation, with an initial concentration of 27.62 wt.-% compared to 30.45 wt.-% by HCl titration, resulting in a weight difference of 2.83 wt.-% and a relative difference of 10.23 %. In contrast, the recent calibration shows an initial concentration of 30.95 wt.-%, which is much closer to the HCl titration value, with a negligible relative difference of -1.65 %.

As the experiment progresses, the weight difference and relative difference between the HPLC and HCl titration methods increase when using the old calibration, indicating a growing discrepancy due to potential degradation products reacting with HCl and affecting the titration results. This is reflected in the increasing weight difference from 2.83 wt.-% to 4.78 wt.-% and relative difference from 10.23 % to 24.40 %.

In contrast, the recent calibration maintains a much smaller weight difference and relative difference, indicating improved accuracy. The weight difference increases only slightly from -0.51 wt.-% to 1.69 wt.-%, with the relative difference increasing from -1.65 % to 7.46 %. This suggests that the recent calibration curve provides more reliable HPLC measurements that are less influenced by the degradation products over time.

Overall, the comparison demonstrates that the recent HPLC calibration provides a more accurate and reliable measure of MEA concentration during degradation experiments, aligning more closely with HCl titration results and exhibiting less variation over time.

V.1.2.e MEA concentration from experiment 4

Regarding the analysis of samples from Experiment 4, an initial HPLC analysis was performed using the previous calibration (see Figure V.4), which was conducted a few days earlier. However, as the results were significantly different from those obtained by HCl titration, a new HPLC analysis was performed concurrently with a new calibration (see Figure V.3). This approach allows for verification of whether the large discrepancies were due to the calibration.

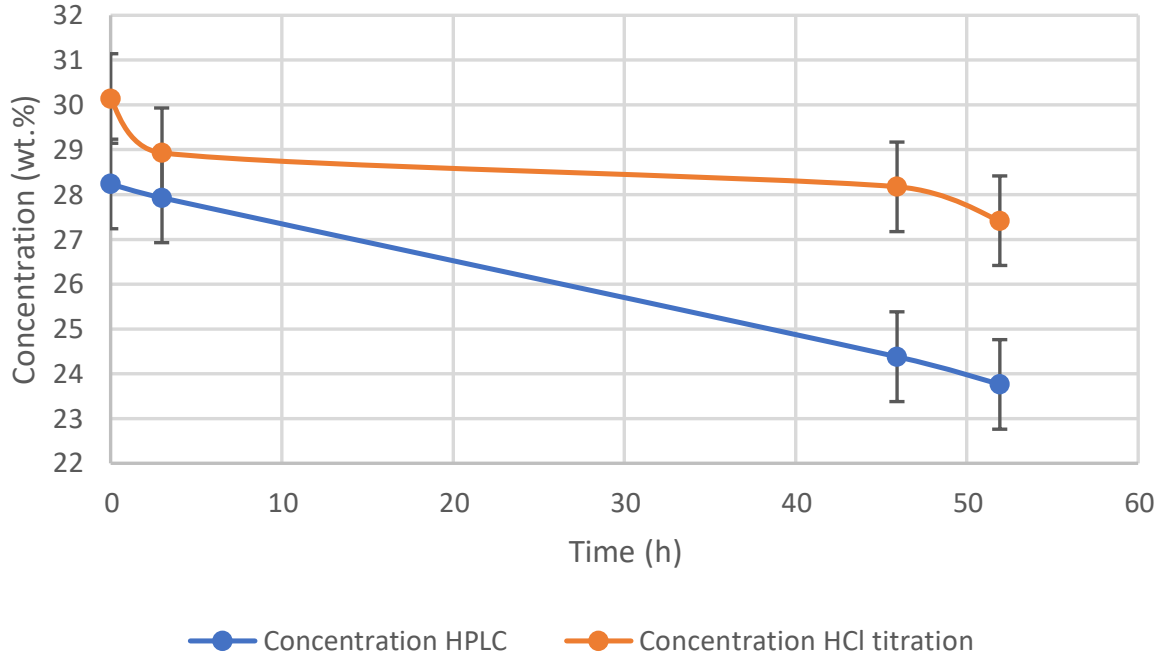

Figure V.9: MEA concentration through experiment 4 using old calibration

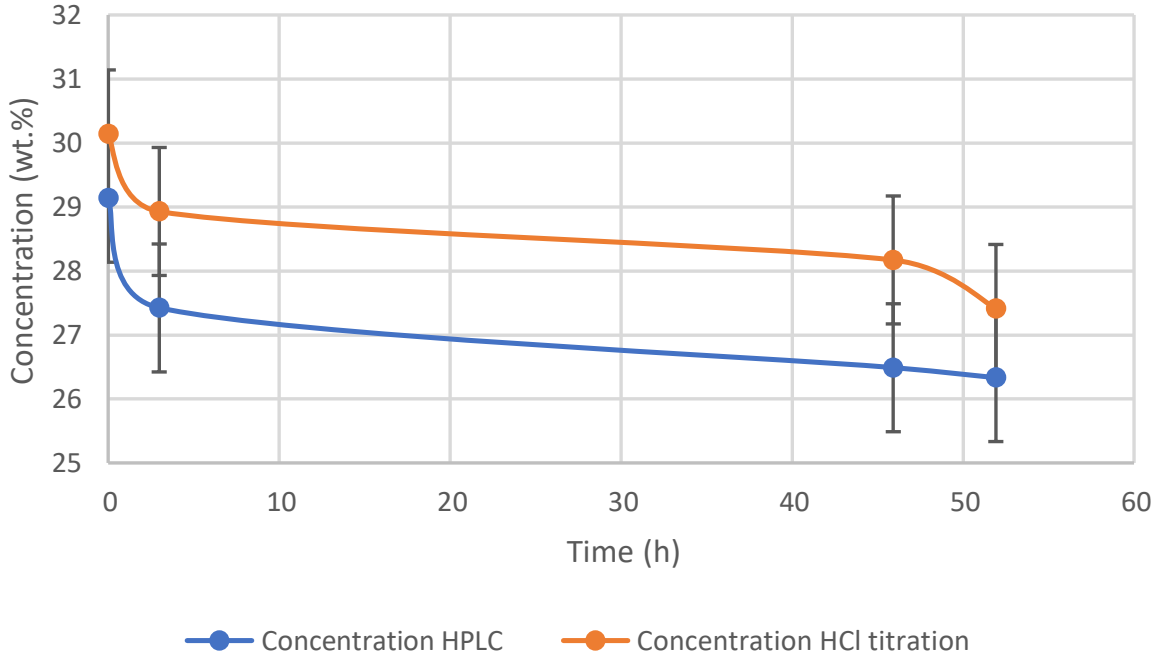

Figure V.10: MEA concentration through experiment 4

Time (h)	Concentration HPLC (wt.-%)	Concentration HCl titration (wt.-%)	wt.-% difference (%)	Relative difference (%)
0	28.24	30.14	1.90	6.75
3	27.93	28.93	1.00	3.59
46	24.38	28.17	3.79	15.56
52	23.76	27.41	3.65	15.37

Table V.10: MEA concentration through experiment 4 using old calibration curve

Time (h)	Concentration HPLC (wt.-%)	Concentration HCl titration (wt.-%)	wt.-% difference (%)	Relative difference (%)
0	29.14	30.14	1.00	3.45
3	27.42	28.93	1.51	5.49
46	26.49	28.17	1.68	6.35
52	26.33	27.41	1.08	4.11

Table V.11: MEA concentration through experiment 4

Figures V.9 and V.10 alongside Tables V.10 and V.11 illustrate the MEA concentration throughout experiment 4, using both the old and recent calibration curves for HPLC analysis.

The results from the HPLC using the recent calibration (Figure V.10 and Table V.11) show a closer agreement with the HCl titration method compared to the old calibration (Figure V.9 and Table V.10). Initially, the HPLC results using the old calibration showed a significant deviation, with an initial concentration of 28.24 wt.-% compared to 30.14 wt.-% by HCl titration, resulting in a weight difference of 1.90 wt.-% and a relative difference of 6.75 %. In contrast, the recent calibration shows an initial concentration of 29.14 wt.-%, which is much closer to the HCl titration value, with a relative difference of 3.45 %.

As the experiment progresses, the weight difference and relative difference between the HPLC and HCl titration methods increase when using the old calibration, indicating a growing discrepancy due to potential degradation products reacting with HCl and affecting the titration results. This is reflected in the increasing weight difference from 1.90 wt.-% to 3.65 wt.-% and relative difference from 6.75 % to 15.37 %.

In contrast, the recent calibration maintains a much smaller weight difference and relative difference, indicating improved accuracy. The weight difference increases only slightly from 1.00 wt.-% to 1.68 wt.-% (instead of 1.90 wt.-% to 3.65 wt.-% for old calibration), with the relative difference varying from 3.45 % to 6.35 % (instead of 6.75 % to 15.37 % for old calibration).

Overall, the comparison demonstrates that the recent HPLC calibration provides a more accurate and reliable measure of MEA concentration during degradation experiments, aligning more closely with HCl titration results and exhibiting less variation over time.

V.1.2.f MEA concentration from experiment 5

Regarding the analysis of samples from Experiment 4, an initial HPLC analysis was performed using the previous calibration (see Figure V.4), which was conducted a few days earlier. However, as the results were significantly different from those obtained by HCl titration, a new HPLC analysis was performed concurrently with a new calibration (see Figure V.3). This approach allows for verification of whether the large discrepancies were due to the calibration.

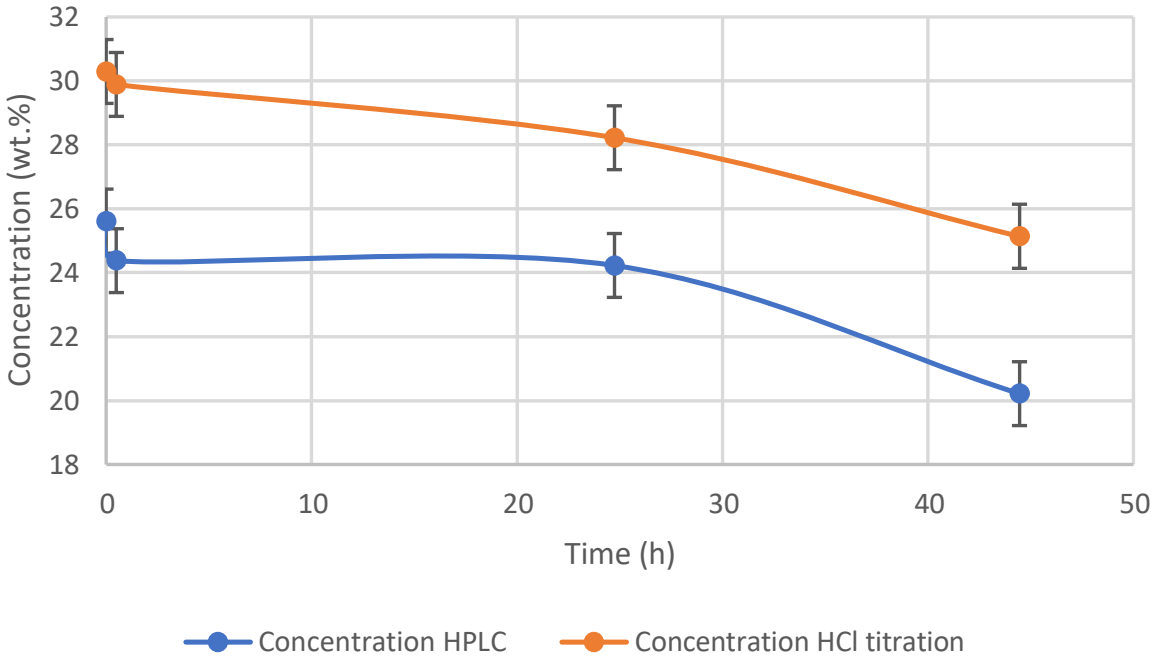

Figure V.11: MEA concentration through experiment 5 using old calibration

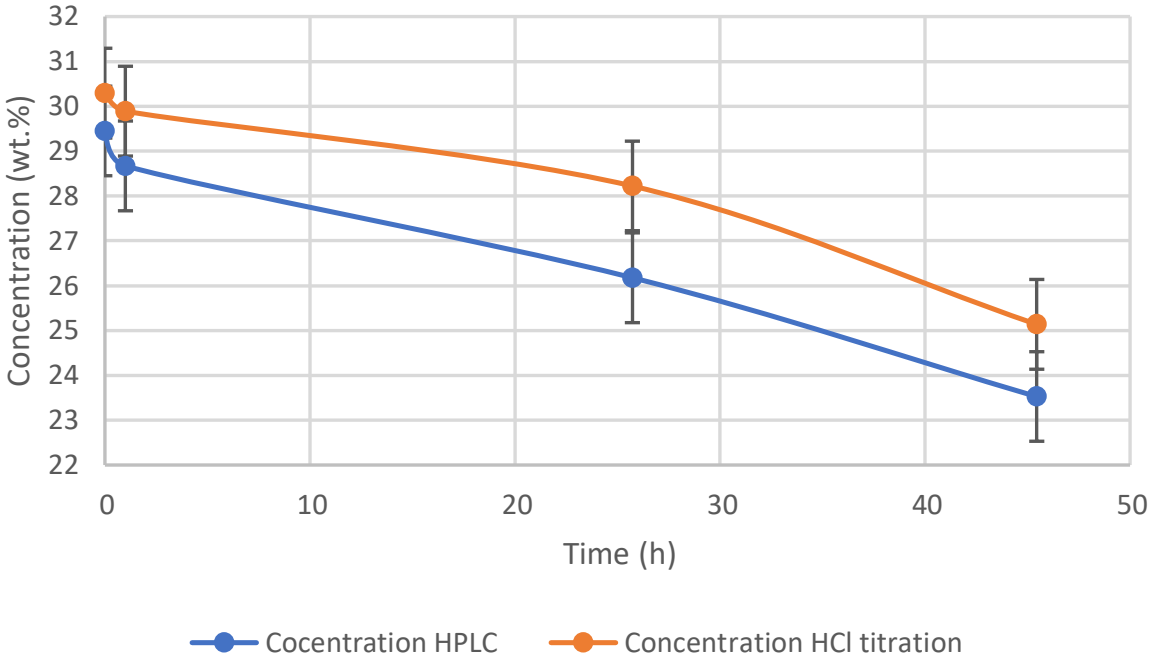

Figure V.12: MEA concentration through experiment 5

Time (h)	Concentration HPLC (wt.-%)	Concentration HCl titration (wt.-%)	wt.-% difference (%)	Relative difference (%)
0	25.61	30.29	4.68	18.27
1	24.38	29.89	5.51	22.60
25	24.23	28.22	3.99	16.50
44	20.22	25.14	4.92	24.36

Table V.12: MEA concentration through experiment 5 using old calibration curve

Time (h)	Concentration HPLC (wt.-%)	Concentration HCl titration (wt.-%)	wt.-% difference (%)	Relative difference (%)
0	29.45	30.29	0.84	2.87
1	28.67	29.89	1.22	4.25
25	26.18	28.22	2.04	7.81
44	23.53	25.14	1.61	6.84

Table V.13: MEA concentration through experiment 5

Figures V.11 and V.12 alongside Tables V.12 and V.13 illustrate the MEA concentration throughout experiment 5, using both the old and recent calibration curves for HPLC analysis.

The results from the HPLC using the recent calibration (Figure V.12 and Table V.13) show a closer agreement with the HCl titration method compared to the old calibration (Figure V.11 and Table V.12). Initially, the HPLC results using the old calibration showed a significant deviation, with an initial concentration of 25.61 wt.-% compared to 30.29 wt.-% by HCl titration, resulting in a weight difference of 4.68 wt.-% and a relative difference of 18.27 %. In contrast, the recent calibration shows an initial concentration of 29.45 wt.-%, which is much closer to the HCl titration value, with a relative difference of 2.87 %.

As the experiment progresses, the weight difference and relative difference between the HPLC and HCl titration methods remain relatively stable when using the recent calibration, indicating improved accuracy. The weight difference varies between 0.84 wt.-% and 2.05 wt.-%, with the relative difference ranging from 2.87 % to 7.81 %.

In contrast, the old calibration exhibits a larger and more variable weight difference, increasing from 4.68 wt.-% to 4.92 wt.-%, with the relative difference ranging from 12.91 % to 24.36 %. This suggests that the recent calibration curve provides more reliable HPLC measurements that are less influenced by the degradation products over time.

Overall, the comparison demonstrates that the recent HPLC calibration provides a more accurate and reliable measure of MEA concentration during degradation experiments, aligning more closely with HCl titration results and exhibiting less variation over time.

V.1.3 Aqueous MDEA sample

In this section, 50 wt.-% MDEA samples have been used in HCl titration for precision and accuracy measurement and in HPLC for calibration. Due to the high viscosity of the samples, a mass measurement has been applied before HCl titrations in order to avoid a volume error.

For each type of sample, 5 HCl titrations were performed with a sample volume of 2 mL, measured using an analytical balance for mass measurement. Tables V.14 and V.15 show the results of titrations for each MDEA sample, depending on whether the measurement was based on mass or volume.

Sample weight (g)	**Predicted required HCl volume (mL)**	**Measured HCl volume (mL)**	**Measured MDEA concentration (wt.-%)**	**Relative error (%)**
2.07	8.70	8.70	50.02	0.04
2.07	8.68	8.73	50.27	0.54
2.06	8.64	8.65	50.04	0.07
2.06	8.66	8.68	50.09	0.18
1.94	8.16	8.20	50.26	0.53

Table V.14: HCl titration results for 50 wt.-% MDEA (weight reference)

Volume Sample (2 mL)	**Predicted required HCl volume (mL)**	**Measured HCl volume (mL)**	**Measured MDEA concentration (wt.-%)**	**Relative error (%)**
2	8.24	8.70	52.83	5.54
2	8.24	8.73	52.98	5.84
2	8.24	8.65	52.52	4.93
2	8.24	8.68	52.67	5.23
2	8.24	8.20	49.73	-0.53

Table V.15: HCl titration results for 50 wt.-% MDEA (volume reference)

According to results, the repeatability and precision of HCl titration in MDEA samples are stronger for weight reference than volume reference. The relative error is in the order of 0.5 % by measuring the sample weight and 5 % for volume sample reference which means that the error precision in volume sample reference results to the sample take that has increased the real volume sample. This may be due to the high viscosity of MDEA that conducts to an adding of sample droplets in the solution.

Then, a single calibration curve has been made in order to use it for HPLC analysis on MDEA degraded samples of the single MDEA experiment and can be seen in Figure V.13. 6 MDEA solutions between 0 and 50 wt.-% MDEA are used for the calibration. Examples of peaks can be found in Appendix C.

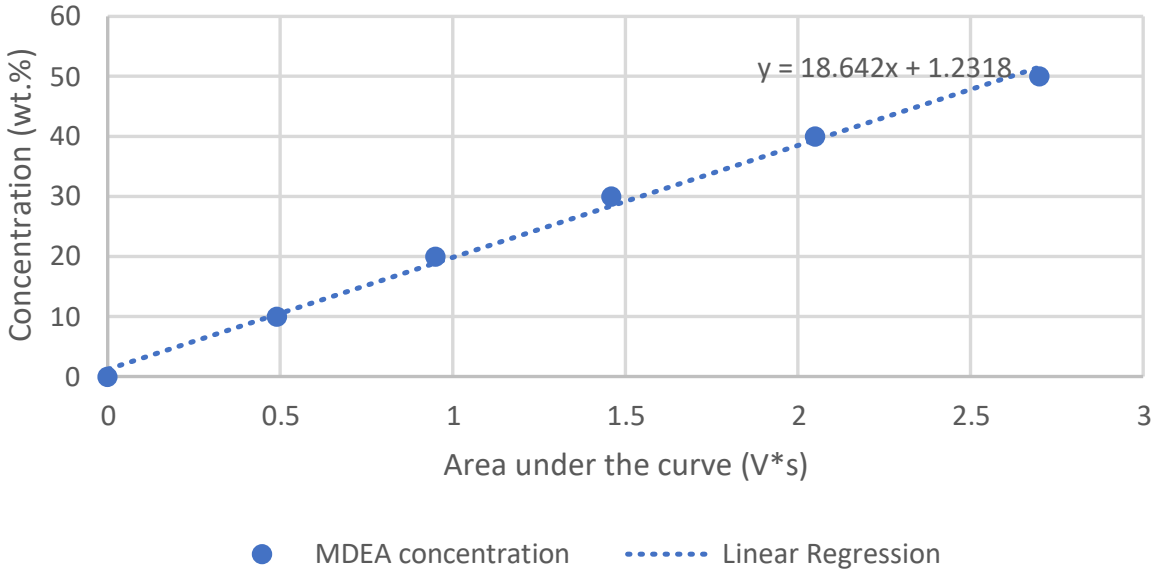

Figure V.13: Calibration curve for MDEA experiment

V.1.4 Degraded MDEA samples

V.1.4.a MDEA concentration from MDEA experiment

For the MDEA experiment, a fully detailed protocol about the experiment is written in Appendix F. However, some issues happen after the first day. As a result, a simple analysis on the beginning and the end of the experiment was made that can be seen in Table V.16.

Time (h)	Concentration HPLC (wt.-%)	Concentration HCl titration (wt.-%)	wt.-% difference (%)	Relative difference (%)
0	50.07	51.49	1.42	2.84
167	45.97	51.49	5.52	12.01

Table V.16: MDEA concentration through the experiment

Table V.16 shows a decrease in the MDEA concentration based on HPLC analyses of approximately 4 wt.-%, which is not observed in the HCl titration results, where the concentration remains constant. There are two possible explanations for these results: the first relates to the precision during the HCl titration. The most common precision error with 50 wt.-% degraded MDEA is the sampling process, as the sample in question is extremely viscous, which distorts the measured sample volume and can result in the addition of a few extra drops. The second reason involves potential reactions between the MDEA degradation products and HCl. Some degradation products such as DEA and formate have a basic nature, requiring more hydrochloric acid during titration to react with these other species in addition to the MDEA.

V.1.4.b Repeatability in HPLC for MDEA samples

To verify the repeatability of the method, five 50 wt.-% MDEA samples highly degraded[2] and non-degraded are analysed with HPLC. This HPLC analysis was made a week after the calibration.

Sample type	Area under the curve (V· s)	Concentration (wt.-%)	Mean area (V· s)	Highest area gap (V· s)	Highest concentration gap (wt.-%)
Non-degraded 50 wt.-% MDEA	2.35	45.04	2.31	0.32	5.97
Non-degraded 50 wt.-% MDEA	2.33	44.67			
Non-degraded 50 wt.-% MDEA	2.41	46.16			
Non-degraded 50 wt.-% MDEA	2.36	45.23			
Non-degraded 50 wt.-% MDEA	2.09	40.19			
High degraded 50 wt.-% MDEA	1.97	37.96	1.90	0.14	2.61
High degraded 50 wt.-% MDEA	1.88	36.28			
High degraded 50 wt.-% MDEA	1.83	35.35			
High degraded 50 wt.-% MDEA	1.96	37.77			
High degraded 50 wt.-% MDEA	1.84	35.53			

Table V.17: Repeatability on MDEA degraded samples in HPLC

Table V.17 shows that obtained concentration values can be significantly different to the desired value for 50 wt.-% non-degraded MDEA samples and can have high variance.

Among the five 50 wt.-% non-degraded MDEA samples, four samples have a calculated concentration between 44.5 wt.-% and 46.2 wt.-% which are far from the true value which is 50 wt.-% MDEA. This shows that the previous calibration is too old to be used with a general weight percentage difference of around 5 wt.-%. A fifth value is close to 40 wt.-% MDEA which may result to a high error during the dilution step[3]. If the fifth value is taken into account, the highest concentration gap has a value close to 6 wt.-%. If the fifth value is not taken into account, the average area increases from V· s with an "area gap" of 0.08 instead of 0.32. The "concentration gap" is reduced to 1.4913 wt.-% instead of 5.9653 wt.-%. This demonstrates that it is advisable to conduct multiple analyses on the same sample, even if it is not degraded.

For highly degraded samples, the calculated concentration of MDEA is between 35.3 and 38 wt.-%. If the gap between previous calibration and repeatability on 50 wt.-% non-degraded MDEA is taken into account, the true concentration value for the degraded samples is higher than 40 wt.-%.

This repeatability test shows that HPLC analysis concentration values can be varied by 2.6098 wt.-% due to some precision errors. This value seems to increase when degraded MDEA is analyzed.

[2]These samples are taken at the end of the experiment.

[3]Each sample was diluted separately, which means that the dilution step may influence the concentration differences observed between each sample.

V.1.5 PZ samples

In this section, HCl titrations have been applied on pure piperazine samples and HPLC has been applied on a 5 wt.-% piperazine sample[4] to verify the precision of the method on PZ samples.

During HCl titrations, PZ samples are initially in a solid state. Their mass has been measured before titration then distilled water has been added to dissolve it. Notice that PZ is a secondary amine meaning that PZ reacts with two molecules of HCl which leads to a change in the equation used to calculate the concentration of amine:

$$n_{amine} = \frac{C_{HCl} \cdot V_{HCl,titration}}{2} \tag{V.1}$$

Notice that n_{amine} is the number of mol in the sample.
Table V.18 regroups three results of HCl titration with predicted and measured HCl volume that must be added to have a colour change and the relative error (with predicted required HCl volume as reference):

Sample mass (g)	**Predicted required HCl volume (mL)**	**Measured HCl volume (mL)**	**Relative error (%)**
0.4873	11.31	11,15	-1.45
0.3973	9.22	9.1	-1.35
0.3038	7.05	6.95	-1.47

Table V.18: HCl titration results for pure PZ

Through these results, the relative error has a close value of -1.5 % which means that the equation V.1 is validated and small errors may be due to the manipulation mistakes.

For the HPLC detection, no peak has been detected for 5 wt.-% PZ sample. It is maybe due to the low concentration of PZ and the 1:8 dilution step that reduces the amine content in the analysed sample which make the detection peak too low to be perceived. However, this hypothesis does not align with the detection of other amines at low concentrations (10 wt.-% during calibration). An alternative hypothesis suggests that the column or the eluent used may not be suitable for PZ, as the interactions between the amine and these different elements are too weak for detection to occur.

[4]The choice of this concentration is due to the fact that solvents containing PZ are often mixtures with other types of amines, and PZ is present at much lower concentrations.

V2. Determination of CO_2 loading

The next step is to analyze the CO_2 loading of the various samples from different experiments in order to compare the different analytical methods in question.

V.2.1 Aqueous CO_2-loaded MEA samples

In this section, different CO_2-loaded MEA samples from different experiments are analyzed to obtain how much CO_2 was absorbed in the solution. On each of them, a $BaCl_2$ titration and a density measurement are applied. Additionally, a mass measurement before and after CO_2 loading has been done in order to calculate the mass difference of the reactor and so the CO_2-loaded mass and so the CO_2 loading. Table V.19 regroups all experimental CO_2 loading values from different experiments (more details in Appendix F). Please note that the relative difference pertains to the CO_2 loading values derived from density correlation and $BaCl_2$ titration, with the latter serving as the reference method.

Experiment number	**CO_2 loading from mass measurement**	**CO_2 loading from density correlation**	**CO_2 loading from $BaCl_2$ titration**	**Relative difference (%)**
0	0.5305	0.5474	0.5504	-0.5493
3	0.562	0.5622	0.5708	-1.5176
4	0.528	0.5292	0.5155	2.6609
5	0.558	0.5660	0.5855	-3.3203

Table V.19: CO_2 loading of loaded samples

The absolute relative difference between calculated CO_2 loading from $BaCl_2$titration and density correlation for the four experiments varies between 0.5 and 3.5 %. Regarding mass measurement, the relative differences for $BaCl_2$ titration are generally between 1.5 % and 4.7 %, while the relative differences for the density correlation are typically between 0.5 % and 3.3 %. Additionally, analyzing the results in Table V.19, the mass measurement method determines concentration values that are closer to those obtained by the density correlation method than to those obtained by $BaCl_2$ titrations.

For experiment 5, the CO_2 loading was measured using $BaCl_2$ titration for samples taken each hour after the loading, as depicted in Figure V.14.

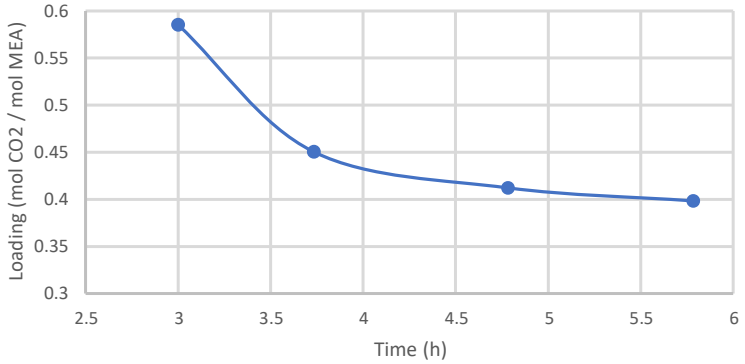

Figure V.14: CO_2 loading of experiment 5 (first day)

According to Figure V.14, the CO_2 loading is decreased during 1 hour and continue to be decreased slowly for the next hours. According to Zhang et al. (2022), CO_2 desorption occurs at high tempera-

tures, with or without the presence of a catalyst (primarily above 100 °C), over a period of 120-150 minutes, after which the decrease in CO_2 loading becomes negligible. In Experiment 5, conducted at 120 °C, CO_2 desorption was observed. Thus, for each experiment, CO_2 desorption occurs during the initial hours following the loading of the solvent with CO_2, resulting in a maximum loading at the beginning of the experiment.

V.2.2 Degraded MEA samples

For this section, $BaCl_2$ titration has been applied on each sample of three experiments (protocols of experiments 3, 4 and 5 are located in Appendix F). The CO_2 loading has been calculated using equation IV.1 to calculate the CO_2 concentration and HPLC results to obtain the amine concentration. A density correlation was made on a single degraded sample which is the last sample of experiment 3.

For each CO_2 loading graphs, two types of curve are drawn. These curves represent the two types of calculations used to determine the loading: calculation type 1 involves dividing the CO_2 concentration by the remaining MEA concentration and calculation type 2 involves dividing the CO_2 concentration by the initial MEA concentration (30 wt.-% or 4.8964 mol/L). The loading values in the tables are calculated using calculation type 1.

V.2.2.a CO_2 loading from experiment 3

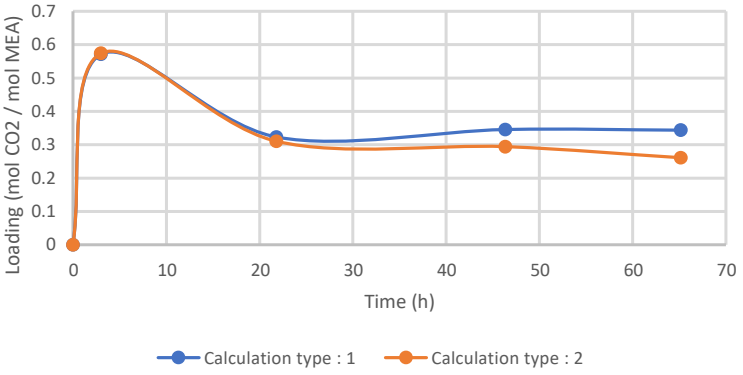

Figure V.15: CO_2 loading of experiment 3 samples

Time (h)	CO_2 concentration (mol CO_2/L)	MEA concentration (mol MEA/L)	CO_2 loading Type 1 (mol CO_2/mol MEA)	CO_2 loading Type 2 (mol CO_2/mol MEA)
0	0.0000	5.0805	0.0000	0.0000
3	2.8100	4.9227	0.5708	0.5739
22	1.5200	4.7017	0.3233	0.3104
46	1.4400	4.1651	0.3457	0.2941
65	1.2800	3.7232	0.3438	0.2614

Table V.20: CO_2 loading of experiment 3 samples

Figure V.15 and Table V.20 show a high CO_2 loading peak at the beginning of the experiment followed by the decreasing of the CO_2 concentration and the MEA concentration. The CO_2 loading depends on both concentrations. As a result, the CO_2 loading is decreasing right after the loading step according

to the Section V.2.1 that confirms discharging phenomena at high temperature and the CO_2 loading is increasing during the second day due to the high MEA degradation. At the end of the experiment, the CO_2 loading is varying less due to a balancing between MEA degradation and CO_2 discharge. The CO_2 concentration has been reduced from 1.44 mol CO_2/L to 1.28 mol CO_2/L and the MEA concentration has been reduced from 4.17 mol MEA/L to 3.72 mol MEA/L which have similar reductions of concentration.

The second calculation shows CO_2 loading with the initial MEA concentration as a reference. The difference between both calculation types increases with the degradation. The more the solvent is degraded, the more the MEA concentration decreases, which reduces the denominator and consequently increases the CO_2 loading value according to calculation method 1. This is not the case for calculation method 2, which does not use MEA concentration values from degraded samples.

A density correlation was performed on the final sample. The CO_2 loading calculated using this density correlation is 0.3401 mol CO_2 per mol MEA, compared to 0.3438, resulting in a relative error of 0.91%.

V.2.2.b CO_2 loading from experiment 4

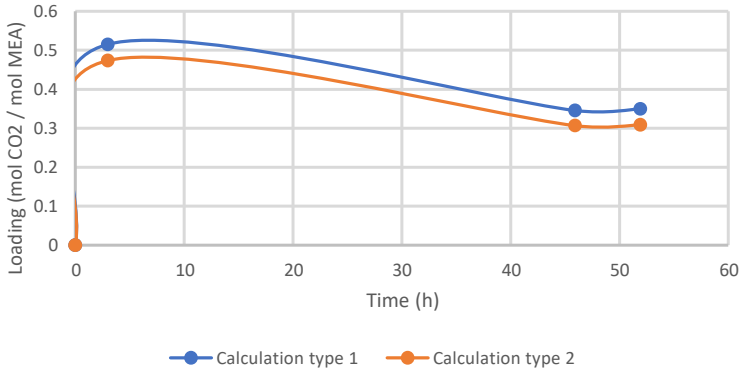

Figure V.16: CO_2 loading of experiment 4 samples

Time (h)	CO_2 concentration (mol CO_2)	MEA concentration (mol MEA)	CO_2 loading Type 1 (mol CO_2/mol MEA)	CO_2 loading Type 2 (mol CO_2/mol MEA)
0	0.0000	4.7823	0.0000	0.0000
3	2.3200	4.5009	0.5155	0.4738
46	1.5025	4.3474	0.3456	0.3069
52	1.5125	4.3218	0.3500	0.3089

Table V.21: CO_2 loading of experiment 4 samples

Figure V.16 and Table V.21 present results similar to those from Experiment 3, with a peak in CO_2 loading at the beginning of the experiment, followed by a decrease in CO_2 loading after the peak. However, Experiment 4 provides fewer samples due to a 43-hour interval between the collection of two samples. This results in less information on the rate of CO_2 desorption, making the trend curve less accurate.

A notable difference between the two experiments lies in the concentrations of amine and CO_2. At the end of Experiment 3, the amine and CO_2 concentrations are 1.28 mol CO_2/L and 3.72 mol MEA/L, respectively, which are lower than the corresponding values at the end of Experiment 4, where they are 1.51 mol CO_2/L and 4.32 mol MEA/L. The CO_2 loading values are quite similar between the two experiments using the first calculation method (0.3438 mol CO_2/mol MEA at the end of Experiment 3 and 0.3500 mol CO_2/mol MEA at the end of Experiment 4). This is because, despite the different species concentrations, their ratio remains similar. Regarding the second calculation method, due to the lower degradation in Experiment 4, the difference between the two calculation methods is less significant.

V.2.2.c CO_2 loading from experiment 5

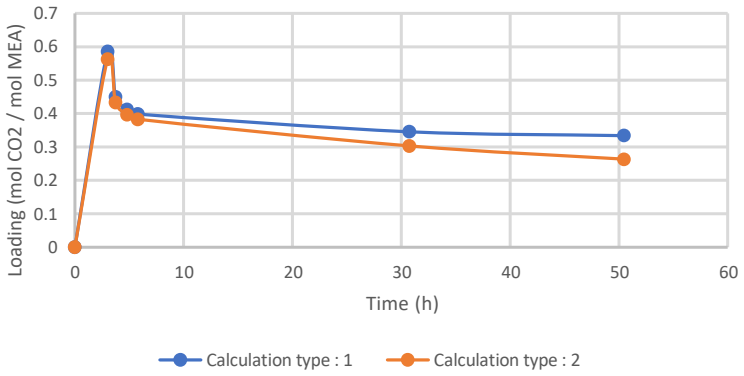

Figure V.17: CO_2 loading of experiment 5 samples

Time (h)	CO_2 concentration (mol CO_2)	MEA concentration (mol MEA)	CO_2 loading Type 1 (mol CO_2/mol MEA)	CO_2 loading Type 2 (mol CO_2/mol MEA)
0	0.0000	4.8335	0.0000	0.0000
3	2.7550	4.7055	0.5855	0.5627
4	2.1200	4.7055	0.4505	0.4330
5	1.9400	4.7055	0.4123	0.3962
6	1.8750	4.7055	0.3985	0.3829
31	1.4850	4.2962	0.3457	0.3033
50	1.2900	3.8612	0.3341	0.2635

Table V.22: CO_2 loading of experiment 5 samples

Figure V.17 and Table V.22 show certain similarities with the results from Experiments 3 and 4, such as the peak in CO_2 loading at the beginning of the experiment and the subsequent decrease in CO_2 loading after the peak. This decrease is even more pronounced in this experiment because samples were analyzed 1, 2, and 3 hours after the loading stage, allowing for a trend curve that more closely reflects reality.

Compared to Experiments 3 and 4, Experiment 5 exhibits the highest CO_2 loading value at the initial loading stage (0.5855 mol CO_2/mol MEA) and the lowest at the end of the experiment (0.3341 mol CO_2/mol MEA) according to the first calculation method. As degradation steadily increases over time, the results from the two calculation methods become increasingly different as the experiment progresses, similar to what was observed in Experiment 3.

Chapter VI

Conclusion and perspectives

VI1. Conclusion related to the results

The comparative analysis of various analytical methods in this study provided significant insights into the precision and reliability of each technique when measuring amine concentrations and CO_2 loading. The key findings from Section V are summarized and interpreted below to highlight the implications of the results.

The comparison between HPLC analysis and HCl titration for determining amine concentrations revealed substantial discrepancies. The HPLC method, particularly with recent calibration, demonstrated greater accuracy and consistency in measuring MEA concentrations, aligning more closely with the true values and showing minimal variation over time. In contrast, the HCl titration method consistently overestimated the concentrations, likely due to precision errors such as excess droplet addition during titration and potential reactions between HCl and degradation products. These findings underscore the importance of using advanced analytical techniques like HPLC, especially with up-to-date calibrations, to ensure reliable results in the presence of degradation compounds.

The evaluation of CO_2 loading methods, specifically BaCl2 titration and density correlation, indicated that both techniques yielded comparable results with relative differences not exceeding 3.5 %. However, the density correlation method required significantly larger sample sizes and was influenced by degradation, as the correlation tables used were based on non-degraded samples. Despite these drawbacks, the density correlation method offers the advantage of not requiring amine concentration measurements, which simplifies the process and reduces potential error sources. This comparison highlights the need to balance precision and practicality when selecting analytical methods for CO_2 loading measurements.

Experiment 5 provided further evidence of the impact of degradation on analytical accuracy. The results showed that as degradation increased over time, the divergence between the two CO_2 loading calculation methods became more pronounced. This trend was consistent with observations from Experiment 3, emphasizing the dynamic nature of degradation processes and their influence on analytical outcomes. The initial high CO_2 loading values and the subsequent decrease observed across experiments underscore the necessity of accounting for degradation in long-term studies to ensure accurate and meaningful data interpretation.

VI2. General conclusion about the analytical methods used

First, a comparison between HCl titration and the HPLC method is conducted across various categories to determine which method is more efficient based on the most impactful variable.

	HCl titration	**HPLC**
Time required for 1 sample analysis (minutes):	5-10	20
Volume sample required (mL)	1 - 4	0.1 - 1
Consumable required for 1 sample analysis	- HCl 1 M: 5 - 10 mL - Orange methyl: 2 - 3 drops - Distilled water	- HCl 0.1 M: 2 - 3 mL - NH_4HCO_2: 6.306 mg - Formic acid: 10 μL - HPLC-grade acetonitrile: 18 mL - Distilled water
Precision error sources	- Sample take - Color change - Burette precision - Titrated degradation products	- Sample take - Dilution step - Calibration age
Cost of materials	+	+++

Table VI.1: HCl titration and HPLC comparison

According to Table VI.1, the HCl titration is a faster and cheaper method and requires less different consumables than HPLC method. However, HPLC analysis requires less sample quantity and HCl titration has a non-negligible precision error due to the titration of some degradation products.

Both methods contain several sources of precision errors, and certain solutions can be implemented to mitigate these errors:

- For both methods, using additionally an analytical balance to measure the sample mass before titration or dilution improves precision. The utilisation of graduated pipette is less precise than an analytical balance.
- For HCl titration, the utilisation of pH-meter may be added to the system still using an indicator. Repeating the method may verify the results
- For HPLC, conducting a calibration concurrently with sample analysis and including a greater number of calibration samples can enhance the validity of the calibration. Moreover, incorporating samples with known amine concentrations during the sample analysis can provide ongoing verification of the calibration's accuracy throughout the analysis process.

Then, a comparison between $BaCl_2$ titration, the correlation density method as well as the mass measurement method is conducted across various categories to determine which method is more efficient based on the most impactful variable.

	$BaCl_2$ titration	**Density correlation**	**Mass measurement**
Time required for 1 sample analysis (minutes):	30 - 40	15	≤ 5
Volume sample required (mL)	0.5	4 - 6	/
Consumable required for 1 sample analysis	- HCl 0.1 M: 10 - 40 mL - NaOH 0.1 M: 60 - 80 mL - $BaCl_2$ 0.5 M: 25 mL - Distilled water	Distilled water	/
Precision error sources	- Sample take - Precipitation recuperation - Burette precision - Amine concentration calculation	- Correlation determination - Non-linearity at high CO_2 loading - Degradation influence on density	- Material addition - Material release
Cost of materials	++	+++	+

Table VI.2: $BaCl_2$ titration and density correlation comparison

According to Table VI.2, most categories favor the mass measurement method, which solely involves mass differentiation. However, the third method exhibits precision errors due to the release and absorption of non-CO_2 species, such as the release of water vapor at high temperatures or the absorption of other gases.

In contrast, density correlation offers several advantages over $BaCl_2$ titration, except for the volume of sample required and the cost of materials. However, density correlations are based only on experimental data from non-degraded samples with very specific amine concentrations. Thus, for density correlations, it is first necessary to establish the equation that relates density to loading, requiring preliminary experiments to determine the parameters, which can introduce errors. Moreover, these correlations may not be valid for highly degraded samples and those with high CO_2 loading, where the correlation is less linear.

The $BaCl_2$ titration method contains several sources of precision errors, and certain solutions can be implemented to mitigate these errors:

- During sample collection, using an analytical balance to measure the sample mass before titration or dilution improves precision. The utilisation of a graduated pipette is less precise than an analytical balance.
- During precipitate recuperation, a mass measurement of the filter before and after the filtration may give an idea of total $BaCO_3$ and so the CO_2 concentration. However, the precipitate may contain other elements such as water or other precipitates.

VI3. Perspectives

Building on the insights and findings from this research, several avenues for future work can be identified to further advance the study of analytical methods for determining amine concentration and CO2 loading in the context of CO2 capture using chemical absorption.

First, expanding the range of comparative studies between different analytical methods is crucial. Exploring titrations using chemicals other than HCl or $BaCl_2$ could provide valuable insights into the impact of protocol variations on measurement accuracy and precision. Investigating the effectiveness of the Chittick Apparatus for simultaneous determination of CO_2 loading and amine concentration would be particularly beneficial. Such studies could help ascertain whether this integrated method offers a more efficient and reliable alternative to the use of separate methods for each parameter.

Additionally, extending these comparative analyses to a broader spectrum of amine solvents beyond MEA, MDEA, and PZ is essential. Conducting more experiments with these and other amines, including mixtures, could uncover potential variations in degradation patterns and analytical challenges. This would not only enhance the robustness of the developed methods but also provide a more comprehensive understanding of solvent behavior under different conditions.

Further research should also focus on the long-term stability and degradation dynamics of amine solvents. The results of this study highlighted the significant impact of degradation on analytical accuracy over time. Therefore, investigating the degradation kinetics and developing strategies to mitigate its effects would be valuable. This could involve studying the influence of operational parameters such as temperature, pressure, and solvent composition on degradation rates and patterns.

Another important aspect to explore is the environmental and economic implications of solvent degradation. Quantifying the lifecycle environmental impacts of using degraded solvents versus fresh ones, as well as assessing the cost-effectiveness of various analytical methods, could provide a holistic view of the sustainability and feasibility of CO2 capture processes. This would support the development of more efficient and environmentally friendly carbon capture technologies.

Finally, integrating advanced analytical techniques, such as spectroscopy and mass spectrometry, could offer new dimensions of data and enhance the understanding of degradation mechanisms. These techniques could provide more detailed information on the chemical changes occurring during solvent degradation, thereby informing the design of more stable and effective amine solvents.

Bibliography

AgriTech, V. (2023), 'Carbon capture projects: Success stories from around the world'. Accessed: 2024-06-02. https://blog.verde.ag/en/carbon-capture-success-stories/.

Ali, A. H. (2022), 'High-performance liquid chromatography (hplc): a review', *Ann. Adv. Chem* **6**, 010–020.

Arachchige, U., Aryal, N., Eimer, D. A. and Melaaen, M. C. (2013), 'Viscosities of pure and aqueous solutions of monoethanolamine (mea), diethanolamine (dea) and n-methyldiethanolamine (mdea)', *Annual Transactions of the Nordic Rheology Society* **21**(8).

Aryal, S. (2024), 'Gas chromatography: Principle, parts, steps, procedure, uses'. Accessed: 2024-06-04. https://microbenotes.com/gas-chromatography/.

Baggio, L. (2022), 'Modelling study on CO_2 purification via a liquefaction process'.

BASF (2022), 'Basf and samsung heavy industries collaborate on carbon capture & storage onboard maritime vessels'. Accessed: 2024-06-02. https://www.basf.com/global/en/who-we-are/sustainability/whats-new/sustainability-news/2022/BASF-and-Samsung-Heavy-Industries-collaborate-on-Carbon-Capture-Storage-onboard-maritime-vessels.html.

Bedell, S. A. (2011), 'Amine autoxidation in flue gas co2 capture—mechanistic lessons learned from other gas treating processes', *International Journal of Greenhouse Gas Control* **5**(1), 1–6.

Bruckner, M. Z. (2006), 'Ion chromatography'. Accessed: 2024-06-04. https://serc.carleton.edu/microbelife/research_methods/biogeochemical/ic.html.

Buvik, V., Høisæter, K. K., Vevelstad, S. J. and Knuutila, H. K. (2021), 'A review of degradation and emissions in post-combustion co2 capture pilot plants', *International Journal of Greenhouse Gas Control* **106**, 103246.

Cerato, A. (2023), 'Determination of soil carbonate content: Chittick apparatus'. University of Oklahoma.

Chiarella, L. (2018 - 2019), 'Experimental study about mdea aqueous solution degradation for carbon capture technology'.

Closmann, F. and Rochelle, G. T. (2011*a*), 'Degradation of aqueous methyldiethanolamine by temperature and oxygen cycling', *Energy Procedia* **4**, 23–28.

Closmann, F. and Rochelle, G. T. (2011*b*), 'Degradation of aqueous methyldiethanolamine by temperature and oxygen cycling', *Energy Procedia* **4**, 23–28.

Cuzuel, V., Gouedard, C., Cuccia, L., Brunet, J., Rey, A., Dugay, J., Vial, J., Perbost-Prigent, F., Ponthus, J., Pichon, V. et al. (2015), 'Amine degradation in co2 capture. 4. development of complementary analytical strategies for a comprehensive identification of degradation compounds of mea', *International Journal of Greenhouse Gas Control* **42**, 439–453.

Delfort, B., Carrette, P.-L. and Bonnard, L. (2011), 'Mea 40% with improved oxidative stability for co2 capture in post-combustion', *Energy Procedia* **4**, 9–14.

Delft, T. (2024), 'High-performance liquid chromatography (hplc)'. Accessed: 2024-06-02. https://www.tudelft.nl/en/ceg/about-faculty/departments/watermanagement/research/waterlab/equipment/high-performance-liquid-chromatography-hplc.

Dubois, L. (2023), 'Annexe b : Méthodes de dosage du CO_2 dans les solvants aminés (alternatives au toc)'. Capture du CO_2 par absorption dans des solvants aminés.

Ghosh, P. (2023*a*), Investigation of mea degradation in presence of sox and nox species in co2 capture systems, Master's thesis, University of Liège, Liège, Belgium. Thesis presented for obtaining the Master's degree in Advanced Materials: Innovative recycling.

Ghosh, P. (2023*b*), Quantitative analysis of mea solvent degradation in samples from co2 capture unit, Technical report, ULiège.

Guardian, T. (2021), 'From pollutant to product: the companies making stuff from co2'. Accessed: 2024-06-02. https://www.theguardian.com/environment/2021/dec/05/carbon-dioxide-co2-capture-utilisation-products-vodka-jet-fuel-protein.

Hoff, K. A. (2003), Modeling and experimental study of carbon dioxide absorption in a membrane contactor, PhD thesis, Norwegian University of Science and Technology.

Horwitz, W. (1970), *Official Methods of Analysis of the Association of Official Analytical Chemists*, Vol. 2, Association of Official Analytical Chemists.

Hwang, G. S., Stowe, H. M., Paek, E. and Manogaran, D. (2015), 'Reaction mechanisms of aqueous monoethanolamine with carbon dioxide: a combined quantum chemical and molecular dynamics study', *Physical Chemistry Chemical Physics* **17**(2), 831–839.

Langa, P., Denesb, F. and Hegelya, L. (2017), 'Comparison of different amine solvents for the absorption of co2', *CHEMICAL ENGINEERING* **61**.

Lepaumier, H. (2008), Etude des mécanismes de dégradation des amines utilisées pour le captage du CO2 dans les fumées, PhD thesis, Chambéry.

Léonard, G. (2013), Optimal design of a CO2 capture unit with assessment of solvent degradation, PhD thesis, ULiège, Liège.

Léonard, G. (2021-2022), 'Gestion durable des combustibles: approvisionnement, synthèse et utilisation'. Cours: La capture et le stockage du CO2.

MacDowell, N., Florin, N., Buchard, A., Hallett, J., Galindo, A., Jackson, G., Adjiman, C. S., Williams, C. K., Shah, N. and Fennell, P. (2010), 'An overview of co 2 capture technologies', *Energy & Environmental Science* **3**(11), 1645–1669.

Masohan, A., Ahmed, M., Nirmal, S. K., Kumar, A. and Garg, M. O. (2009), 'A simple ph-based method for estimation of co 2 absorbed in alkanolamines', *Indian Journal of Science and Technology* pp. 59–64.

Mitsubishi Heavy Industries, Ltd. (2022), 'CO2 capture technology: CO2 capture process'. Accessed: 2024-06-02. https://www.mhi.com/products/engineering/co2plants_process.html.

Nakagaki, T., Tanaka, I., Furukawa, Y., Sato, H. and Yamanaka, Y. (2014), 'Experimental evaluation of effect of oxidative degradation of aqueous monoethanolamine on heat of co2 absorption, vapor liquid equilibrium and co2 absorption rate', *Energy Procedia* **63**, 2384–2393.

Poluzzi, A., Guandalini, G. and Romano, M. C. (2022), 'Flexible methanol and hydrogen production from biomass gasification with negative emissions', *Sustainable Energy & Fuels* **6**(16), 3830–3851.

Ritchie, H., Rosado, P. and Roser, M. (2023), 'Greenhouse gas emissions', *Our world in data* .

Saleh, S., Razali, A., Hanafiah, R., Tamidi, A. and Chan, Z. P. (2021), Optimization of mdea-pz ratio and concentration for co2 removal in semi-lean membrane contactor process, *in* 'E3S Web of Conferences', Vol. 287, EDP Sciences, p. 03009.

Santos, S. P., Gomes, J. F. and Bordado, J. C. (2016), 'Scale-up effects of co2 capture by methyldiethanolamine (mdea) solutions in terms of loading capacity', *Technologies* **4**(3), 19.

Schurink, A. (2022), 'Renewable trias energetica: The path to emission free, renewable energy at your event'. Accessed: 2024-06-02. https://www.linkedin.com/pulse/renewable-trias-energetica-path-emission-free-energy-your-schurink.

Spietz, T., Stec, M., Wilk, A., Krotki, A., Tatarczuk, A. and Więcław-Solny, L. (2018), 'Density correlation of carbonated amine solvents for co2 loading determination', *Asia-Pacific Journal of Chemical Engineering* **13**(6), e2248.

Strazisar, B. R., Anderson, R. R. and White, C. M. (2003), 'Degradation pathways for monoethanolamine in a co2 capture facility', *Energy & fuels* **17**(4), 1034–1039.

Voice, A. K. and Rochelle, G. T. (2011), 'Oxidation of amines at absorber conditions for co2 capture from flue gas', *Energy Procedia* **4**, 171–178.

Voice, A. K., Wei, D. and Rochelle, G. T. (2012), Sequential degradation of aqueous monoethanolamine for co2 capture, *in* 'Recent advances in post-combustion CO2 capture chemistry', ACS Publications, pp. 249–263.

Zanco, S. E., Pérez-Calvo, J.-F., Gasós, A., Cordiano, B., Becattini, V. and Mazzotti, M. (2021), 'Postcombustion co2 capture: a comparative techno-economic assessment of three technologies using a solvent, an adsorbent, and a membrane', *ACS Engineering Au* **1**(1), 50–72.

Zhang, B., Peng, J., Li, Y., Shi, H., Jin, J., Hu, J. and Lu, S. (2022), 'Evaluating co2 desorption activity of tri-solvent mea+ eae+ amp with various commercial solid acid catalysts', *Catalysts* **12**(7), 723.

Zhang, R., Yang, Q., Liang, Z., Puxty, G., Mulder, R. J., Cosgriff, J. E., Yu, H., Yang, X. and Xue, Y. (2017), 'Toward efficient co2 capture solvent design by analyzing the effect of chain lengths and amino types to the absorption capacity, bicarbonate/carbamate, and cyclic capacity', *Energy & Fuels* **31**(10), 11099–11108.

Appendix A

Preparation of liquid reservoir used for Chittick apparatus

The operating mode is related to the Cerato (2023) procedure:

1. In a 1 or 2 L Erlenmeyer Flask, dissolve 100 g of sodium chloride (NaCl) in 350 mL of distilled water ;
2. Add 1 g of sodium bicarbonate ;
3. Add 2 mL of methyl orange solution or 15 mg of methyl orange powder ;
4. Add 1:5 dilute sulfuric acid (1 part concentrated sulfuric acid to 5 parts distilled water) until the solution turns a deep pink (usually about 10 mL) ;
5. Stir overnight ;
6. Add distilled water to fill up to 1 L ;
7. Stir for 1 hour.

Appendix B

Pictures during HCl titration

This section contains images of the setup used for the HCl titration, as well as photos of both degraded and non-degraded samples, taken before and after titration. These photos support the observation that color changes may be less perceptible during titration of highly degraded samples.

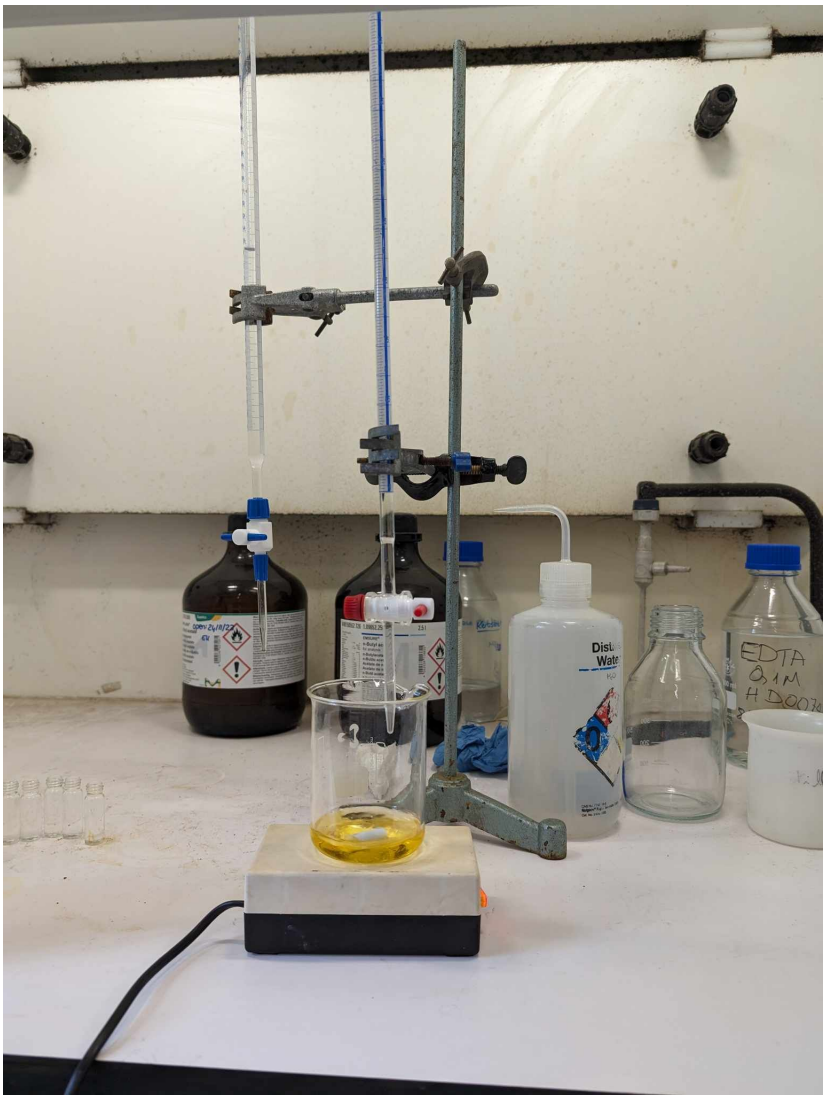

Figure B.1: HCl titration equipment

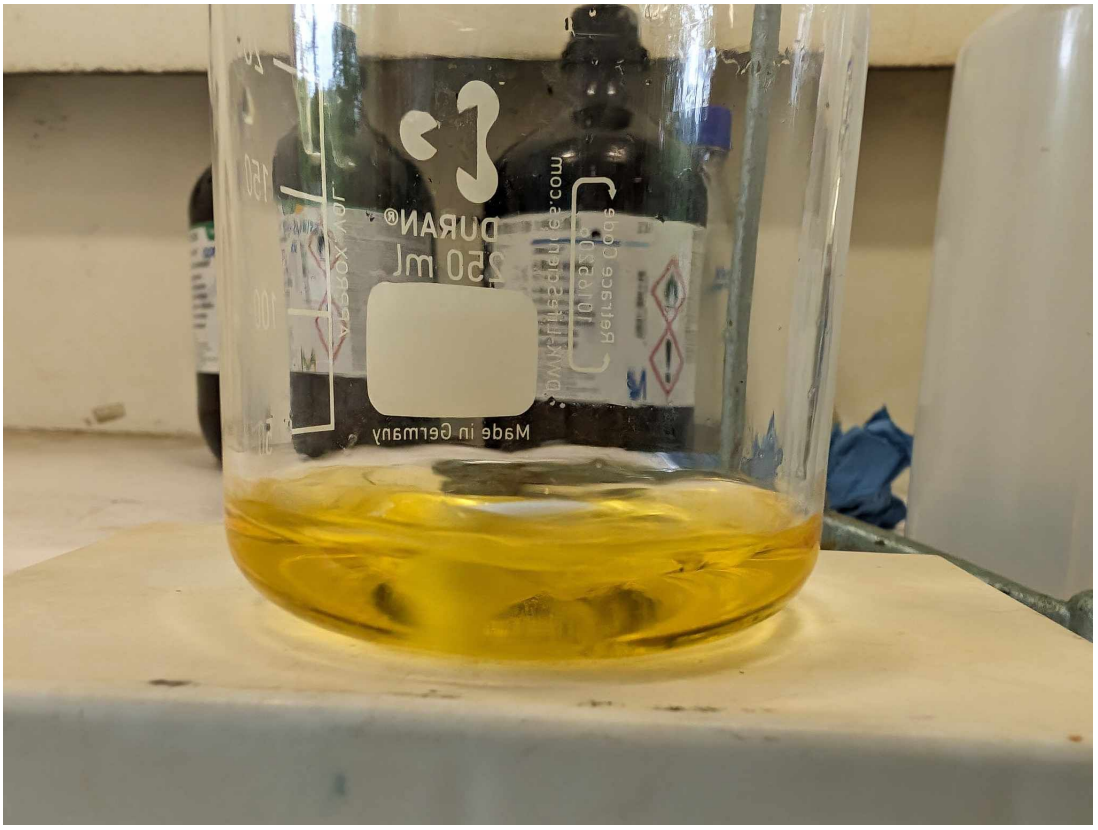

Figure B.2: Solution before HCl titration (low degraded sample)

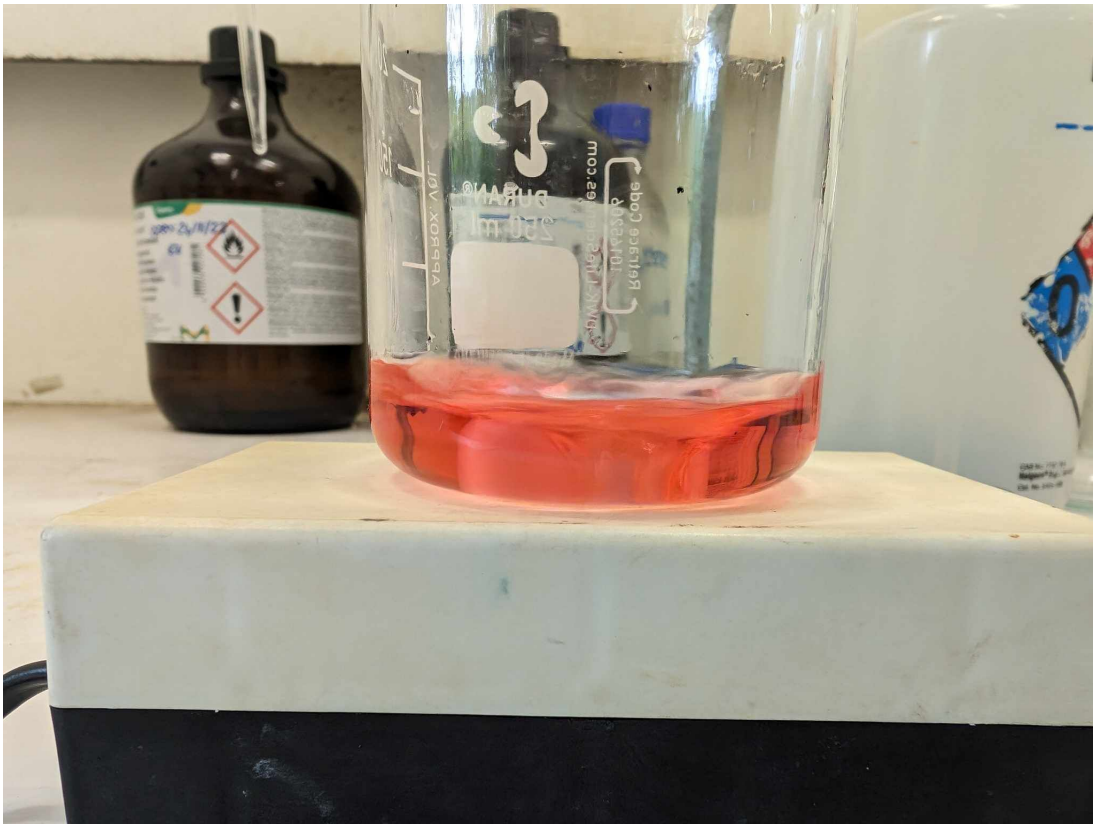

Figure B.3: Solution after HCl titration (low degraded sample)

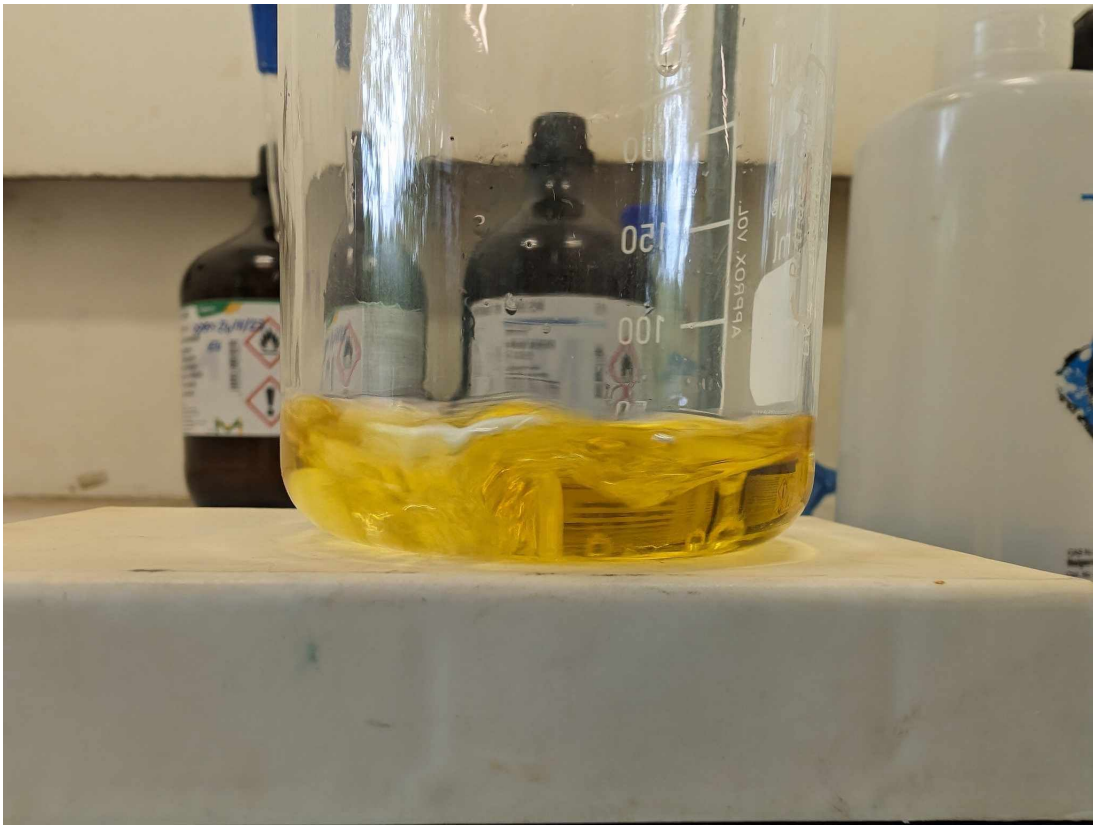

Figure B.4: Solution before HCl titration (high degraded sample)

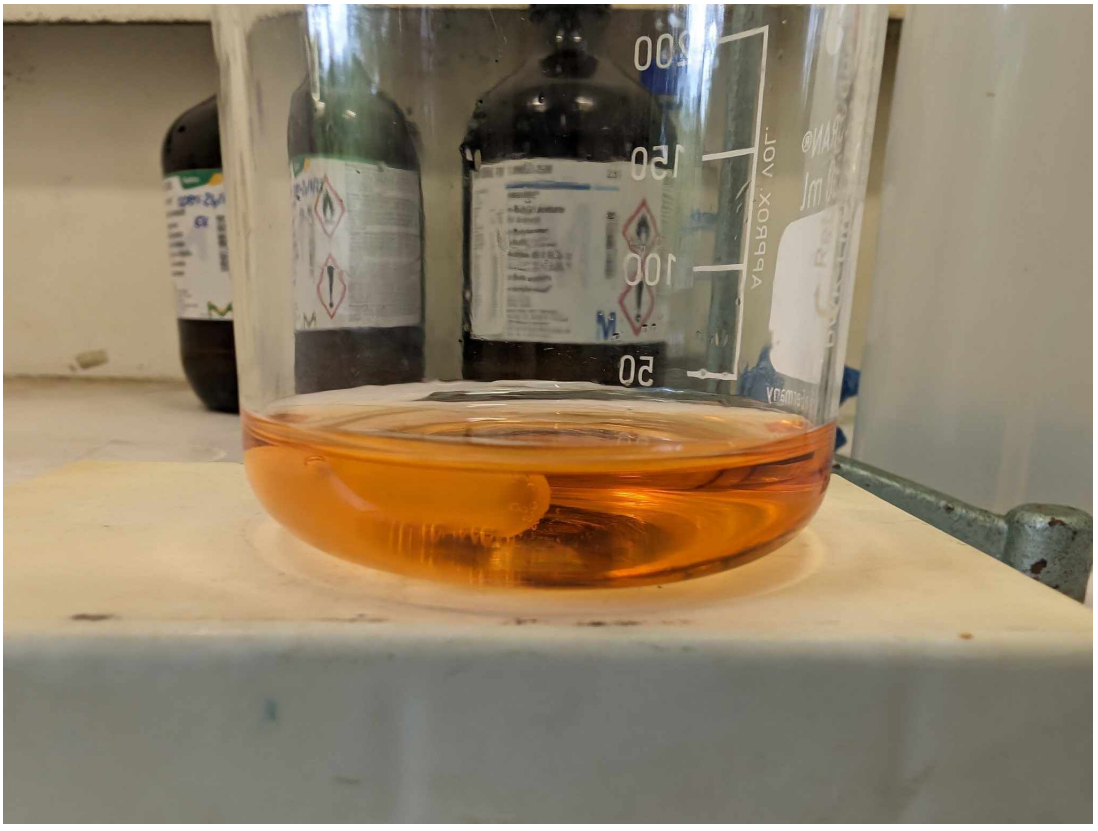

Figure B.5: Solution after HCl titration (high degraded sample)

Appendix C

Examples of peaks in PowerChrome

This section consolidates several intensity peaks observed during HPLC analysis. The graphs feature time on the horizontal axis (in minutes) and signal intensity on the vertical axis (in volts). The analysis commences with an initial intensity peak, attributed to the activation of the automatic injector unit just prior to the sample injection into the column.

The intensity peaks of the amine solvents appear subsequent to a drop in intensity, with the areas under these peaks highlighted in pink. Small peaks may emerge following the amine peaks, which correspond to degradation products. For instance, Figure C.2 illustrates two discernible peaks appearing one minute after the MEA peak.

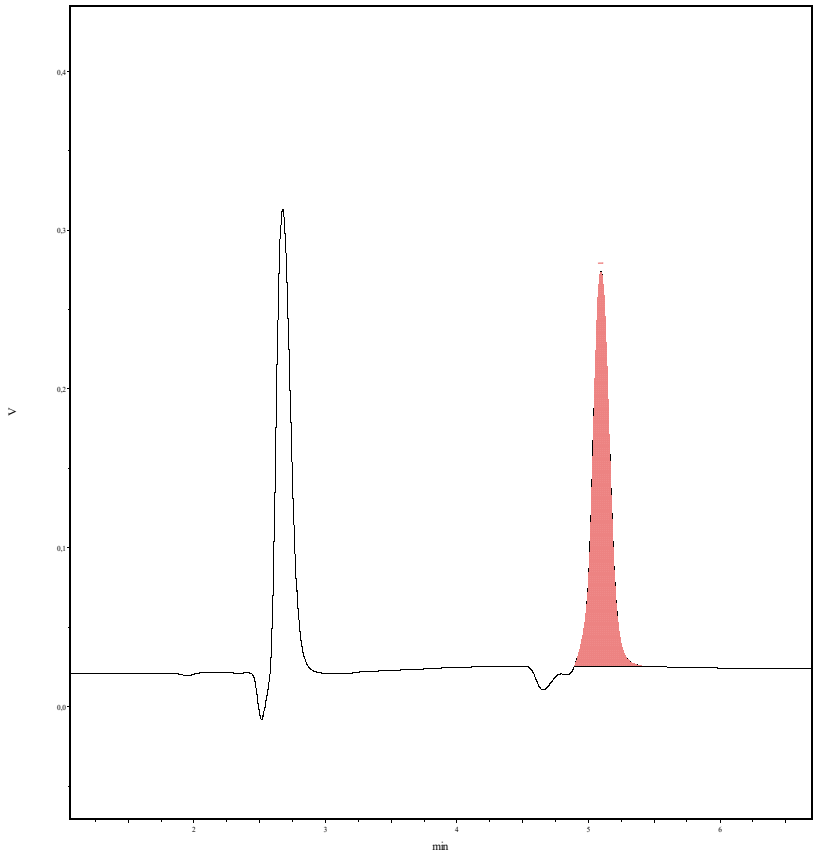

Figure C.1: MEA 30 % peak first calibration curve

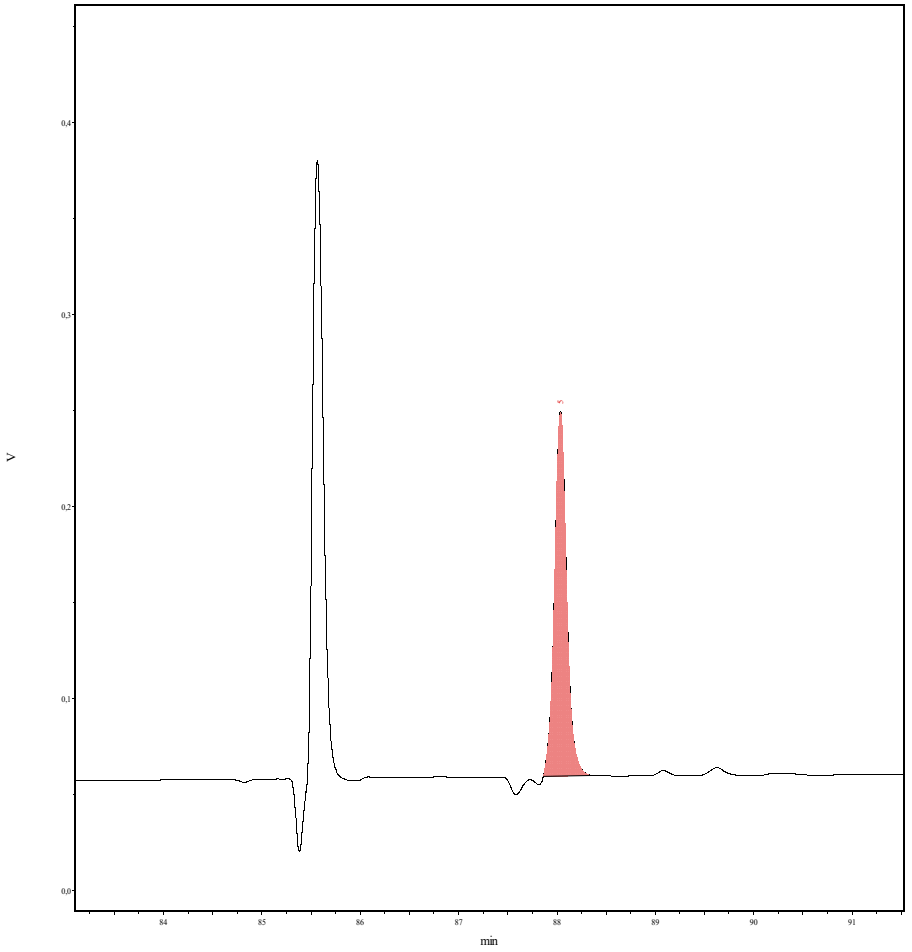

Figure C.2: MEA 30 % degraded sample (Experiment 1)

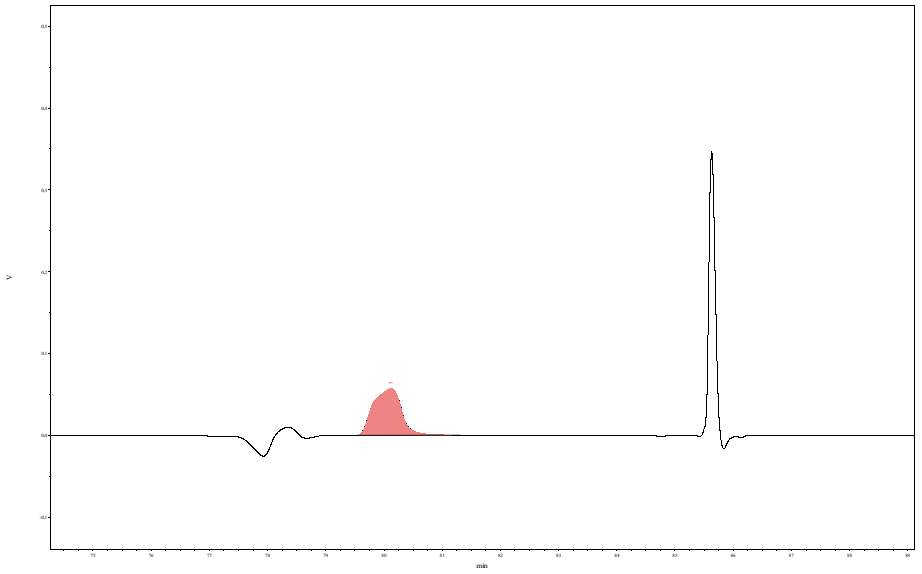

Figure C.3: MEA 30 % peak second calibration curve

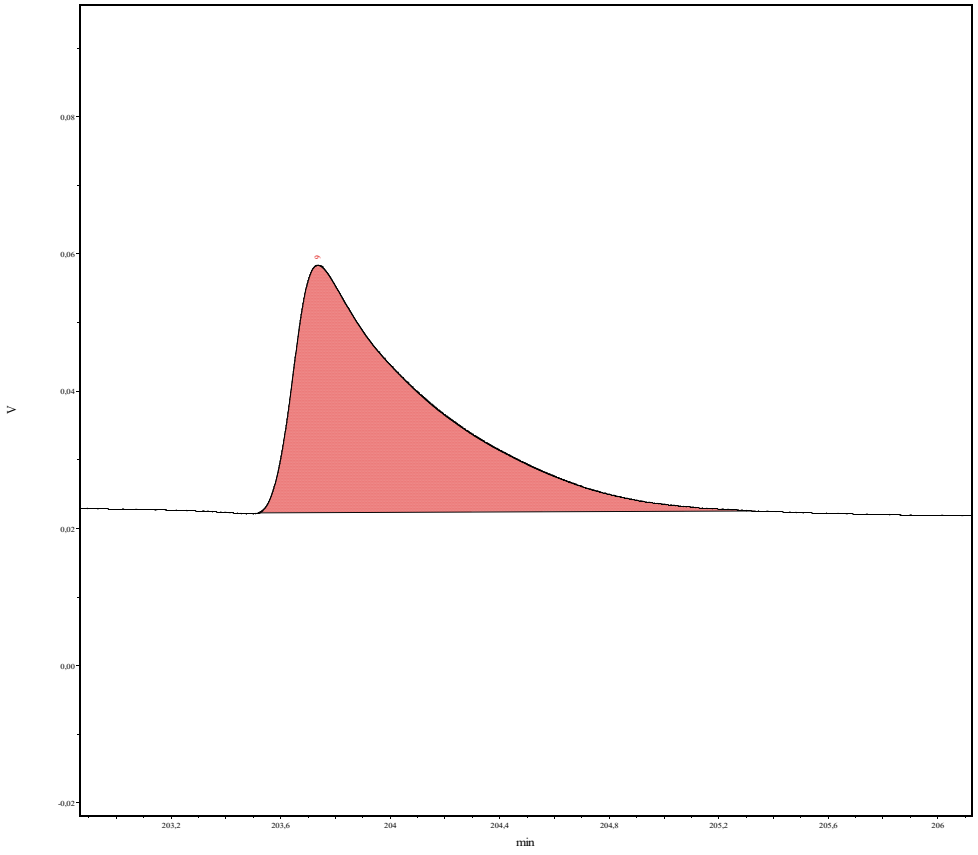

Figure C.4: MEA 30 % degraded sample (Experiment 3)

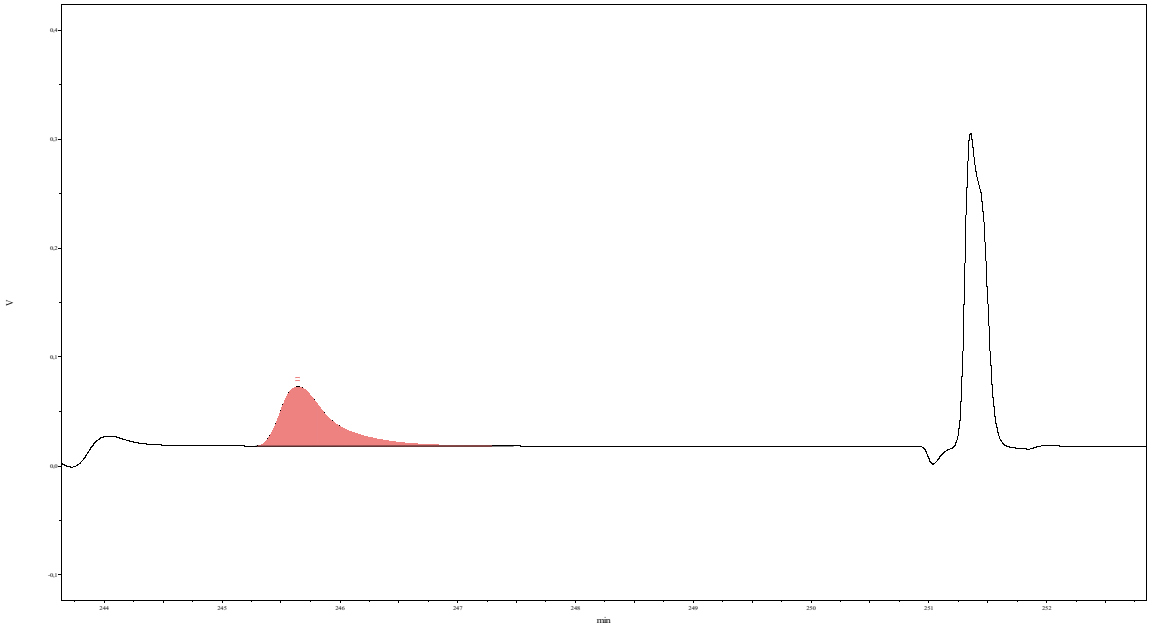

Figure C.5: MEA 30 % degraded sample (Experiment 5)

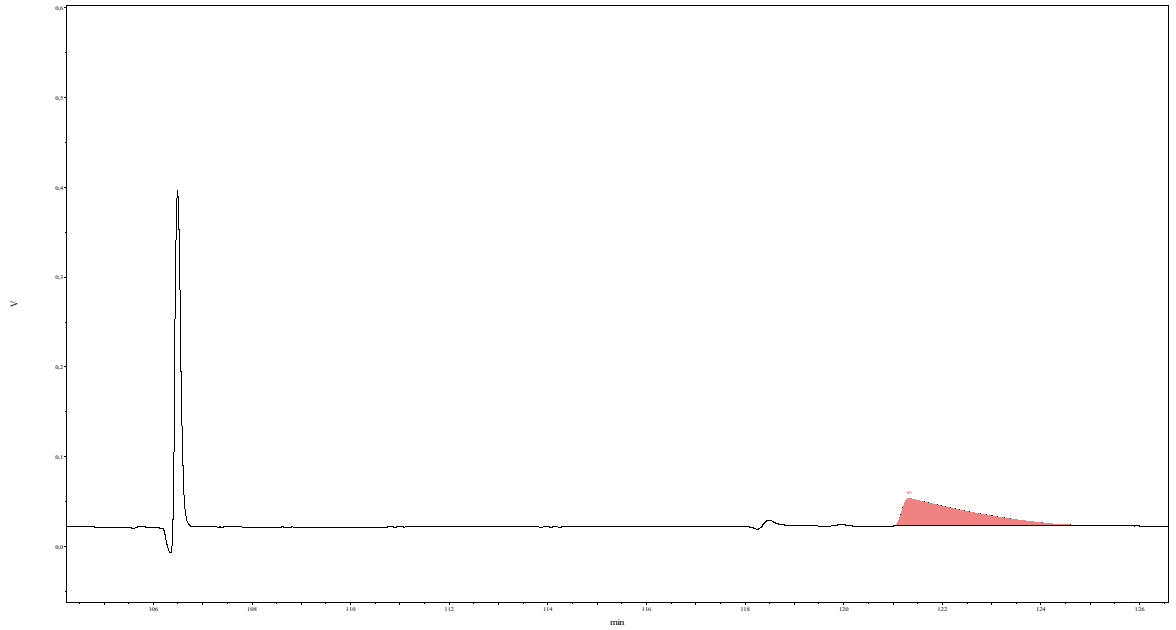

Figure C.6: MDEA 50 % peak calibration curve

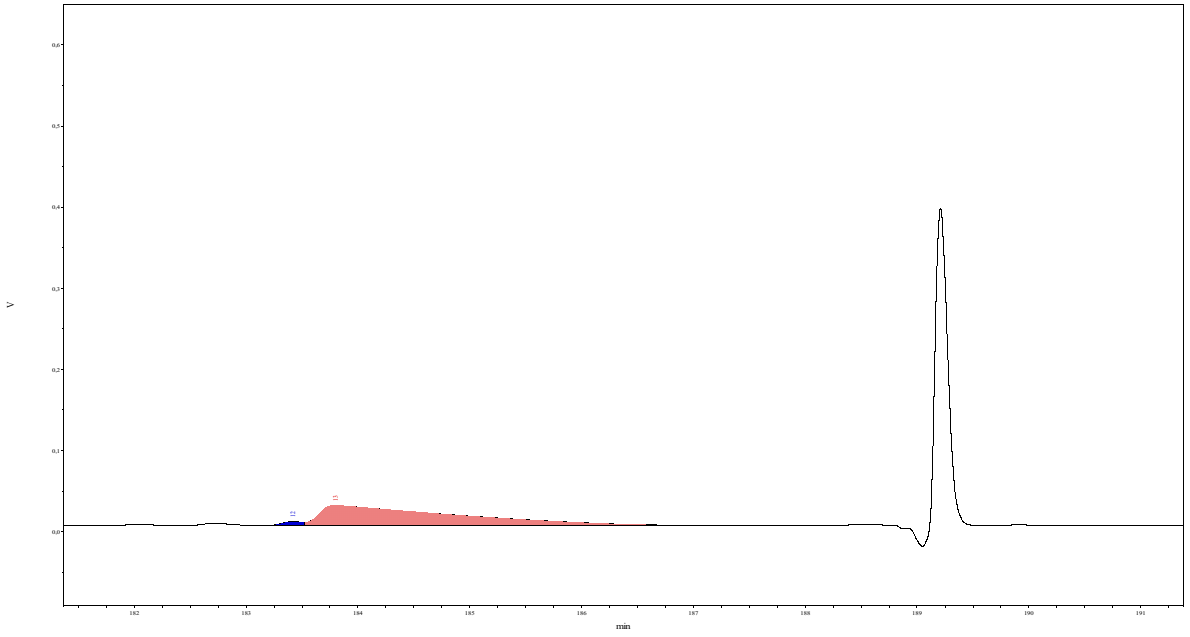

Figure C.7: MEA 50 % degraded sample (Experiment 1)

Appendix D

Pictures during $BaCl_2$ titration

This section displays images of the various setups used during the BaCl2 titration, as well as the condition of the sample at different stages of the process.

Figure D.1: Boiling solution during $BaCl_2$ titration

Figure D.2: Vacuum filtration equipment

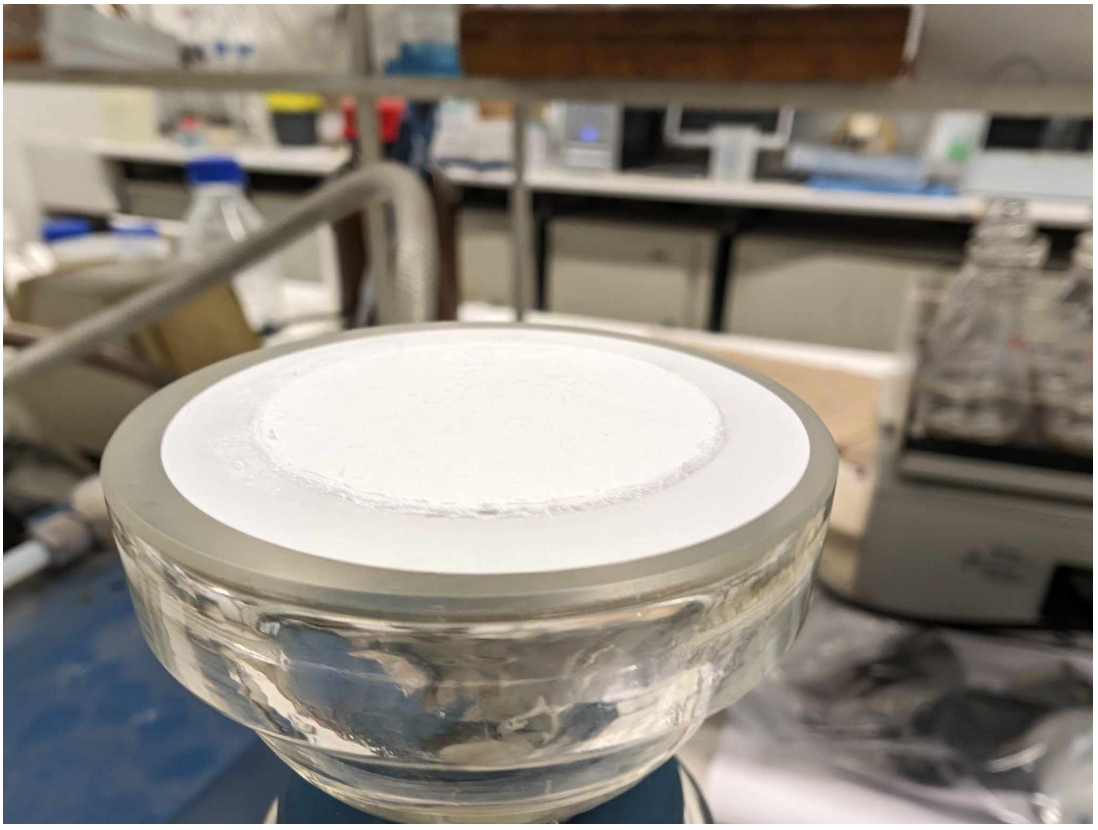

Figure D.3: Precipitate after filtration

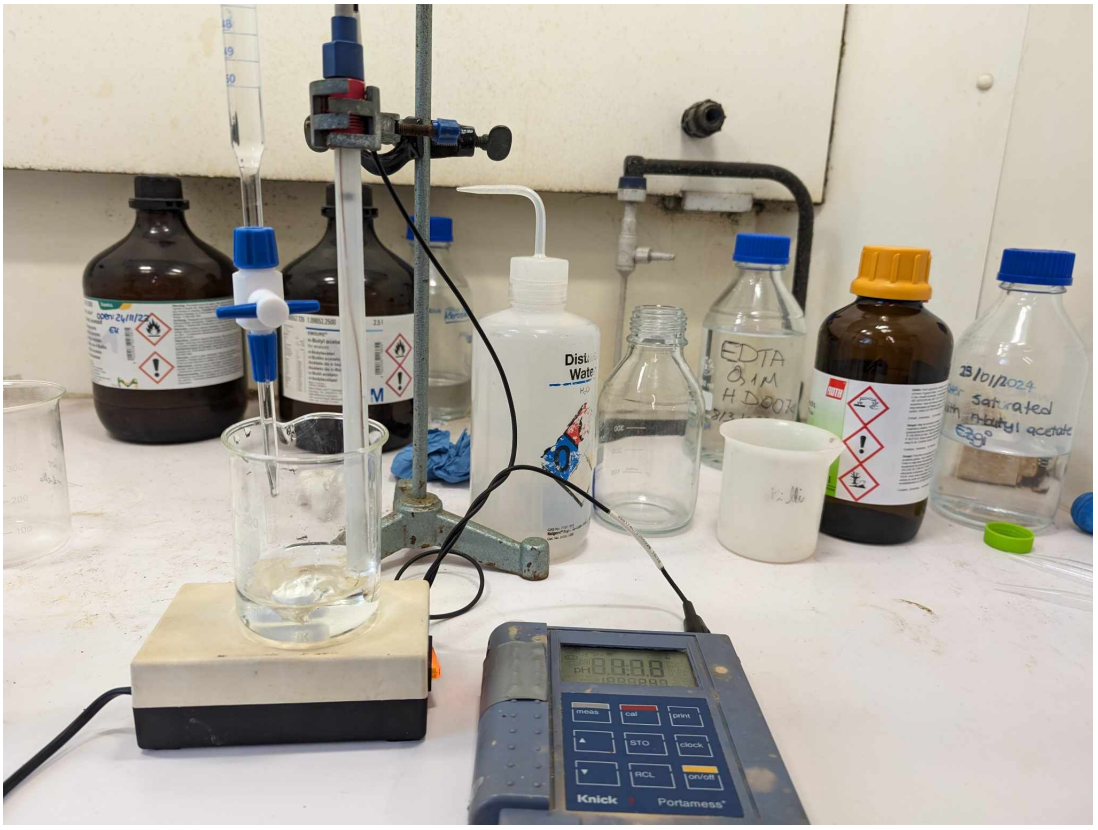

Figure D.4: $BaCl_2$ titration equipment

Appendix E

Samples color

This section compiles samples from the five MEA experiments and the single MDEA experiment. For each figure, the order of the samples is from left to right. It can be observed that the color of the solvent changes progressively throughout the experiment, indicating the extent of degradation. Except for Experiment 1, the leftmost sample was collected at the very beginning of the experiment and is thus undegraded with a transparent coloration. A yellowish color signifies the onset of degradation, followed by orange/red, and finally dark red or even black for the most degraded samples.

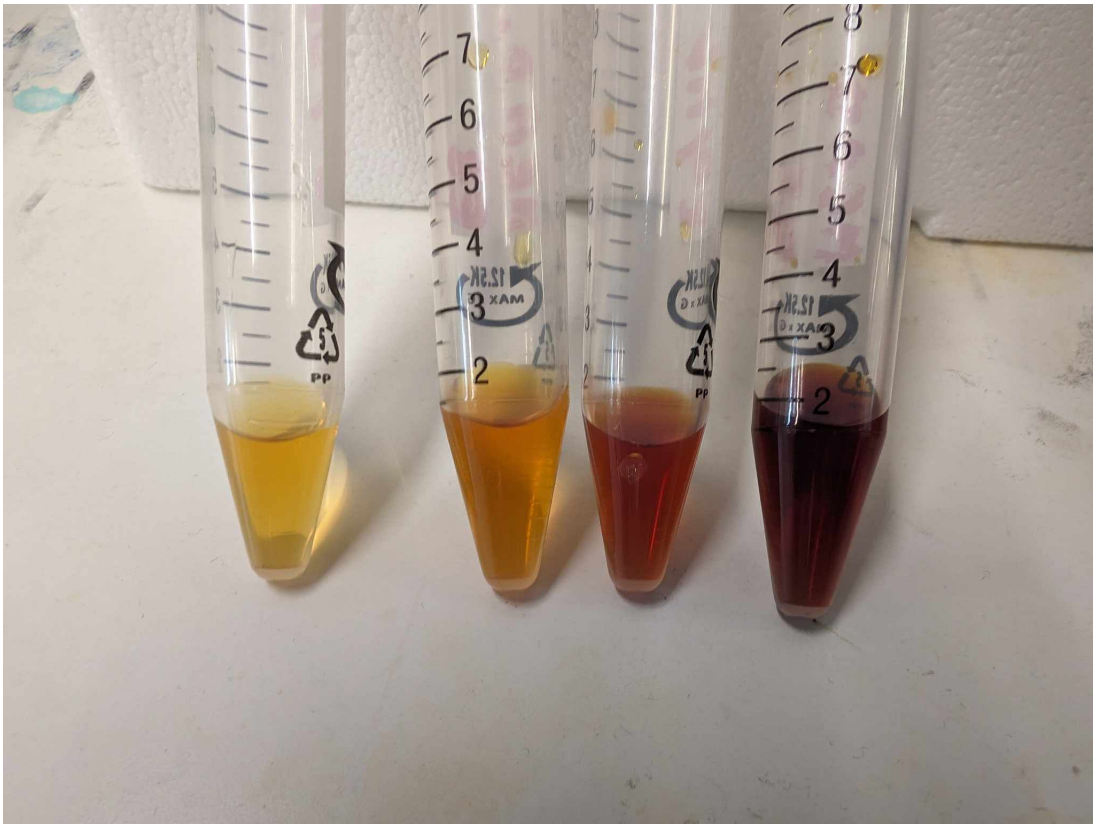

Figure E.1: Samples experiment 1

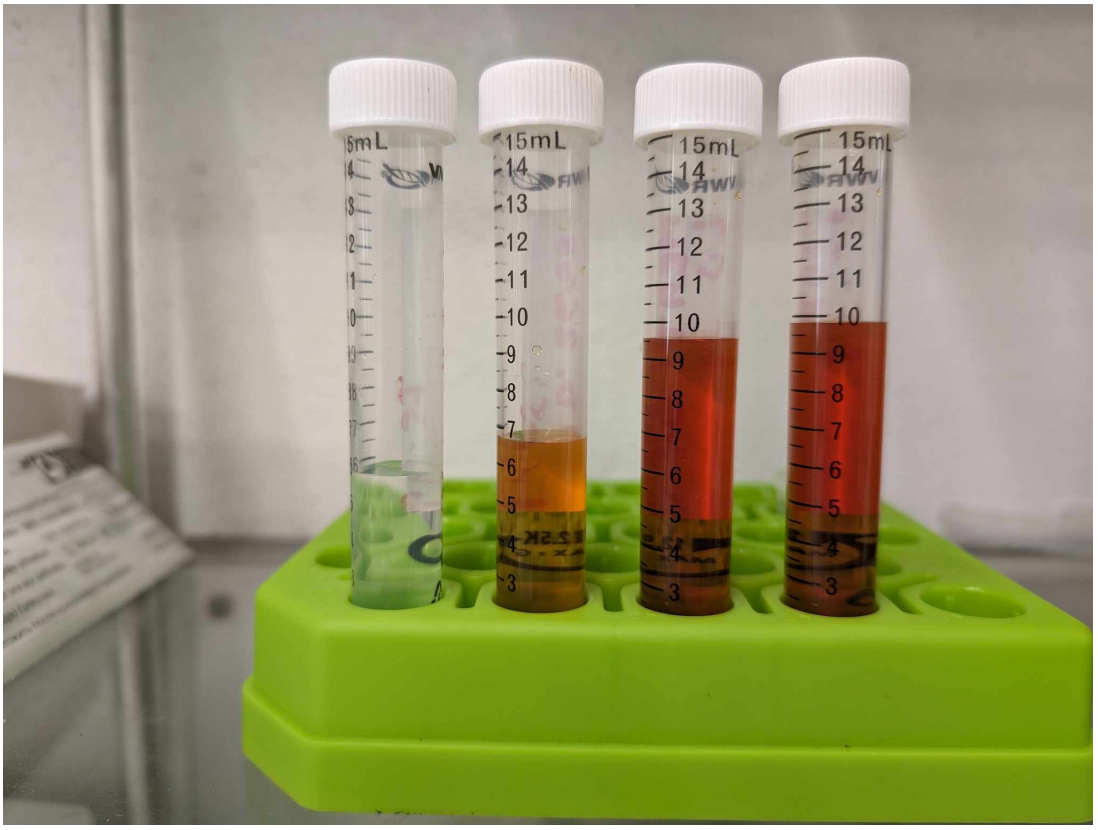

Figure E.2: Samples experiment 2

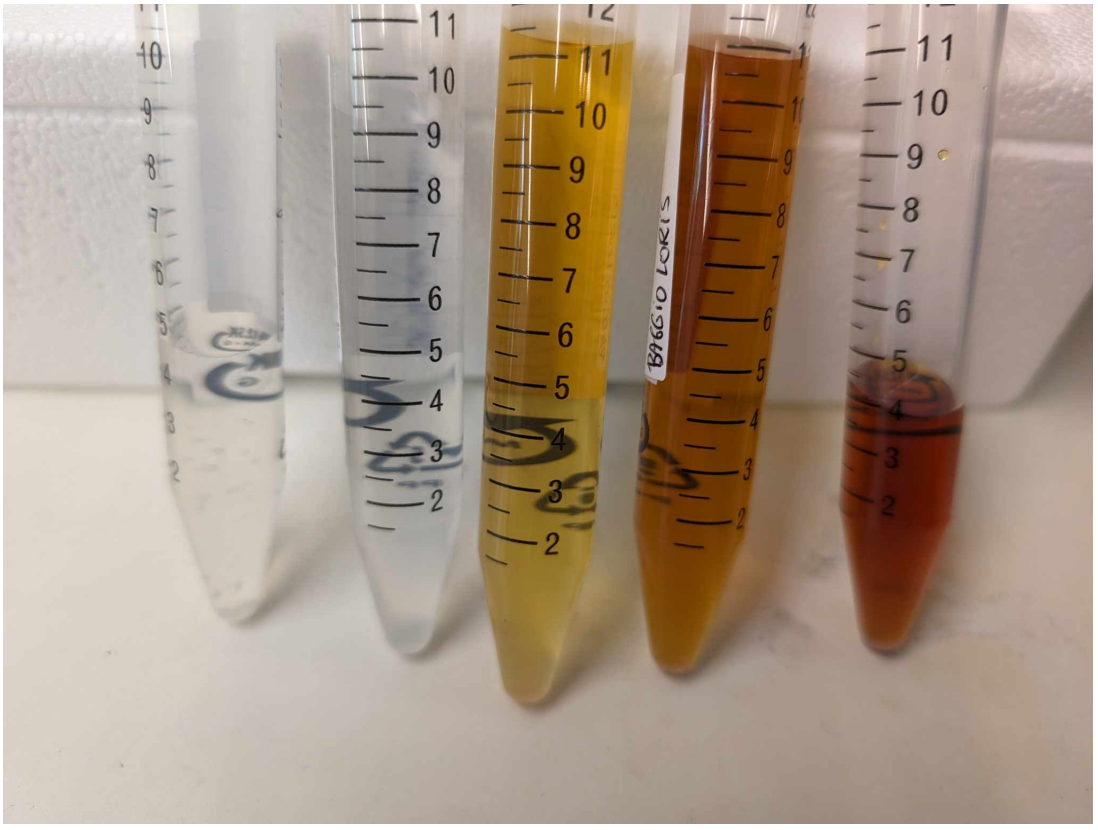

Figure E.3: Samples experiment 3

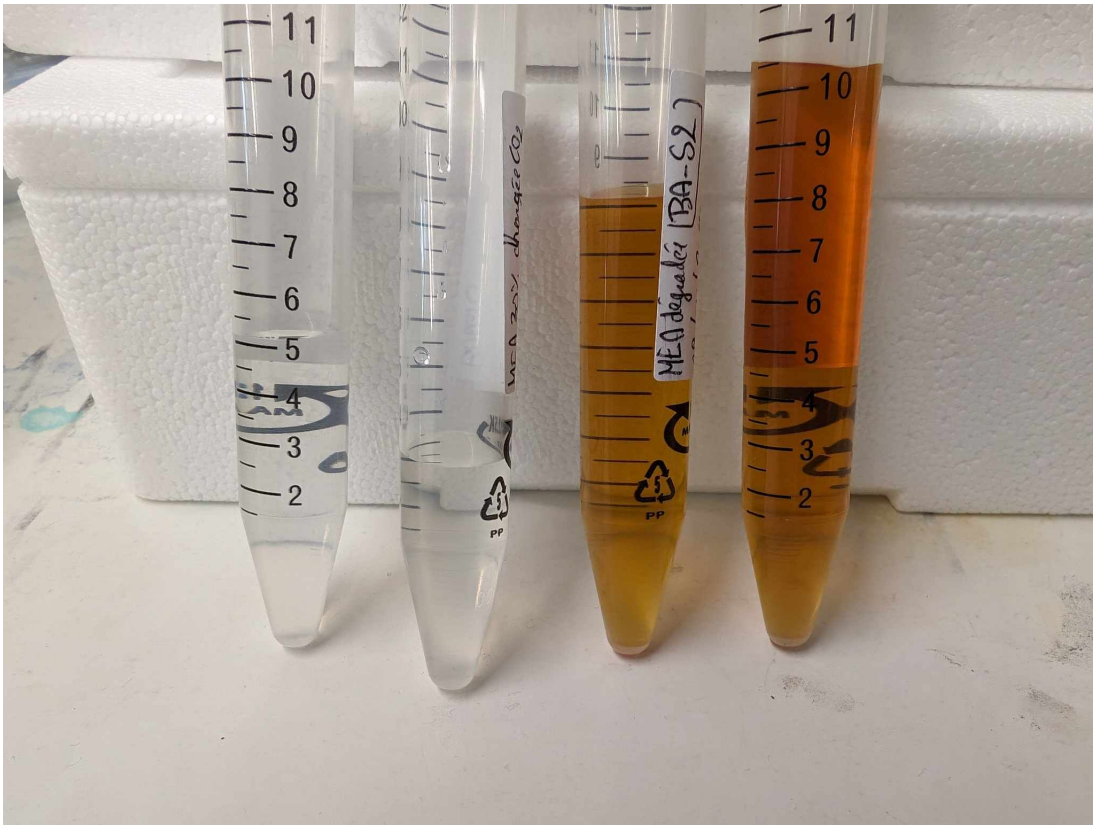

Figure E.4: Samples experiment 4

Figure E.5: Samples experiment 5

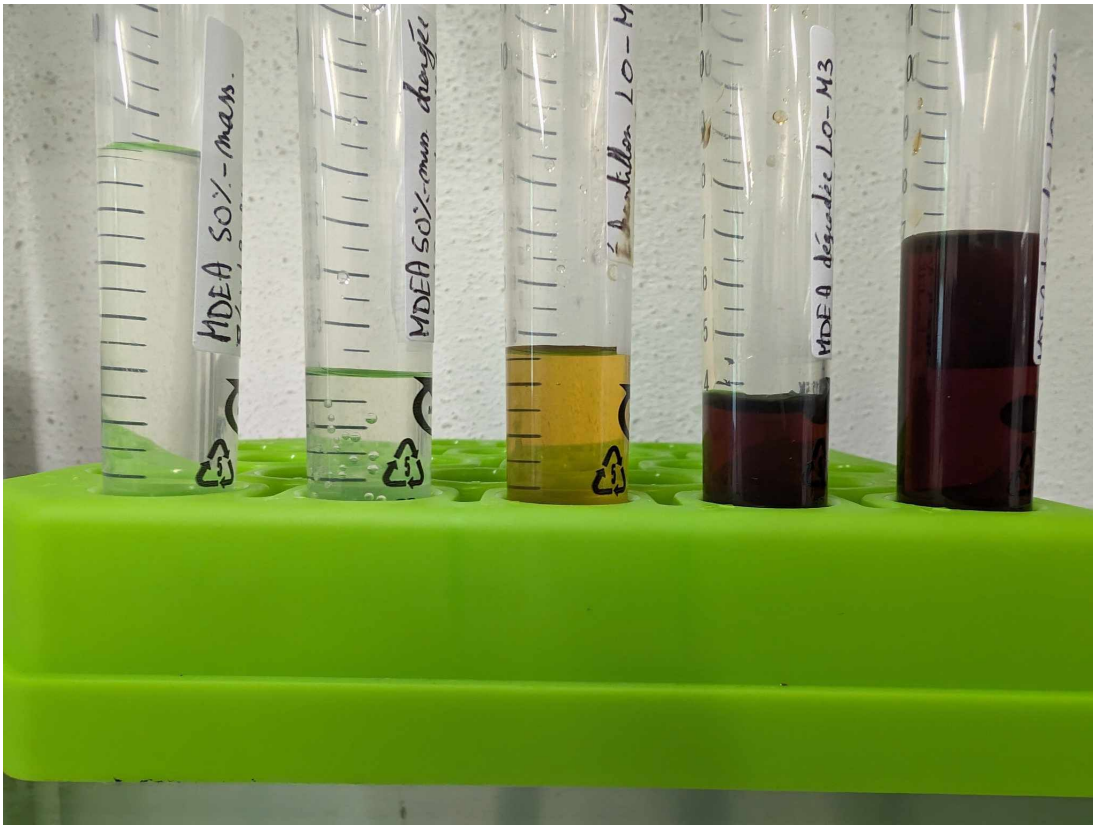

Figure E.6: Samples experiment MDEA

Appendix F

Protocol from all DTR experiments

This annex regroups all DTR experiments concerning MEA CO_2 loading (experiment 0), CO_2 loading with degradation (experiment 1 to 5) and MDEA degradation (experiment MDEA)

VI1. Experiment 0

This experiment was a simple first test of CO_2 loading. Here are the details about the experiment:

- **Initial mass of the reactor:** 3105.0 g
- **Mass after loading:** 3139.4 g
- **Mass of CO_2:** $M_i - M_f = 34.4$ g
- **MEA details:**
  - 90 g of MEA $\rightarrow$ 1.473405 moles (300 g of 30%-mass MEA solution)
- **CO_2 details:**
  - 34.4 g ofCO_2 $\rightarrow$ 0.7816405 moles
- **Loading:** ≈ 0.5305 mol CO_2 per mol MEA

VI2. Experiment 1

Objective: base case for a first test since 2023.

O_2	CO_2	N_2	T°	P	Stirring	Flow rate
%-vol.	%-vol.	%-vol.	°C	barg	rpm	ml/min
5	15	80	120	4	700	160

Table F.1: Input data experiment 1

Initial Conditions

- **Initial weight of the reactor with solution:** 3104.6 g (empty weight: 2804.6 g)

- **Solution composition:** 105 g MEA and 245 g H_2O, with 50 g kept as a sample

Day 1

- 15:33: Start of loading
- 16:33: Weighing of the reactor shows that loading has not yet occurred
- 16:50: Start of the experiment with an uncharged solution and sample 1.1 of the solution

Day 2

- 08:22: Pressure at 5.9 barg (relief valve too tight)
- 08:30: Sample 1.2 (8.5 mL) taken after discarding two dead volumes (2x 1.5 mL)
- 08:36 – 08:56: Condenser cleaning
- 09:00: Restart based on initial conditions

Day 3

- 09:58: Pressure at 4.7 barg (and steady over the last 12 hours according to continuous graphs from Parr software) – 720 rpm
- 10:00: Sample 1.3 (10.2 mL) taken after discarding two dead volumes (2x 1.5 mL)
- 10:05 – 10:30: Cleaning and observation of well-formed crystals
- 10:36: Restart based on initial conditions and stable at 3.9 barg

Day 4

- 09:05: Pressure stable at 4.5 barg over the last 12 hours – 721 rpm
- 09:10: Sample 1.4 (10.5 mL) taken after discarding two dead volumes (2x 1.5 mL)
- 09:15 – 09:50: More complicated cleaning due to significant crystals at the upper junction of the valve and the condensed pipe
- 09:58: System restart based on initial conditions and pressure at 3.9 barg

Day 5

- 09:30: Pressure at 6 barg, but outlet pressure at 0 barg indicating a blockage at the condenser; additionally, white deposit seen at the junctions with the condenser, estimated via graphs to have occurred around 16:40 on Day 4
- 09:40: Sample 1.5 (10.5 mL) taken after discarding two dead volumes (2x 1.5 mL)
- Reactor weight at 3055 g, evaluating the samples taken (± 53.3 g), giving a total of 3108.3 g (3.7 g more than initially, indicating slight solution loading during the experiment)

Post-Experiment Observations After cleaning, it was evident that the crystals had blocked the junction from the reactor outlet to the valve and the valve itself.

VI3. Experiment 2

Objective: observe the oxygen influence.

O_2	CO_2	N_2	T°	P	Stirring	Flow rate
%-vol.	%-vol.	%-vol.	°C	barg	rpm	ml/min
10	15	75	120	4	700	160

Table F.2: Input data experiment 2

Initial Conditions

- **Initial weight of the reactor with solution:** 3104.7 g (empty weight: 2804.7 g)
- **Solution composition:** 93 g MEA and 210.3 g H_2O, with 10.3 g kept as a sample (sample 2.1)

Day 1

- 10:30: Start of CO_2 loading, temperature rises but pressure drops to 0 barg
- 13:18: After replacing the reactor clamp and the cooling system hoses, restart of loading
- 15:00: End of loading indicated by pressure increase; reactor weighed at 3139.3 g (estimated 34.6 g of CO_2 absorbed, charge of 0.533 mol CO_2/mol MEA)
- 15:24: 76 °C – 699 rpm – 4.4 barg
- 15:38: 119 °C – 701 rpm – 3.9 barg

Day 2

- 08:40: 120 °C – 704 rpm – 4.0 barg
- 15:04: Pressure increased to 7.6 barg due to an ammonium carbonate crystal blockage, estimated to have formed around 14:45
- 15:10: Sample 1.2 (10.5 mL) taken after discarding 1 dead volume (1.5 mL)
- 15:22: Restart after cleaning parts above the valve
- 15:25: Adjusted cooler setpoint to 18 °C instead of 16 °C
- 16:28: 120 °C – 703 rpm – 4.9 barg

Day 3

- 08:32: 120 °C – 705 rpm – 4.5 barg (stable over the last 12 hours according to Parr graph)
- 08:42: Pressure increased to 5.2 barg and outlet pressure decreased
- 08:45: Started cleaning phase for the condenser to remove significant crystals
  - Restarted, but no return of outlet pressure indicating crystals between reactor outlet and valve
  - Experiment stopped due to crystal location needing clearing

- 09:38: Samples 1.3 and 1.4 (13 mL and 13.5 mL) taken without discarding dead volume
- Reactor weighed at 3065.1 g
  - Initial mass after loading: 3139.3 g
  - Mass of all samples: ~37 g
  - Mass of dead volume: ~2 g
  - Mass difference: 35 g (losses in pipes and mostly crystals)
- 12:15: Started Phase II cleaning (400 rpm, 120 °C, 4 barg)

Day 4

- Pressure loss noticed as only 0.9 barg in the reactor
- Water conductivity at 73 μS
- After cleaning, it was noted that the condensed pipe had leaks and needed to be tightened entirely

VI4. Experiment 3

Objective: basic case.

O_2	**CO_2**	**N_2**	**T°**	**P**	**Stirring**	**Flow rate**
%-vol.	%-vol.	%-vol.	°C	barg	rpm	ml/min
5	15	80	120	4	700	160

Table F.3: Input data experiment 3

Initial Conditions

- **Initial weight of the reactor with solution:** 3120.7 g (empty weight: 2804.7 g)
- **Solution composition:** 99.1 g MEA and 231 g H_2O, with approximately 15 g kept as a sample (sample 3.0)
- 330 g of solution prepared and charged with 316 g of solution.

Day 1

- **CO_2 loading started** (700 rpm – 150 ml/min CO_2):
  - 10:14: 27 °C – 679 rpm – 0.7 barg
  - 11:19: 33 °C – 701 rpm – 1.6 barg
  - 11:39: 36 °C – 706 rpm – 1.7 barg
  - 12:00: 38 °C – 709 rpm – 1.7 barg
  - 13:23: 38 °C – 711 rpm – 2.8 barg (peak T = 40 °C around 13:10)
- Reactor mass = 3159.2 g (38.5 g of CO_2)

- Charge = (38.5/44.01)/(316*0.3/61.083) = 0.562
- **Base case experiment started for 72h after sampling** (sample 3.1), approximately 14 mL (and 2 dead volumes):
  - 13:44: 66 °C – 708 rpm – 3.8 barg
  - 13:51: 95 °C – 710 rpm – 4.4 barg
  - 14:00: 116 °C – 710 rpm – 3.8 barg
  - 14:54: 118 °C – 716 rpm – 3.4 barg
  - 15:11: 120 °C – 707 rpm – 3.7 barg
- Note: The door of the room housing the DTR will remain open during the experiment.

Day 2

- 08:22: 120 °C – 704 rpm – 3.4 barg (tightened the relief valve)
- 08:33: Sample of 14.5 mL solution taken (sample 3.2) (+ 2 dead volumes)
- **Flow rate adjustments to match an initial situation of 300 mL:**
  - Approximately 5
    - 160*0.95 = 152 ml/min distributed as follows:
      - O_2 = 7.6 mL (5
      - CO_2 = 22.8 mL (15
      - N_2 = 121.6 mL (80
- No apparent signs of crystal formation, no cleaning (goal of 72h without cleaning).
- 08:35: 120 °C – 705 rpm – 3.8 barg
- 08:50: 120 °C – 705 rpm – 4.0 barg

Day 3

- 08:59: 120 °C – 705 rpm – 3.9 barg
- 09:05: Sample of 14.5 mL solution taken (sample 3.3) (+ 2 dead volumes)
- **Flow rate adjustments to match an initial situation of 300 mL:**
  - Approximately 10
    - 160*0.90 = 144 ml/min distributed as follows:
      - O_2 = 7.2 mL (5
      - CO_2 = 21.6 mL (15
      - N_2 = 115.2 mL (80
- No apparent signs of crystal formation, no cleaning (goal of 72h without cleaning).
- 10:07: 120 °C – 705 rpm – 4.0 barg

Day 4

- 15:33: 120 °C – 705 rpm – 7.2 barg
- Blockage due to ammonium carbonate formation, likely stopping the experiment around 10:00 (pressure went from 4.1 barg to 6.1 barg)
- Slight pressure still observed at reactor outlet...
- 15:40: Sample of 14.5 mL solution taken (sample 3.4) (+ 2 dead volumes)
- The gas outlet valve is completely blocked (crystals), solution extracted via the sampler:
  - 238.3 g of solution weighed
  - Reactor weighed after releasing pressure, measured at 2831.5 g
- Final reactor mass = 3069.8 g.
- **Phase II cleaning started** (after cleaning all piping and removing crystals):
  - Reactor mass = 3190.5 g
  - 17:16: 25 °C – 402 rpm – 1.8 barg
  - 17:25: 37 °C – 405 rpm – 3.7 barg

Day 5

- 08:10: 120 °C – 411 rpm – 3.8 barg at the end of cleaning
- Reactor mass = 3179.2 g (+10 g taken for cleaning the sampler) indicating very low or no loss.

VI5. Experiment 4

Objective: basic case.

O_2	**CO_2**	**N_2**	**T°**	**P**	**Stirring**	**Flow rate**
%-vol.	%-vol.	%-vol.	°C	barg	rpm	ml/min
5	15	80	120	4	700	160

Table F.4: Input data experiment 4

Initial Conditions

- **Initial weight of the reactor with solution:** 3129.8 g (empty weight: 2804.6 g)
- **Solution composition:** 102.1 g MEA and 237.9 g H_2O, with approximately 15 g kept as a sample (sample 4.0)
- 340 g of solution prepared and charged with 325.1 g of solution.

Day 1

- **Reactor mass before CO_2 loading:** 3129.8 g
- **CO_2 loading started:**

  - 11:05: 30 °C - 704 rpm - 0.9 barg
  - 12:15: 37 °C - 710 rpm - 2 barg
  - 12:43: 40 °C – 723 rpm – 2 barg
  - 13:13: 43 °C – 694 rpm – 2.1 barg
  - 14:04: 43 °C – 695 rpm – 2.6 barg (loading completed)
- Reactor mass = 3166.9 g, corresponding to an addition of 37.1 g of CO_2. Sample of 15 mL taken (sample 4.1).
- Charge = $(37.1/44.01)/(97.53/61.083) = 0.528$ mol CO_2/mol MEA
- **Program launched:** 8 mL O_2 – 24 mL CO_2 – 128 mL N_2
  - 14:19: 40 °C – 689 rpm – 2.7 barg (heating stage II)
  - 14:27: 61 °C – 691 rpm – 4.2 barg (heating stage I)
  - 14:42: 117 °C – 693 rpm – 4.0 barg
  - 14:48: 122 °C – 693 rpm – 4.2 barg
  - 14:55: 123 °C – 693 rpm – 4.0 barg
  - 15:45: 119 °C – 696 rpm – 3.8 barg (adjusting the relief valve)
  - 16:28: 120 °C – 699 rpm – 4.1 barg

Day 3

- 09:07: 120 °C – 687 rpm – 4.5 barg (over the last 12 hours, pressure decreased from 4.7 barg to 4.5 barg)
- 09:15: Sample of 12 mL taken (sample 4.2) (+ 2 dead volumes)
- 15:15: Sample of 15 mL taken (sample 4.3) (+ 2 dead volumes)
- 15:20: End of experiment (only 48h)
  - Note: Low presence of crystals compared to previous experiments, and no intermediate cleaning of the condenser tube was required.
- Reactor mass = 3105.7 g – total mass of samples = approximately 43 g – mass of dead volumes = approximately 7 g
- **Total loss:** approximately 11 g
- Phase I cleaning followed by Phase II cleaning (started at 16:17)
- Reactor and water mass = 3154.3 g

Day 4

- End of cleaning at 16:18 (120 °C – 415 rpm – 4.3 barg)
- Reactor and water mass = 3153.9 g (loss of 0.4 g)
- Conductivity = 128 μS from a 50 mL sample kept in the refrigerator

VI6. Experiment 5

Objective: repeatability of basic case.

O_2	CO_2	N_2	T°	P	Stirring	Flow rate
%-vol.	%-vol.	%-vol.	°C	barg	rpm	ml/min
5	15	80	120	4	700	160

Table F.5: Input data experiment 5

Initial Conditions

- **Initial weight of the reactor with solution:** 3118.0 g (empty weight: 2804.7 g)
- **Solution composition:** 99 g MEA and 231 g H_2O, with approximately 15 g kept as a sample (sample 5.0)
- 330 g of solution prepared and charged with 313.3 g of solution.

Day 1

- **CO_2 loading started (700 rpm – 150 ml/min CO_2):**
  - 09:24: 29 °C – 686 rpm – 0.4 barg
  - 09:45: 30 °C – 694 rpm – 1.3 barg
  - 10:07: 32 °C – 697 rpm – 1.5 barg
  - 10:52: 37 °C – 700 rpm – 1.5 barg
  - 11:54: 41 °C – 702 rpm – 1.6 barg
  - 12:04: 40 °C – 702 rpm – 1.7 barg (weighing at 3150 g, continued loading)
  - 12:13: 39 °C – 697 rpm – 1.5 barg
  - 12:18: 38 °C – 697 rpm – 1.7 barg
  - 12:27: 38 °C – 700 rpm – 1.8 barg
  - 12:30: 38 °C – 700 rpm – 1.9 barg (end of loading)
- Reactor mass = 3155.8 g (37.8 g of CO_2)
- Charge = $(37.8/44.01)/(313.3 * 0.3/61.083) = 0.558$
- Sample of 10 mL taken (4.1) (+ 2 mL dead volume)
- **Base case started (72h) at 12:41:**
  - 12:41: 36 °C – 698 rpm – 2.2 barg (heating power on II)
  - 12:50: 58 °C – 699 rpm – 3.5 barg (heating power on I)
  - 13:13: 121 °C – 702 rpm – 4.0 barg
  - 13:21: Sample 1.5 mL (sample 5.1.1) + 2 mL dead volume
  - 14:28: Sample 1.5 mL (sample 5.1.2) + 2 mL dead volume

- 15:28: Sample 1.5 mL (sample 5.1.3) + 2 mL dead volume
- 16:15: 120 °C – 706 rpm – 4.1 barg

Day 3

- 08:36: 120 °C – 705 rpm – 4.0 barg
- 13:24: 120 °C – 706 rpm – 4.2 barg
- Sample of approximately 14 mL taken (sample 5.2) (+ 2 mL dead volume)
- Adapted flow rates: 7.2 mL/min O_2, 21.6 mL/min CO_2, and 115.2 mL/min N_2
- 13:30: 120 °C – 707 rpm – 4.2 barg
- 16:03: 120 °C – 708 rpm – 6.4 barg (crystals present, blockage detected at 15:00)
- Cleaned upper part of gas outlet valve, resumed with 80
- Pressure remained at 6.3 barg, solution transferred to glass bottle to reduce pressure to 0 barg in the reactor, allowing for valve and lower part disassembly and cleaning.
- Solution mass in bottle = 599.3 g - 333.7 g = 265.6 g, reinjected into the reactor with a 2 g loss (bottle reweighed at 335.8 g).
- 16:47: Restarted with 80
- 17:08: 123 °C – 707 rpm – 3.8 barg
- 17:09: 124 °C – 707 rpm – 3.9 barg

Day 4

- 08:55: 120 °C – 711 rpm – 3.8 barg (seems stable)
- Pressure had risen to 5 barg by Wednesday, 01/05/2024
- Outlet pressure ~1 barg and saturator pressure 5.4 barg, indicating an issue (generally a max difference of 0.5 barg between saturator and reactor)
- 09:10: Sample of 15 mL taken (sample 5.3) (+ 2 mL dead volume)
- Solution transferred to bottle to reduce reactor pressure due to blockage below gas outlet valve; pressure remained at 3.8 barg despite cooling to 35 °C, indicating an issue with the pressure sensor.
- Solution mass in bottle = 597.6 g - 353.5 g = 244.1 g
- Reactor mass = 2829.2 g
- Reactor and solution mass (after recalculation) = 3073.3 g
- Total sample mass ~44 g
- Total dead volume mass ~17.5 g

- Transferring loss ~2.2 g
- Recalculated mass ~3137 g (loss of 18.8 g?)

Day 4

- Cleaning revealed pressure was blocked near the pressure sensor due to crystals, causing constant display.
- Phase I cleaning rigorously performed and Phase II cleaning started.
- 12:00: Cleaning procedure started with reactor mass = 3227.2 g
- 12:13: 28 °C – 400 rpm – 0.0 barg
- 12:17: 34 °C – 403 rpm – 2.0 barg
- 12:37: 108 °C – 405 rpm – 4.0 barg (increased opening of drain)
- 12:43: 119 °C – 405 rpm – 3.9 barg
- 12:44: 120 °C – 406 rpm – 4.0 barg
- 12:57: 123 °C – 406 rpm – 3.9 barg
- 14:44: 120 °C – 411 rpm – 4.0 barg
- 16:13: 120 °C – 413 rpm – 4.1 barg (increased opening of drain, which was an error)

Day 5

- 08:36: 120 °C – 412 rpm – 3.3 barg
- From 16:40 the previous day, the pressure was at 3.5 barg due to the increased drain opening, then dropped to 3.3 barg by 03:20 (possible small leak).
- Reactor mass = 3215.7 g (+ 6 g used to clean the sampler), indicating a loss of approximately 5.5 g.
- Conductivity measured at 46 µS.

VI7. Experiment MDEA

Objective: 50 % wt MDEA degradation.

O_2	**CO_2**	**N_2**	**T°**	**P**	**Stirring**	**Flow rate**
%-vol.	%-vol.	%-vol.	°C	barg	rpm	ml/min
5	15	80	120	4	700	160

Table F.6: Input data experiment MDEA

Initial Conditions

- **Initial weight of the reactor with solution:** 3104.7 g (empty weight: 2804.7 g)

- **Solution composition:** 160 g MEA and 160 g H_2O, with approximately 20 g kept as a sample (sample MDEA.1)
- 320 g of solution prepared and charged with 300 g of solution. Reactor mass with solution = 3104.7 g; sample taken (sample MDEA.0) for the 50

Day 1

- **CO_2 loading started:**
  - 09:17: 27 °C – 590 rpm – 1.4 barg
  - 09:51: 29 °C – 606 rpm – 2.7 barg
  - 11:03: 33 °C – 612 rpm – 3.7 barg
  - 12:00: 36 °C – 620 rpm – 4.8 barg
  - 12:44: 37 °C – 623 rpm – 5.7 barg (end of loading)
- Reactor mass = 3140.5 g (35.8 g of CO_2 added); charge = $(35.8/44.01)/(150/119.163) = 0.646$.
- Sample of 10.2 mL taken (sample MDEA.2).
- **Degradation operation started at 13:01:**
  - 13:06: 35 °C – 690 rpm – 3.6 barg
  - 13:21: 92 °C – 695 rpm – 5.9 barg
  - 13:37: 113 °C – 696 rpm – 3.5 barg
  - 14:19: 119 °C – 700 rpm – 3.7 barg

Day 2

- 08:00: 120 °C – 0 rpm – 4.3 barg (stirring system failed around 4 am according to recorded graphs).
- Sample of 11 mL taken (sample MDEA.3) after discarding 2 dead volumes.
- The belt broke at the "arm" connecting the motor turntable to the stirring system; no replacement parts available.
- 09:50: Operation put on standby by closing all valves to conserve gas in the system (gas flow stopped).
- 120 °C – 0 rpm – 3.9 barg

Day 4

- 08:40: 120 °C – 0 rpm – 3.7 barg (belt replacement scheduled for Monday using O-ring from CoJoint).

Day 8

- 08:19: 120 °C – 0 rpm – 3.4 barg

- 08:40: 120 °C – 704 rpm – 3.5 barg (belt replaced)
- 08:45: 120 °C – 698 rpm – 4.0 barg
- Sample of 10 mL taken (sample MDEA.4) after discarding a dead volume; darker color compared to 3.3 indicating degradation of the solution in batch mode from April 9 to April 15.

Day 9

- 08:40: 120 °C – 725 rpm – 3.8 barg
- Nitrogen flow rate dropped to 5 mL/min instead of 128 mL/min due to insufficient remaining pressure in the N_2 bottle.
- Sample of 13 mL taken (sample MDEA.5) (+ 1 dead volume)
- **End of the experiment:** Reactor weighed 3054 g (85.5 g difference):
  - Mass of samples ~45 g
  - Dead volumes ~6 g
  - Losses ~34 g
- Phase I cleaning followed by Phase II cleaning in the afternoon and replacement of the N_2 bottle.
- Reactor mass with water = 3154.7 g:
  - 14:45: 128 °C – 399 rpm – 3.9 barg
  - 15:51: 119 °C – 406 rpm – 3.8 barg
  - 17:15: 120 °C – 409 rpm – 4.0 barg
  - 18:25: 120 °C – 409 rpm – 4.1 barg

Day 10

- **End of cleaning:**
  - 09:43: 120 °C – 410 rpm – 4.0 barg
- Note on temperature impact: Cooling the reactor from 120 °C to 45 °C, pressure drops from 4.0 barg to 2.8 barg.
- Reactor mass at end of cleaning = 3151.5 g (3 g difference due to losses in stirring parts, vapor, etc.); conductivity measured at 36 µS.